NPFC

North Pacific Fisheries Commission

Stock assessment report for chub mackerel – 2025

EXECUTIVE SUMMARY

Background information

Chub mackerel (*Scomber japonicus*) in the Northwest Pacific Ocean (NWPO) are distributed from the coast of southern Japan to offshore waters of Kuril Islands. It is considered that both adults and juveniles are distributed as far east as the 170-degree East longitude line. The feeding migration of adults has expanded to the northeast recently, and since 2018 the distribution of adults during summer and fall has reached 47-degree North, 166-degree East, east offshore of Kuril Island. The spawning ground is known to be located within the range of the Japanese Exclusive Economic Zone (EEZ), with the main spawning ground located in Izu Island waters.

Chub mackerel are harvested by China, Japan and Russia (Figure E-1). Chinese light purse seine and pelagic trawl fisheries operate in the NPFC Convention Area, while Japanese chub mackerel fisheries consist mainly of purse seine and set net fisheries within the Japanese national waters. Russian chub mackerel fisheries mainly operate in the Russian national waters and consist of mid-water trawl and purse seine gears. Russian fisheries also operate bottom trawl gears in the Japanese national waters. The historical total landings have fluctuated largely and recently decreased from approximately 514,000 mt in 2018 to 135,000 mt in the most recent calendar year (CY) 2024. The Conservation and Management Measure for chub mackerel (CMM 2025-07) includes a catch limit of 66,740 mt set in the Convention Area for the 2025 fishing seasons.

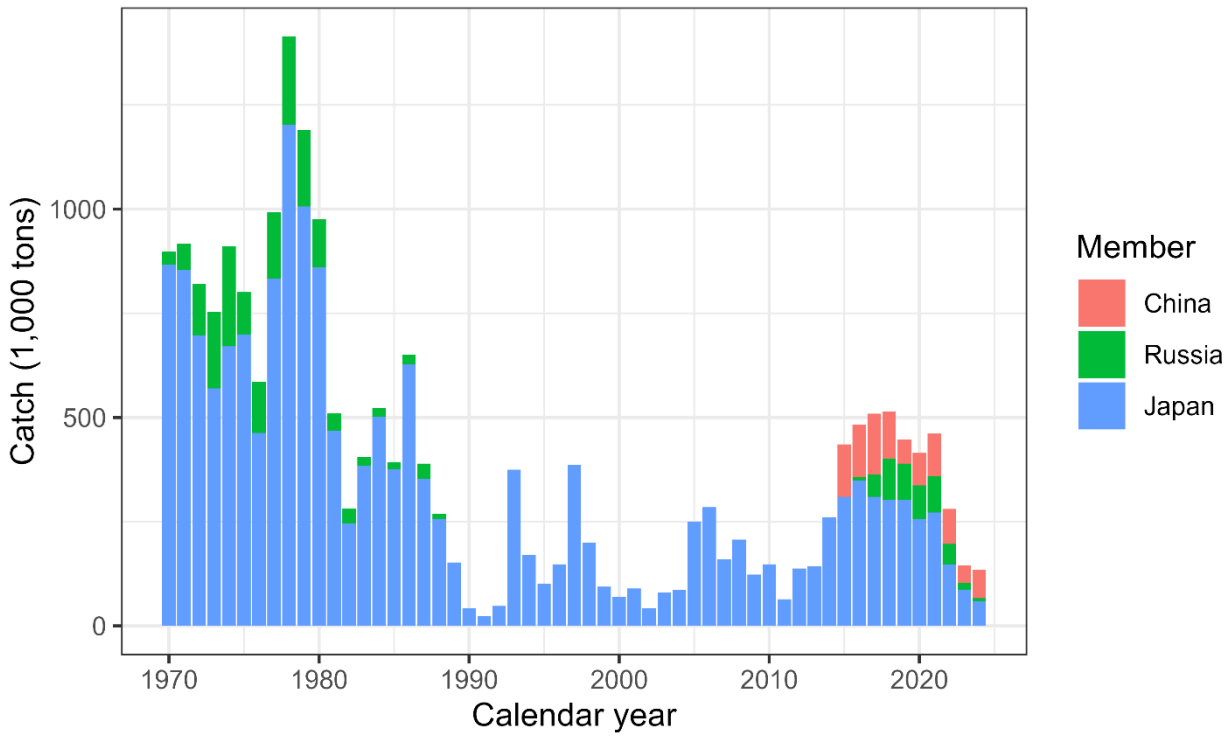

Figure E-1. Historical chub mackerel catch in weight by Member.

2nd Floor Hakuyo Hall
Tokyo University of Marine Science and Technology
4-5-7 Konan, Minato-ku, Tokyo
108-8477 JAPAN

TEL +81-3-5479-8717
FAX +81-3-5479-8718
Email secretariat@npfc.int
Web www.npfc.int

Stock assessment model

A state-space stock assessment model (SAM) was agreed to be used for the chub mackerel stock assessment by the Technical Working Group on Chub Mackerel Stock Assessment (TWG CMSA). SAM accounts for observation errors in catch-at-age data and abundance indices. It uses age-specific data on catch numbers, stock weight, and maturity rate in each year. Recruitment was defined as numbers at age 0, and spawning stock biomass (SSB) was calculated through multiplication of numbers-at-age by maturity-at-age and weight-at-age. SAM consists of two subparts: a population dynamics model and an observation model.

Age-structured population dynamics for chub mackerel estimated by SAM are driven through survival processes such as natural and fishing mortalities, as well as process errors. Reproduction is calculated by a Beverton-Holt stock recruitment relationship. Fishing mortality coefficients by year and age group are assumed to follow a multivariate random walk, consequently allowing estimation of time-varying selectivity.

In the observation model of SAM, the catch-at-age is estimated though the fitting of the Baranov equation to the observed catch-at-age under a lognormal error distribution. SAM also fits to abundance indices with a lognormal error assumption. Non-linear relationships to population abundance estimates were estimated for the three abundance indices specific to ages 0 and 1, linear relationships were applied to the other abundance indices.

Data and biological parameters used in the assessment model

Data are included from the NPFC Convention Area and Members' EEZs.

A fishing year (FY) starting from July and ending in June of the following year was applied in the stock assessment of chub mackerel. The TWG CMSA agreed for the stock assessment period to be FY1970 to FY2023. Seven age groups of ages 0 to 5 and 6+ were defined in the stock assessment. The historical catch-at-age, which was constructed from the quarterly data from each Member, is shown in Figure E-2. Time series of mean weight-at-age are illustrated in Figure E-3. Annual maturity-at-age with decadal time-varying changes is shown in Figure E-4. These data were available up to FY2023.

Seven time series of the relative indices of abundance were used during model development (Figure E-5): relative number of age 0 fish from the summer survey by Japan; relative number of age 0 fish from the autumn survey by Japan; relative number of age 1 fish from the autumn survey by Japan; relative SSB from the egg survey by Japan; relative SSB from the dip-net fishery by Japan; relative vulnerable stock biomass from the light purse-seine fishery by China; and relative vulnerable stock biomass from the trawl fishery by Russia. The indices from Japan and Russia were available until FY2024 and until FY2023 for China.

An age-specific natural mortality (M), corresponding to 0.80 for age 0, 0.60 for age 1, 0.51 for age 2, 0.46 for age 3,0.43 for age 4, 0.41 for age 5, and 0.40 for age 6+, was applied for the stock assessment by the TWG CMSA.

Overall, the available data show 1) recent decreases in the relative abundance trends, 2) a shift to older average age at maturity, 3) changes in weight at age, and 4) declining catch trends.

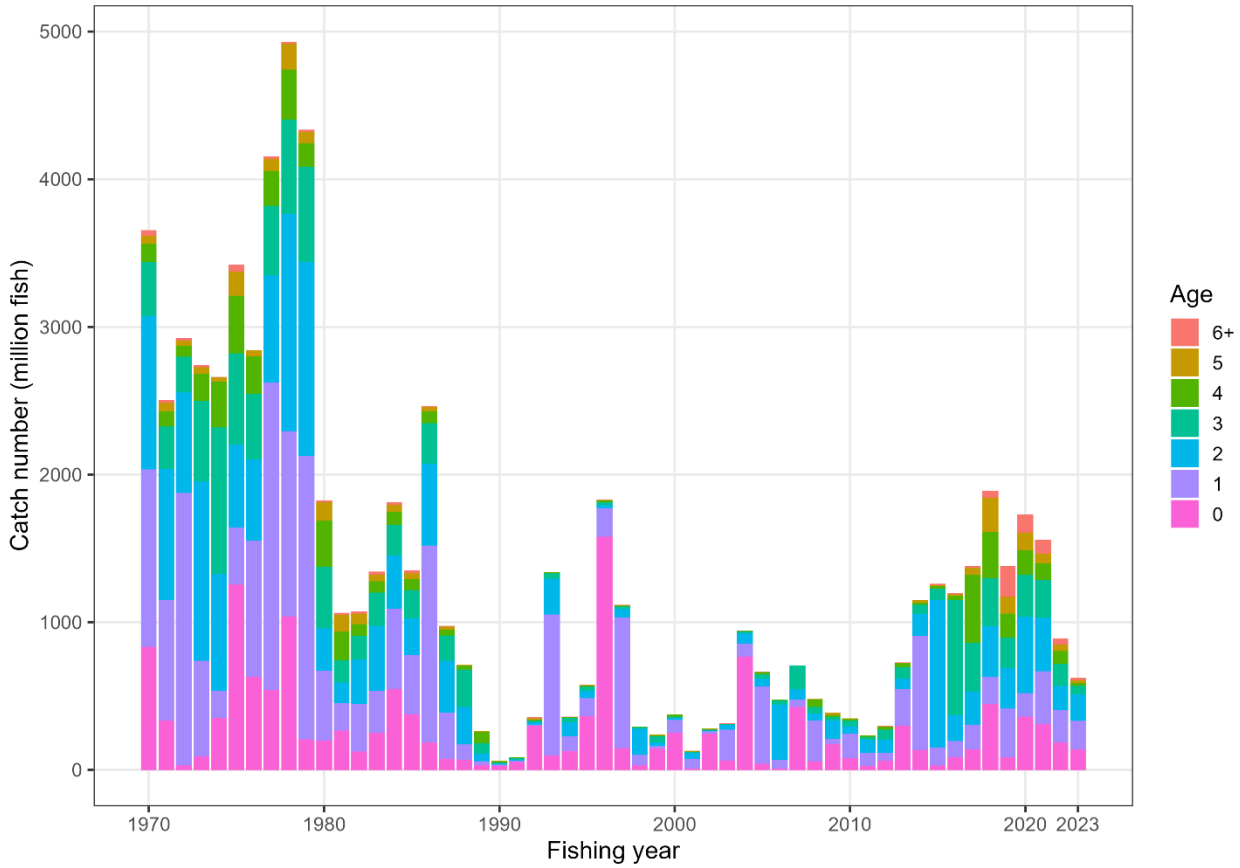

Figure E-2. Historical observed catch-at-age.

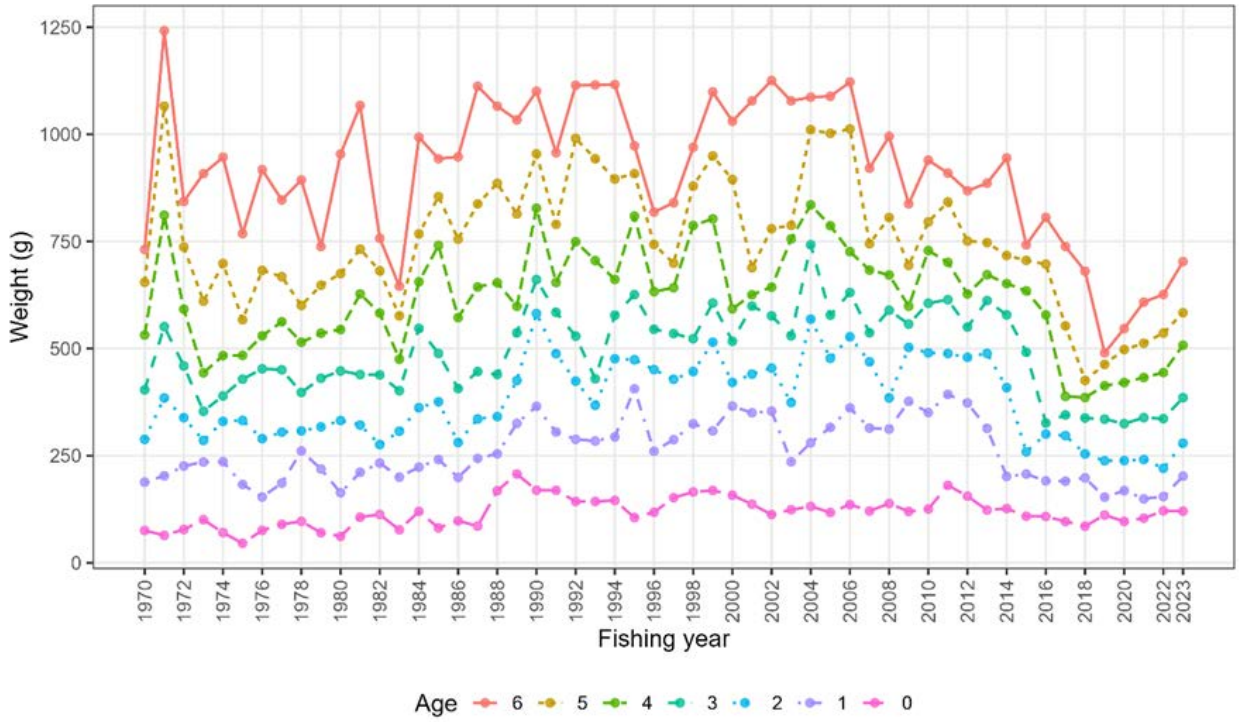

Figure E-3. Time series of weight-at-age.

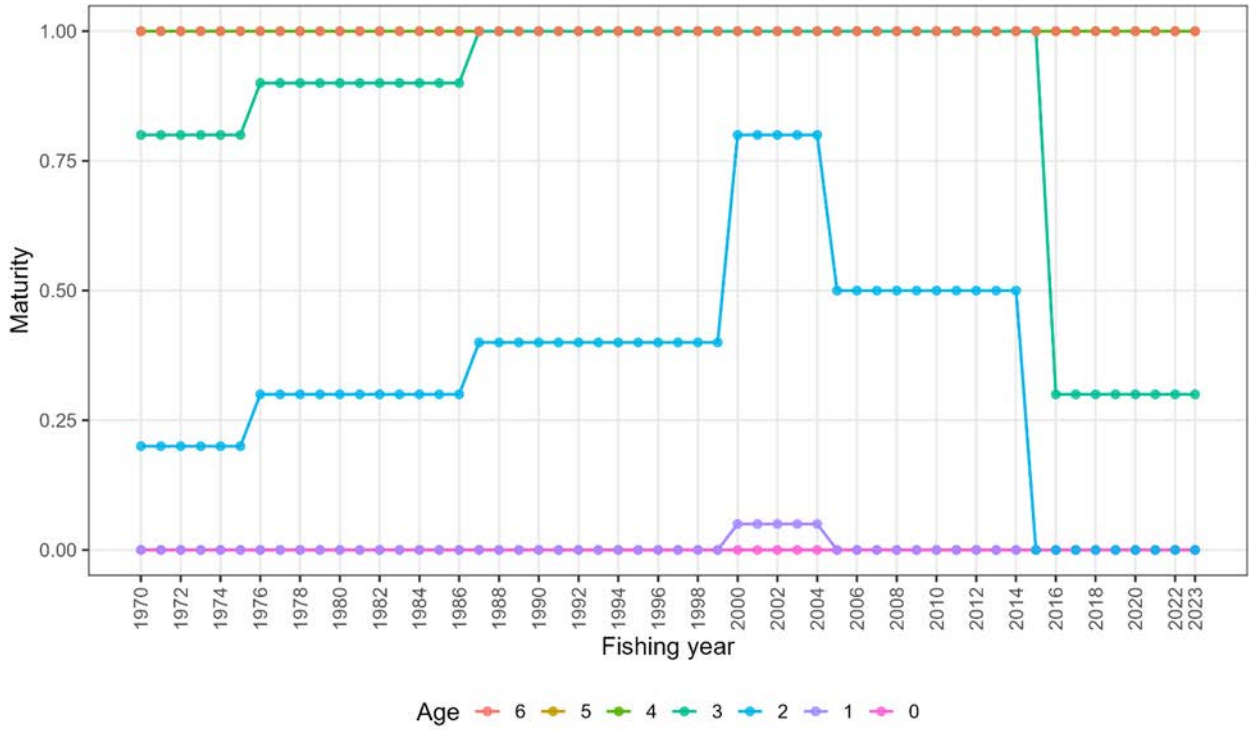

Figure E-4. Time series of maturity-at-age.

Figure E-5. Time series of abundance indices, note that the y- scales differ.

Main stock assessment scenarios

The TWG CMSA based this year's stock assessment on the previous assessment and included the following scenarios as candidate base cases:

- **S01-InitBase.** This scenario is based on the TWG CMSA 09 base case (S28-Proc Est), which excluded the latest abundance indices. Therefore, the abundance indices up to FY2023 were used as input in this scenario (FY2024 indices were excluded).

- **S02-Index24_1.** This scenario included the FY2024 abundance indices from Japanese and Russian fisheries and Japanese surveys. The weight and maturity at age for FY2024 were assumed to be their averages throughout FY2016–FY2023. The proportion of Russian catch out of the total catch was assumed to be its average over FY2021–FY2023. Although the catch in FY2024 is not available, stock status at the start of FY2024 is able to be calculated because stock status is determined before exploitation.

Seventeen other sensitivities were used to investigate the effect of alternative assumptions regarding the biological parameters in FY2024, Russian catch proportion in FY2024, nonlinearity for abundance indices, stock-recruit relationship, maturity processes and assumptions regarding process error in numbers at age. TWG CMSA agreed to select S02-Index24_1 as a base case scenario because of its robustness and better diagnostic performance.

F-based reference points

The TWG CMSA calculated these reference points along with commonly used biological reference points such as F%SPR (30%, 40%, 50%, 60% and 70%), F0.1, with mean biological parameters and selectivity of the current fishing mortality (F_{cur}, average in FY2021 to FY2023) (Table E-1). In particular, the biological parameters such as weight-at-age and maturity-at-age used for calculation of biological reference points are assumed as the average values during the most recent 8 years (FY2016 to FY2023), which represents the recent shift in biological parameters. As a comparable, the average of the biological parameters over the stock assessment period is used for the calculation of these reference points.

B-based reference points

While the F-based reference points are relatively robust to the time-varying biological parameters, commonly used B-based reference points such as SSB_{MSY} and SSB0 are found to be significantly affected by the changes of biological parameters in this stock as well as by the assumptions of stock recruitment relationships and model configurations. Owing to the uncertainty, the TWG CMSA explored some empirical reference points based on percentiles of historical SSB in FY1970–FY2023 (Figure E-6). The 25th percentile of SSB could be regarded as the limit, being above the SSB levels when the stock has been severely depleted during the 1990's and early 2000's. The remaining two reference points ($SSB_{REFERENCE\_A}$ and $SSB_{REFERENCE\_B}$) are the 50th and 70th percentiles of historical estimated SSB.

Although these levels of SSB are significantly lower than the theoretically calculated SSB_{MSY} under the assumption of Beverton-Holt type SR relationship without considering the time-varying nature of biological parameters, the two SSB reference points are about 20% of $SSB_{F=0\_RECENT}$ and about 40% of $SSB_{F=0\_RECENT}$, respectively, which is calculated as the multiplier between average lifetime contribution to the spawning stock biomass per fish assuming no fishing (SPR0) and average number of recruitment during the most recent 8 years. The quantity roughly approximates the level of SSB that could have been attained on average over the last decade if there had been no fishing.

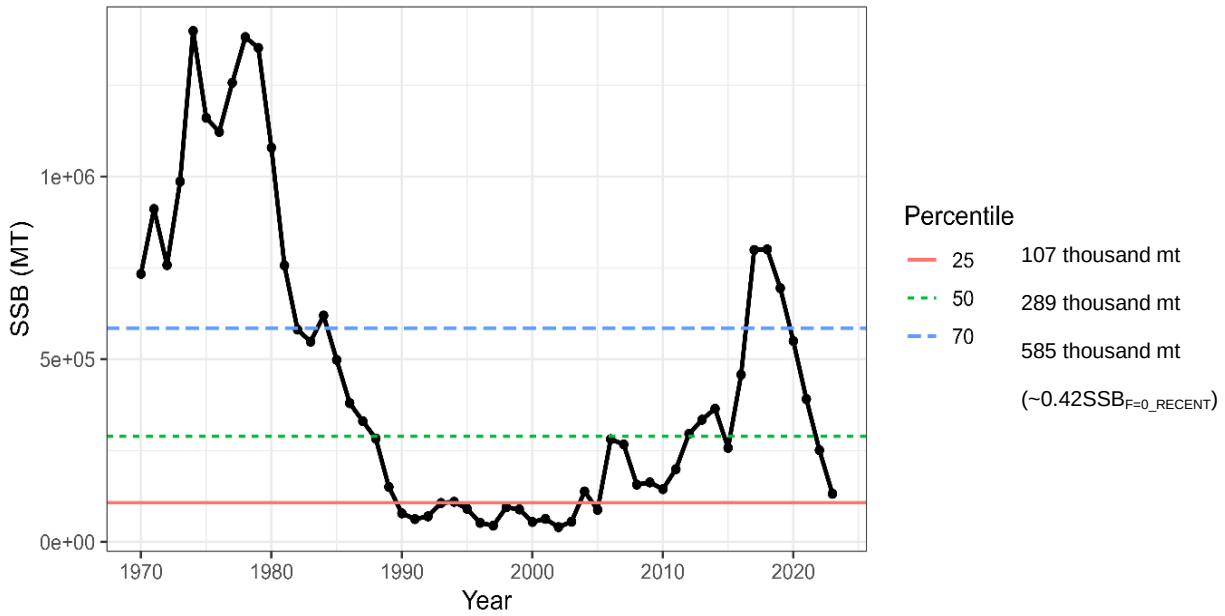

Figure E-6. Estimated spawning stock biomass and its 25th, 50th and 70th percentiles.

Description of specification of future projections

The population dynamics model for stochastic future projections is the same as is used in SAM. Future projections were conducted assuming a constant catch a fixed amount (ranging from 0 to 200 thousand mt in increments of 10 thousand mt) each year from FY2026 to FY2036. Constant F projections were also conducted under F_{cur} and Constant-F scenarios where the catch was calculated by a fixed fishing mortality (ranging from F30%SPR to F70%SPR in increments of 5%SPR) each year since FY2026. For all scenarios the catch in FY2024 and FY2025 is based on the assumption that the fishing mortality in FY2024 and FY2025 would be the same as the FY2023 fishing mortality estimated by SAM.

Two assumptions regarding biological parameters were used for the calculation of reference points, one where the future biological parameters are assumed to equal the average of the recent eight (FY 2016–FY2023) years, and another where the mean biological parameters for the entire model time period (FY1970–FY2023) are used to calculate the reference points. The TWG CMSA recommends the use of the recent average based on the assumption that the prevailing conditions will likely persist for the near future.

Stock status overview

Total biomass, Spawning Stock Biomass

The time series of estimated chub mackerel total biomass and SSB generally declined from the 1970s through the 1990s (Figure E-8). The stock began to recover in the early 2000s, peaking in FY2018, then SSB has declined to 16% of that peak in 2023. The spawning stock biomass in 2023 is slightly higher than SSB_{LIM} (SSB_{2023}/SSB_{LIM}=1.23) but lower than $SSB_{REFERENCE\_A}$ and $SSB_{REFERENCE\_B}$ (Table E-1).

Recruitment

The level of recruitment in the 1970s was estimated to be high (~15 billion individuals on average) and reached a low period between the 1990s and the 2010s (Figure E-8). Recruitment in the most recent decade (FY2014–FY2023) was also high on average (~7.4 billion), but not as high as in the

1970s and had a decreasing trend since the last peak in 2018. The estimated Beverton-Holt stock recruitment relationship was slightly concave (Figure E-9), suggesting that the density-dependent effect in recruitment is not strong.

Exploitation status

Estimated exploitation rate generally fluctuated between 10% and 35%, with over 40% and below 10% in several years, following the estimated F dynamics. No clear temporal trend was observed (Figure E-8). The current fishing mortality (F_{cur}) corresponds to 16% SPR, and higher than the commonly used F-based reference points such as F0.1 and F30–70%SPR (Table E-1). Fishing mortality related reference points indicate that the stock is at approximately 16% SPR, indicating that current fishing mortality are also reported for percent FSPR values, in relation to the current F (F_{cur}, average FY2021–FY2023) for FSPR from the recent period (FY2016–FY2023) as well as over the entire time period (FY1970–FY2023; Table E-1).

Conclusions and recommendations

The chub mackerel stock in the NWPO has experienced large changes in biological parameters over the time period of the model. The main temporal changes are a recent decrease in maturity at age, along with a recent change in the weight at age, both of which were observed to impact the model time period to cause temporal impacts on biological reference points. MSY-based reference points are highly variable over the time series of the assessment because the weight- and maturity- at age of chub mackerel have varied widely (Figures E-3 and E-4), which impacts the productivity of the stock. Unfished spawning biomass per recruit (SPR0) has varied remarkably over time (Figure E-7).

Besides such uncertainty, the current fishing mortality (average FY2021–FY2023) is higher than the commonly used reference points such as F%30–60%, and SSB in FY2024 is lower than the reference levels of median and 70th percentiles ($SSB_{REFERENCE\_A}$ & $SSB_{REFERENCE\_B}$, respectively), but slightly above the SSB_{LIM}.

Harvest Recommendations

Given the uncertainty in biological parameters in future, which has a large impact on the projection results, the TWG CMSA considers it is not appropriate to provide long-term harvesting recommendations at this time. However, in response to the request from COM09, 10 year projection was undertaken to assess the effects of varying catch and F levels based on the most recent eight years' biological data (Figures E-10 and E-11, Tables E-2 to E-5). Projections indicate that current fishing mortality is unsustainable, and probabilities of achieving various reference levels under catch-constant as well as F-constant scenarios are provided in Tables E-2 and E-3. It is recommended to reduce fishing mortality to recover SSB to the reference levels.

Data and Research needs

The assessment results, including projections, are dependent on biological parameters and processes which are uncertain. Therefore, future studies should be focused on collecting and analyzing biological information, e.g., maturity-at-age and weight-at-age, which would improve the assessment. Fisheries-dependent data, such as fleet-specific catch-at-age, are also critical to develop Member-specific fishing fleet and age-specific abundance indices. It is also important to explore the factors that contributed to the lower-than-expected presence of the 2018 year class in catch-at-age data, despite strong signals in survey indices.

A critically important recommendation that should be carried out in 2-3 years is to develop a harvest control rule (HCR) specific to this stock via a Management Strategy Evaluation (MSE) process.

This HCR should be dynamic and able to adjust annual total catches depending on the stock abundance as well as the target and limit reference points. During the process of the development of MSE, uncertainties in parameter estimates, time-varying or density-dependent biological parameters, stock-recruitment assumptions, process errors, and selectivity should be considered.

Timely collection of biological information and further research on biological parameters and processes, including the effect of environment and climate change, are critically important to facilitate the accurate estimation of reference points.

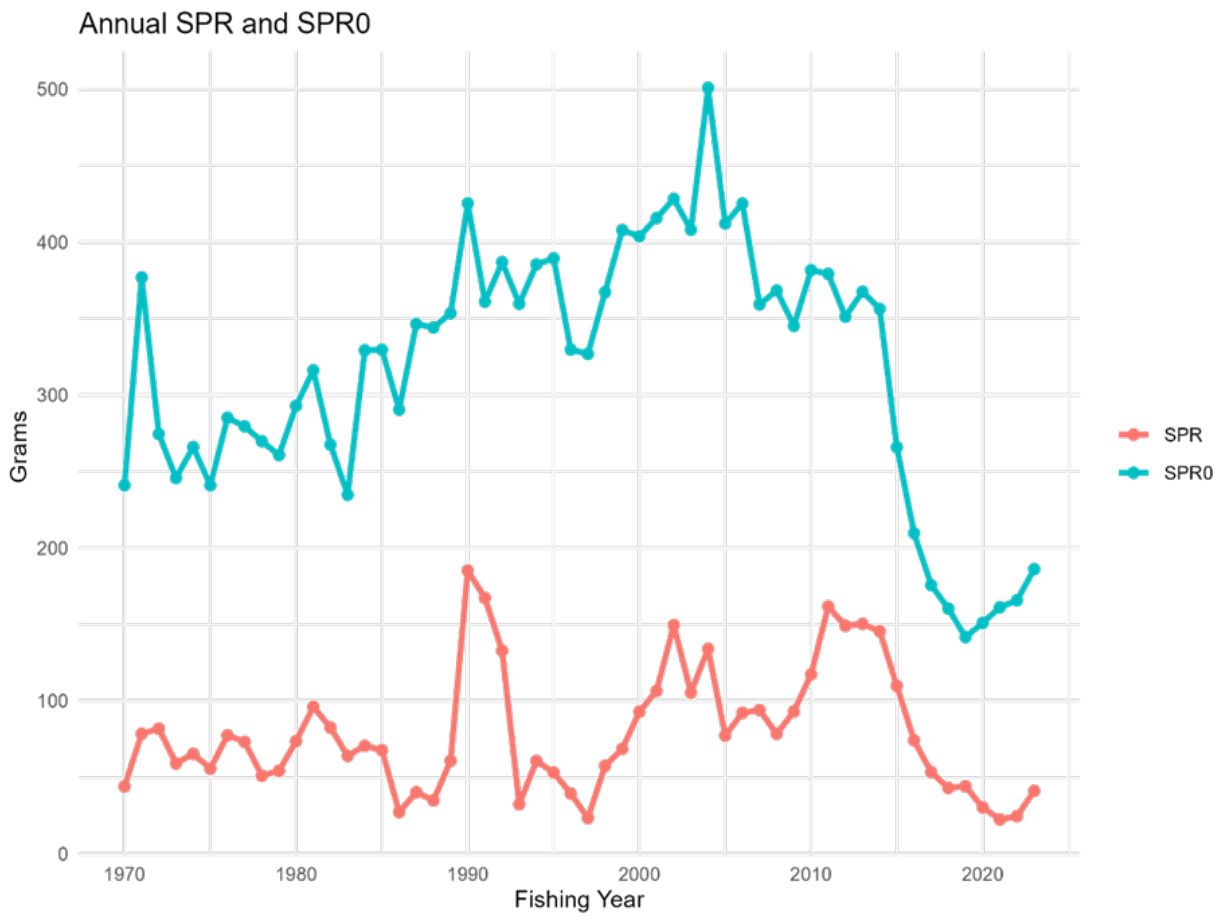

Figure E-7. Trajectories of spawners per recruit with (SPR) and without fishing (SPR0).

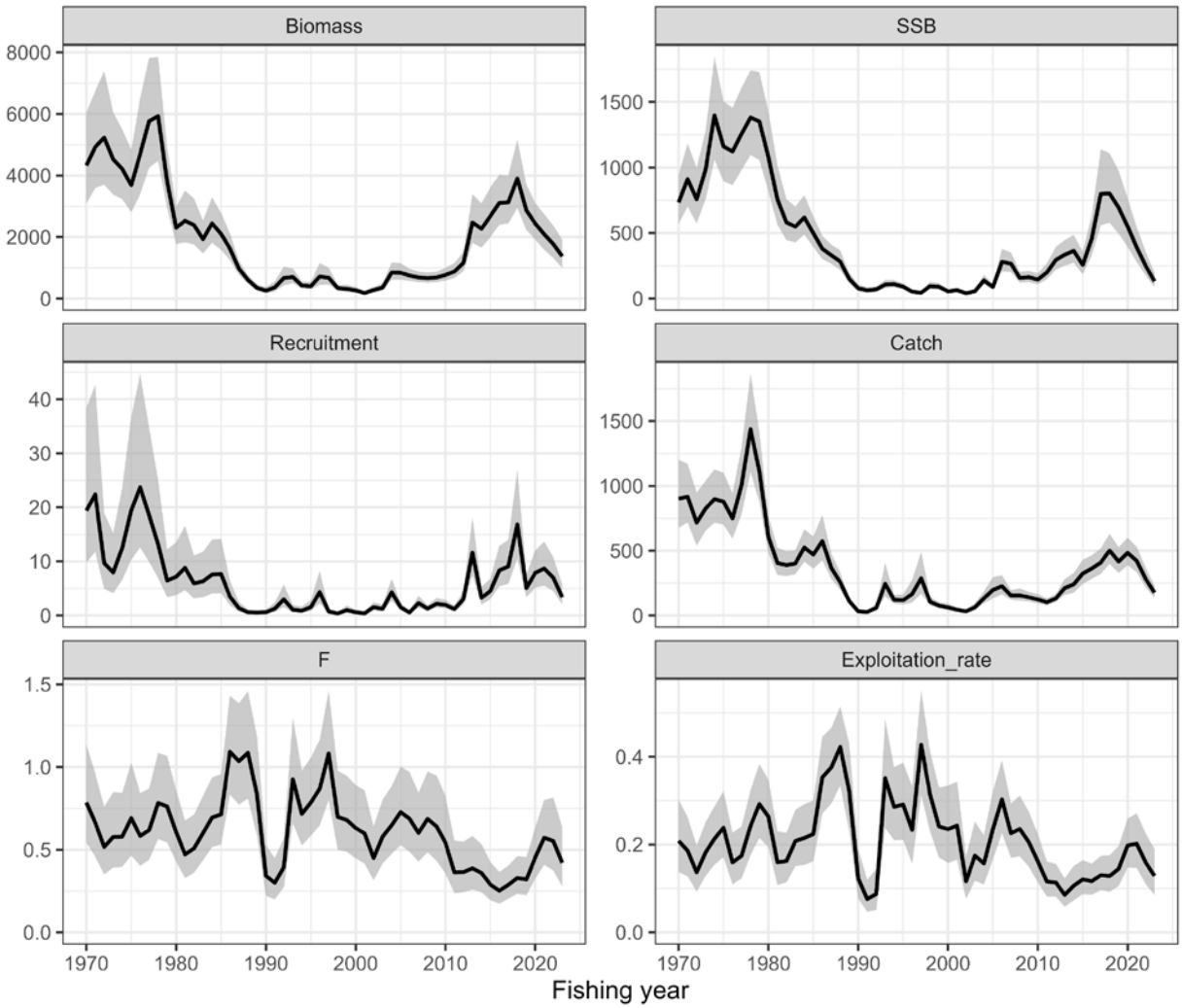

Figure E-8. Time series of estimates of total biomass (thousand mt), SSB (thousand mt), recruitment (billion fish), catch (thousand mt), mean fishing mortality (F) and exploitation rate (catch divided by total biomass) from the base case (S02-Index24_1).

Table E-1. Reference points for the base case scenario (S02-Index24_1). F-based reference point values that are dependent on time varying parameters are calculated by holding F_{cur} the same for all calculations, but by varying the time period (either FY2016–FY2023 or FY1970–FY2023) over which the biological parameters are estimated. Refer to Glossary in the stock assessment report for the definitions.

Reference Points	**Biological parameters**	
	FY2016–FY2023	FY1970–FY2023
F-based reference points		
Current%SPR	**16.2**	27.8
$F0.1/F_{cur}$	**0.838**	0.838
$FpSPR.30.SPR/F_{cur}$	**0.580**	0.911
$FpSPR.40.SPR/F_{cur}$	**0.412**	0.609
$FpSPR.50.SPR/F_{cur}$	**0.295**	0.416
$FpSPR.60.SPR/F_{cur}$	**0.207**	0.282
$FpSPR.70.SPR/F_{cur}$	**0.139**	0.184
Biomass-based reference points		
$SSB_{F=0\_RECENT}$	**1399**	–
25th Percentile Historical SSB (SSB_{LIM}) (thousand mt)	**107**	
50th Percentile Historical SSB ($SSB_{REFERENCE\_A}$) (thousand mt)	**289**	
70th Percentile Historical SSB ($SSB_{REFERENCE\_B}$) (thousand mt)	**585**	
SSB_{2023}/ SSB_{LIM}	**1.23**	
SSB_{2023}/ $SSB_{REFERENCE\_A}$	**0.46**	
SSB_{2023}/ $SSB_{REFERENCE\_B}$	**0.23**	
SSB_{LIM} / $SSB_{F=0\_RECENT}$	**0.08**	–
$SSB_{REFERENCE\_A}$ / $SSB_{F=0\_RECENT}$	**0.21**	–
$SSB_{REFERENCE\_B}$ / $SSB_{F=0\_RECENT}$	**0.42**	–

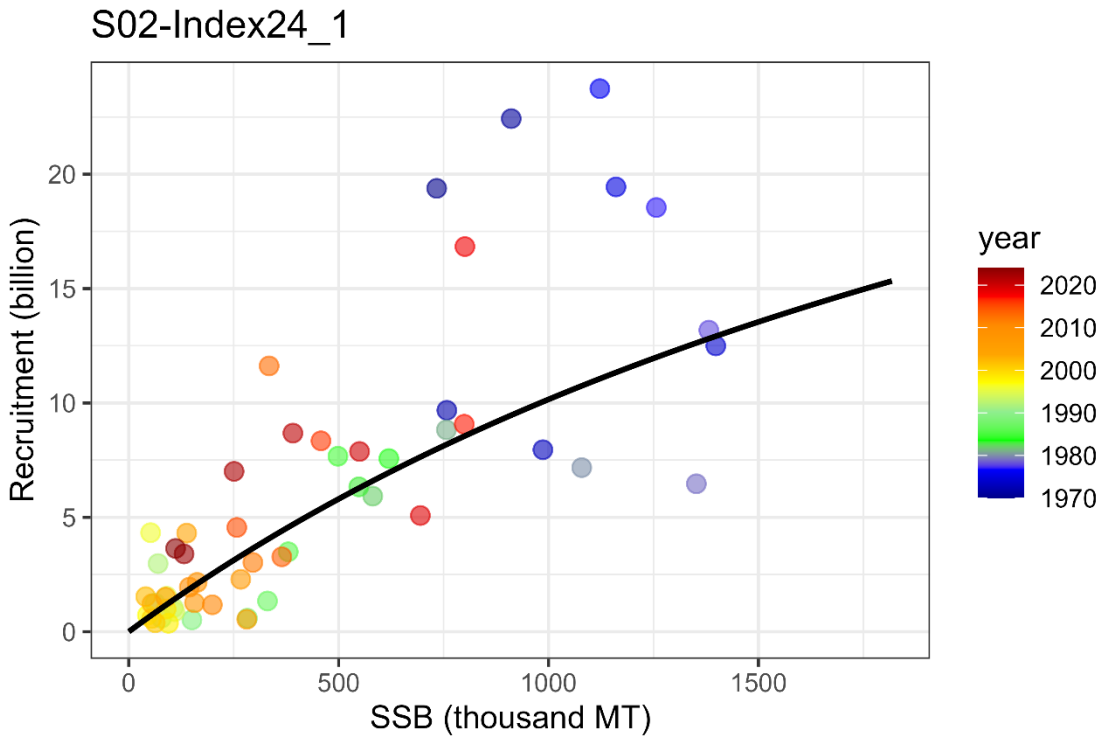

Figure E-9. Estimated stock-recruitment curve (black line) and estimated SSB and number of recruits (circles colored by decade), from the selected base case (S02_Index24_1).

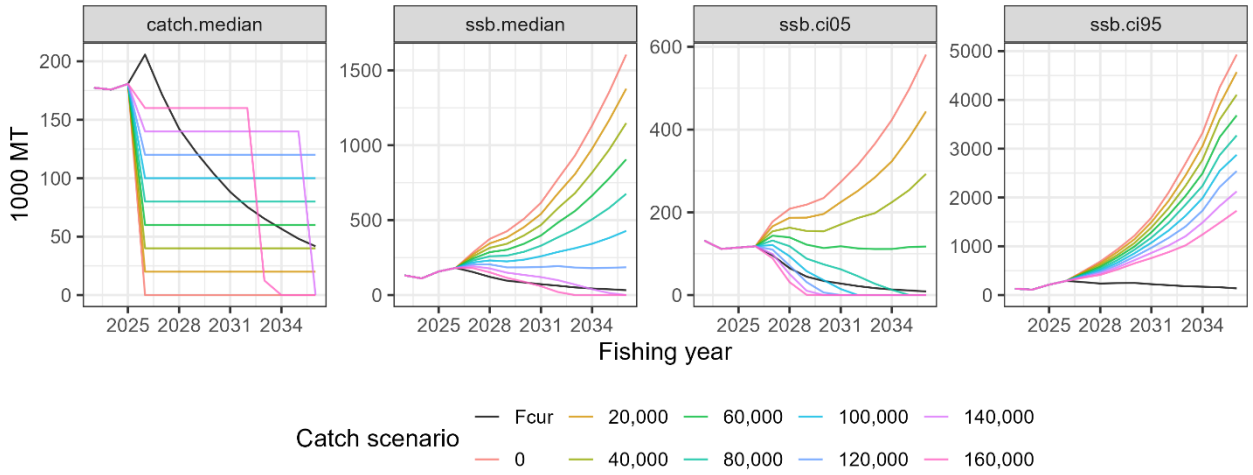

Figure E-10. Future trajectories of median catch (left), median SSB (second from left), 5% lower limit of predictive interval for SSB (third from left) and 95% SSB (right) with mean biological parameters in recent 8 years. Numbers and "F_{cur}" in "Catch scenarios" indicate total amount of catches (mt) in constant catch scenarios of 0 to 160 thousand mt in increments of 20 thousand mt and current fishing morality, respectively.

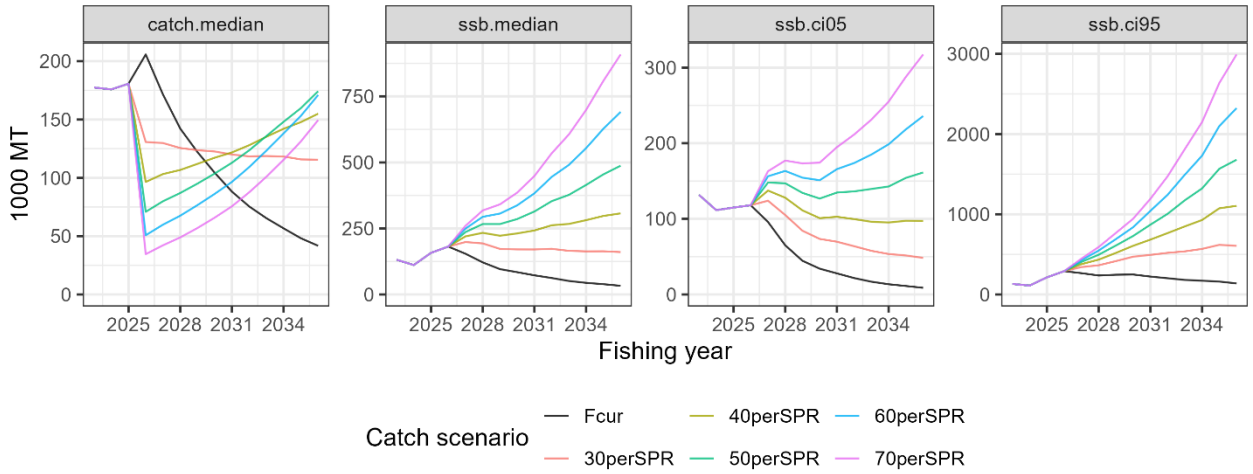

Figure E-11. Future trajectories median catch (left), median SSB (second from left), 5% lower limit of predictive interval for SSB (third from left) and 95% SSB (right) with mean biological parameters for the entire time series. 30–70%SPR and "F_{cur}" in "Catch scenarios" indicate total amount of catches (mt) in constant fishing mortality scenarios of F30–70%SPR in increments of 10% and current fishing morality, respectively.

Table E-2. Probability that future SSB on July 1, at the beginning of the fishing year, is above $SSB_{REFERENCE\_B}$, $SSB_{REFERENCE\_A}$, and SSB_{LIMIT} (70^{th} percentile, 50^{th} percentile and 25^{th} percentile, respectively) under constant catch projections for the base case scenario. The projection towards FY2036 is shown below.

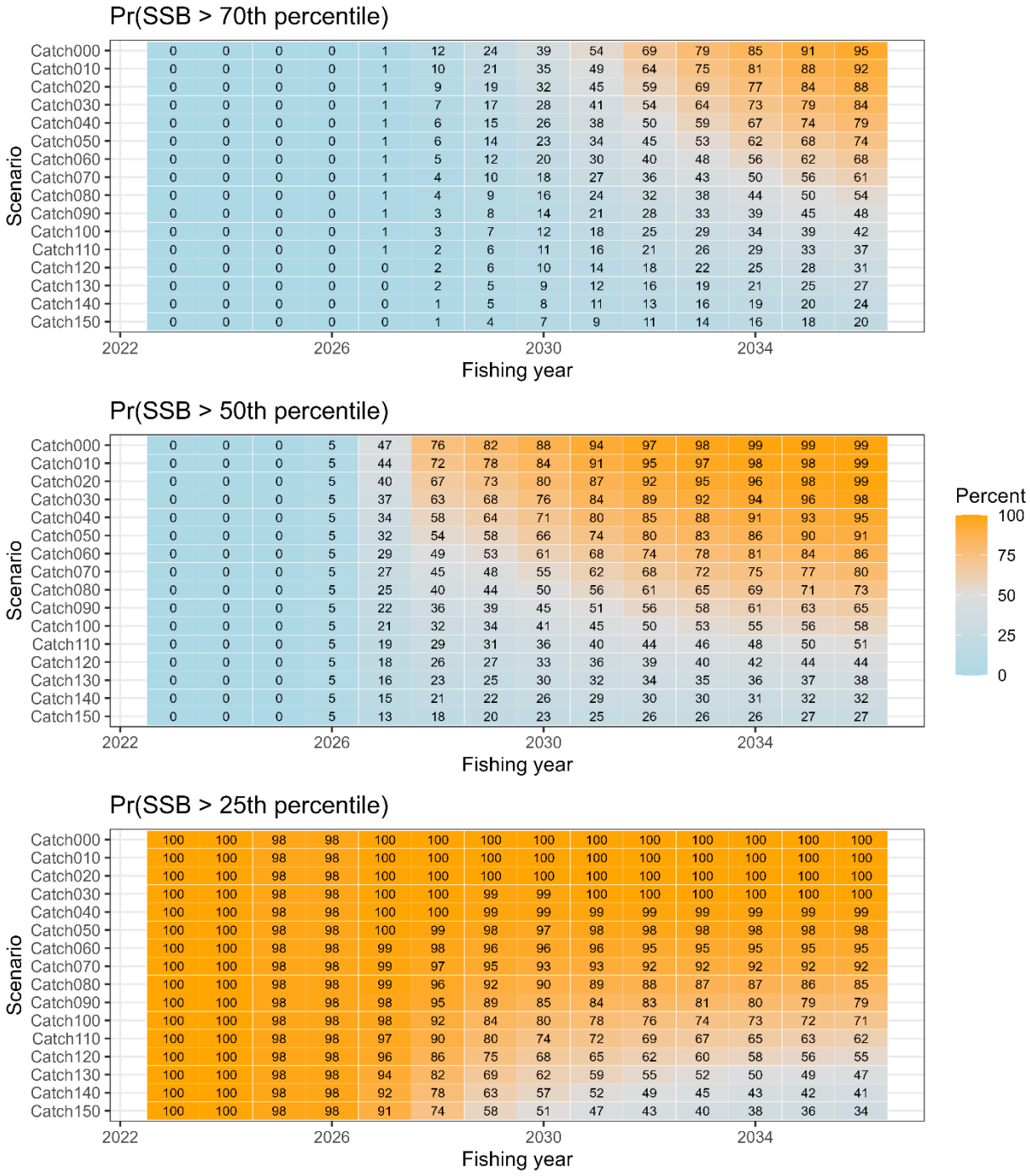

Table E-3. Probability that future SSB on July 1, at the beginning of the fishing year, is above $SSB_{REFERENCE\_B}$, $SSB_{REFERENCE\_A}$, and SSB_{LIMIT} (70^{th} percentile, 50^{th} percentile and 25^{th} percentile, respectively) under constant fishing mortality projections for the base case scenario. The projection towards FY2036 is shown below.

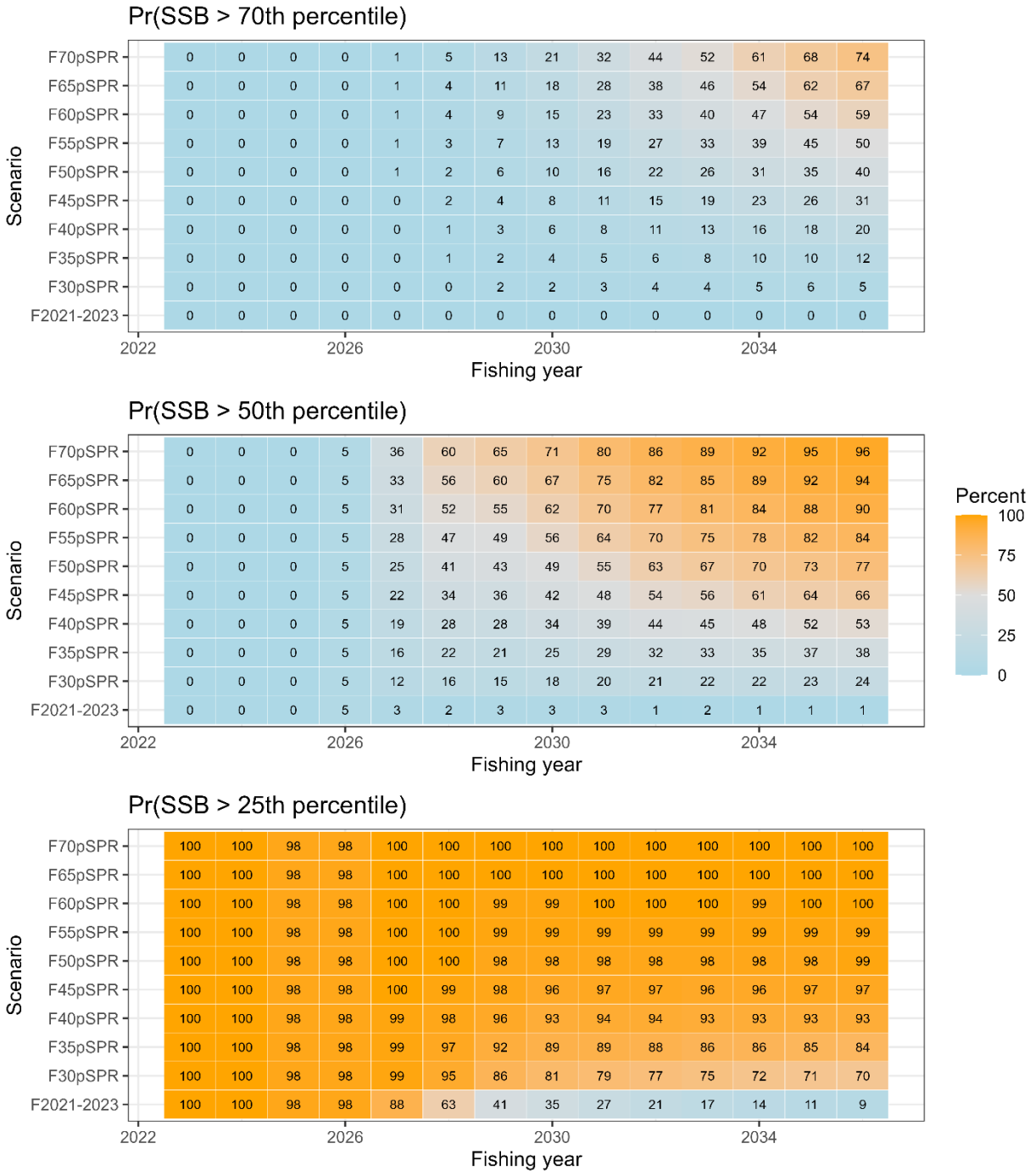

Table E-4. Median catch and median SSB based on constant-catch scenarios (ranging from 0 mt to 150 thousand mt).

Table E-5. Median catch and median SSB based on projections using constant F scenarios.

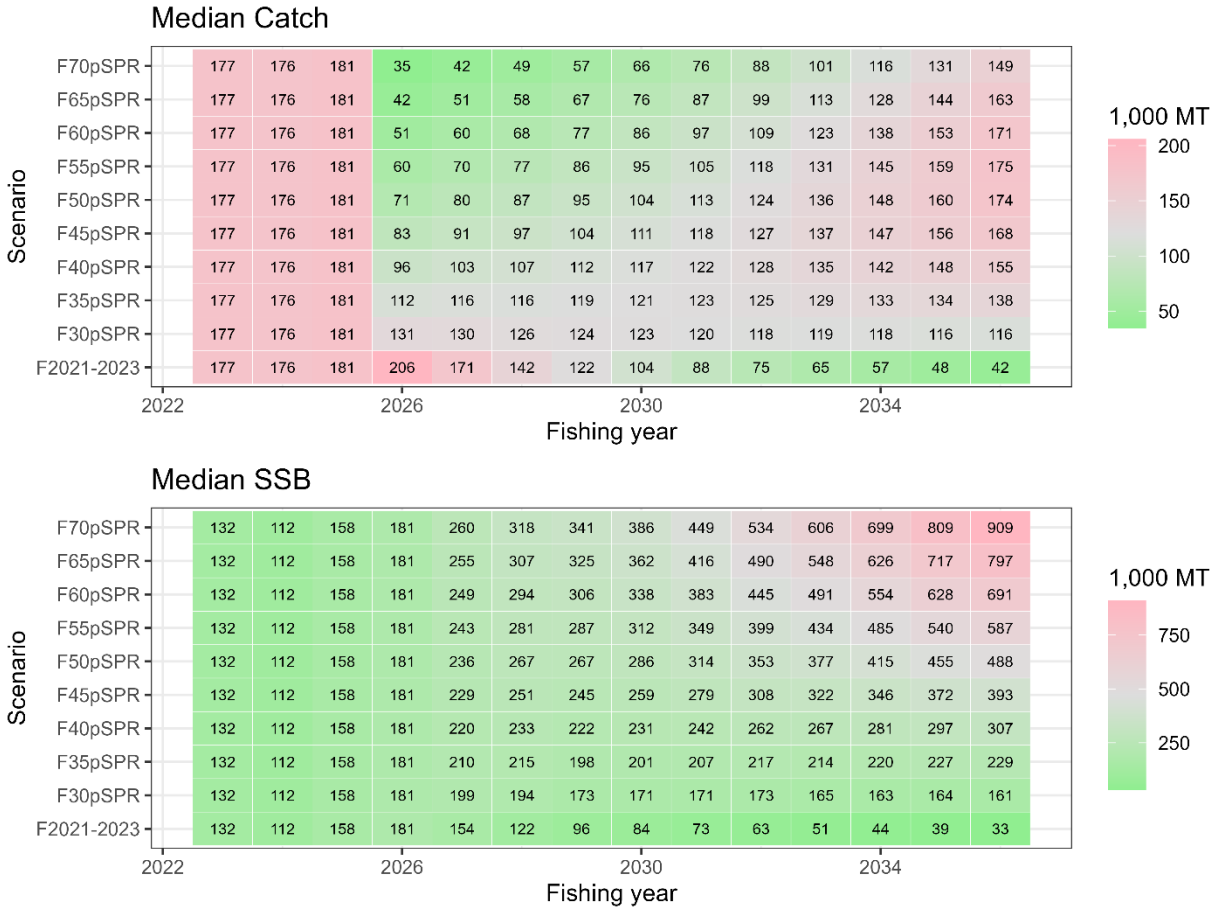

INTRODUCTION

1.1 Distribution and population structure

Chub mackerel (*Scomber japonicus*) is widely distributed throughout in the northwest Pacific, including in the waters of Japan, Korea, China, and Russia. The species exhibits highly migratory behavior, with distinct spawning, feeding, and wintering grounds. Spawning occurs primarily from spring to early summer in the subtropical waters, and the larvae and juveniles are often carried by ocean currents to feeding grounds further north. This migration pattern leads to a dynamic population structure that varies seasonally and spatially, reflecting the species' adaptation to environmental conditions.

In the northwest Pacific, two stocks of chub mackerel are recognized. Although there are no clear genetic differences between the two stocks, they are treated as different stocks due to their biological differences, distribution and spawning grounds. The first is the Tsushima Warm Current stock, which is distributed in the East China Sea and the Sea of Japan, and the latter is the Pacific stock, which can be defined as a straddling stock and is harvested in both national waters of Japan and Russia and the NPFC Convention Area. The Pacific stock, hereafter called chub mackerel in this report, is distributed from the coast of southern Japan to offshore waters of Kuril Islands (Figure 1). It is considered that both adults and juveniles are distributed as far east as 170°E longitude in periods of high abundance. During the low abundance period of 1990s-2000s, juvenile distributes from Japan to around 170°E, but adults were only found to 150°E due to the possible contraction of the feeding ground. The feeding migration of adult extends northeast, with the recent (since 2010) increase of stock abundance, the distribution of adult during the summer to fall season has expanded to 47° N, 166° E, east offshore of Kuril Island, after 2018. Adult fish spawn in Izu Islands waters in spring and then engage northward feeding migration to waters of Sanriku to east Hokkaido from summer to autumn.

1.2 Migration

Adults move to north (March to June) after spawning at Izu Islands area, which is the main spawning ground, and migrate to offshore area of Northeast of Japan (Sanriku and Hokkaido) from summer to fall for feeding (Meguro et al., 2002) (Figs. 1 & 2). Larvae distribute broadly from the Pacific side of southern Japan to Kuroshio extension and Kuroshio-Oyashio transition area in spring. Larvae occurred at Kuroshio-Oyashio transition area and move to offshore of Kuril Island in summer and subadults migrate down south in fall to offshore of Chiba and Ibaraki prefecture for wintering (Kawasaki, 1968; Iizuka, 2002; Nishida et al., 2001; Kawabata et al., 2006). Portion of adult and subadult migrate to Kii strait, Bungo strait and Seto inland sea, while the main spawning adults migrate to waters around Izu Islands area. Because of the occurrence of larvae originated upstream of Kuroshio current at the spawning ground of Izu Islands (Koizumi, 1992), spawning

ground extended from offshore of southern Japan to northern Japan (Kuroda, 1992).

1.3 Reproduction

Chub mackerel mature at about age 2 or 3 and all fish at age 4 and above are supposed to be fully matured (Watanabe and Yatsu, 2006). One functional matured female produces 30–90 thousand eggs several times during a spawning season (Murayama et al., 1995; Watanabe et al., 1999; Yamada et al., 1999). The main spawning grounds are in the Japanese Exclusive Economic Zone (EEZ), in waters around the Izu Islands but also in areas off the Pacific coast of southern Japan, including the Kinan area, Cape Muroto and Cape Ashizuri (Fig. 1). The waters around the Izu Islands are considered the main spawning ground (Watanabe, 1970; Usami, 1973). Although spawning occurs from offshore of southern Japan to northern Japan (Kuroda, 1992) and it has also been observed in the Tohoku waters (Kanamori et al., 2019).

The spawning season for chub mackerel is from January to June. In the main spawning ground of Izu Islands, spawning occurs in March and April, which historically are the peak spawning months (Fig. 2). In the 2000s, the peak spawning timing has shifted to May and June because of the high fraction of younger adults, which tend to spawn eggs at later season (Watanabe, 2010). Additionally, the spawning ground is reported to exhibit northward shifting with extended spawning period associated with climate change (Kanamori et al., 2019).

1.4 Prey and predators

Larvae feed on the eggs of copepods and nauplii, whereas juvenile prey on small zooplankton such as small copepods, noctilucines, cercariae, and salpae (Kato and Watanabe, 2002). The feeding behaviors of immature and adult fish differ depending on the waters and lifecycle, but they mainly prey on other fishes (e.g., anchovies and lantern fish), crustaceans (e.g., krill and copepods) and salpae. In the Sanriku waters, the main prey are mysid shrimp and anchovies.

Before the 1980s, when stock abundances were high, chub mackerel were often observed to be eaten by large fishes such as the mackerel shark, blue shark, pomfret, albacore, and skipjack tuna (Kawasaki, 1965; Nagasawa, 1999), as well as the minke whale (Kasamatsu and Tanaka, 1992). In the 1990s, the lower abundance period, predation of minke whales was not reported (Tamura et al., 1998). From the research report of baleen whale predations, composition of anchovy decreased in the stomach contents after 2012, but mackerels and sardine increased. Especially in the case of sei whale, the main prey item shifted from anchovy in early 2000s to mackerel and sardine in late 2000s and after 2010 (Tamura et al., 2016; Konishi et al., 2016). When the abundance of mackerels is high, they appear to be main prey items for whales.

1.5 Age and growth

Longevity of chub mackerel is estimated to be approximately 8 years, based on age determination of sampled catch, and maximum age was recorded at 11year-old (Iizuka, 2002). Fish at age 6 and above are very rare in the catches in recent years. There is no significant difference in growth between sex. Growth of chub mackerel is density dependent, and the parameters of growth function are variable among the year classes. According to Kamimura et al. (2021), the asymptotic body length *Linf* and growth coefficient *k* of von Bertalanffy growth function varied between 339.9 to 440.5 mm and 0.25 to 0.55 (/year), respectively, for each year class of 2006-2016.

Average size (fork length) and weight of catch in 2018 are shown in Fig. 3, with comparison of those at 2011-2014 which did not show any slow growth. Average weight of 2018 was low comparing with those of 2011-2014 and 1970s, especially for age 5 (extremely high recruitment in the 2013 year class). It is considered that density dependence may be the cause for this change. (Kamimura et al., 2021). However, slower growth has been observed at periods of high abundance, this may be due to poor environmental conditions (i.e. lower temperatures due to range expansion), or feeding competition with Japanese sardine, or other factors (Kamimura et al., 2021).

The growth of chub mackerel is density dependent, and may also be influenced by changes in the ocean environment and recent recruitment (Watanabe and Yatsu, 2004). Maturity at age has changed depending on changes in growth (Watanabe and Yatsu, 2006). The maturity at age for chub mackerel has changed over time, for example the maturity rate of age 3 fish has decreased from 100% to 30% since 2015 (Fig. 4).

FISHERIES AND SCIENTIFIC SURVEYS

2.1 Overview of fisheries

Chub mackerel are harvested by China, Japan and Russia (Figs. 5 & 6). Chinese light purse seine and pelagic trawl fisheries are operated in the NPFC Convention Area. Japanese chub mackerel fisheries consist mainly of purse seine and set net fisheries within the Japanese national waters. The Russian chub mackerel fisheries consist of mid-water trawl, purse seine and bottom trawl gears. They operate in the Russian national waters and the NPFC Convention Area. Some of these fisheries occur in the Japanese national waters. The historical total landings have largely fluctuated. In last decade, the total catch was stable at higher level and subsequently decreased from 516 thousand mt in 2018 to 129 thousand mt in the most recent calendar year (CY) 2024. The Conservation and Management Measure for chub mackerel (CMM 2025-07) includes a catch limit of 66,740 mt set in the Convention Area for the 2025 fishing season (1 June to 31 May).

China harvests this species dominantly by the light purse seine fishery in the NPFC Convention Area. A smaller component of the catch is taken by pelagic trawl. Chinese catch statistics on

mackerels in the NPFC Convention Area are available since 2015. The Chinese mackerel fisheries in the NPFC Convention Area initiated in 2014 and mainly caught chub mackerel, blue mackerel, and Japanese sardine (Zhang et al., 2023). The fishing season of Chinese fleet is from April to December.

The major Japanese fisheries for chub mackerel are purse seine, set net, dip-net fishing, and stick-held dip-net fishing. Large-scale purse seiners, historically the primary source to the total catch in Japan, operate all the year over during the main fishing season from September to February in the offshore waters off Joban and Sanriku coasts on the Pacific side of Japanese main island. Small-scale purse seiners operate year-round in the coastal waters south of Chiba Prefecture. Set net fisheries are deployed extensively along the Japanese coast and yield a large catch from Sanriku coast. Dip-net and stick-held dip-net fisheries which target adult fish in spawning season (age 2 to 4 fish) are mainly operated from January to June in the Izu Islands waters, which is the major spawning ground. Chub mackerel is also caught by angling all over Japan.

Russian fisheries targeting mackerel species and sardine operate in the NW area of the NPFC Convention Area and operate both purse seine vessels and pelagic trawl vessels. Russian fisheries first exploited mackerel in the Far East in the early 1960s and harvested it until the late 1980s, when its stocks in areas accessible to the domestic fleet were completely depleted (Baryshko, 2009, Pozdnyakov and Vasilenko 1994, Pyrkov et al. 2015). Out of 26 years of mackerel fishery for 13 years more than 50 thousand tonnes per year was harvested, including 9 years when the catch was more than 100 thousand mt. Commercial fishing of mackerel in the North-West Pacific Ocean by vessels under the Russian (Soviet) flag began in 1968 (Vasilenko 1990). Since the second half of the 1980s, due to a sharp decline in mackerel abundance, its commercial fishing for mackerel in the Russian EEZ has been rare. Until recently, there has been no target fishing for mackerel by Russia in the Northwest Pacific. Russian fisheries resumed fishing in 2015. In 2021, the chub mackerel catch by the Russian fleet totaled to 87 thousand mt.

2.2 Overview of scientific surveys

China has been conducting a scientific survey program using its fishery research vessel "Song Hang" in the NPFC convention area since 2021 (Ma et al., 2023). The survey is conducted during June-August, with methods of mid-trawling, acoustic and squid jigging, covering about 70 stations per year. The results indicated that Chub mackerel is one of the dominant species in the four years survey.

In Japan, monthly egg surveys have been intensively conducted off the Pacific coast of Japan in the western North Pacific since 1978 by a historical cooperative system among many national and regional fisheries research bodies (Nishijima et al., 2025a). The survey protocol can be found at

Oozeki et al. (2007). The objective of this egg survey is to monitor egg abundance of major small pelagic fish species such as Japanese sardine, Japanese anchovy, chub mackerel, etc. The survey area roughly covered the major spawning grounds of small pelagic fish off the Pacific coast, mainly inshore waters but also offshore waters related to the warm Kuroshio and cold Oyashio currents. In addition, Japan has conducted the surface trawl net surveys in summer (June to July) and autumn (September to October) to monitor abundance of ages 0 and 1 (Nishijima et al., 2025b; 2025c; Yukami et al., 2024). The summer survey has been initiated in 2001 and annually carried out, covering the waters approximately from 141.5º E to 170.0º W and from 32.0º to 45.0º N. It provides information on abundance of age 0 fish. The autumn survey was started in 2005 and has been conducted annually, covering the area approximately of 141.5º–175º E and 37.0º–50.0º N. This survey provides abundance information on ages 0 and 1.

Russia has conducted a summertime acoustic-trawl survey since 2010 that examines mid-water and upper epipelagic species including chub mackerel. This survey completes 60-80 stations per year and aims to assess changes in abundance and migration patterns. Data collected include catch and effort, catch at length, and data for ageing.

DATA

3.1 Data preparation for stock assessment model

The Technical Working Group on Chub Mackerel Stock Assessment (TWG CMSA) agreed to apply a State-space Stock Assessment Model (SAM; Nielsen and Berg, 2014) for its stock assessment (TWG CMSA, 2023). It requires age-specific input data such as catch-at-age, maturity-at-age and weigh-at-age and abundance indices. A fishing year (FY) starting from July and ending in June of the following year was applied in the stock assessment of chub mackerel. The TWG CMSA agreed for the stock assessment period to be FY1970 (CY1970/quarter 3 (Q3)) to FY2023 (CY2024/Q2) (TWG CMSA, 2024). Seven age groups of ages 0 to 5 and 6+ were defined in the stock assessment. The Members submitted their data on quarter basis and then, they were compiled for construction the input data based on the fishing year. Manabe et al. (2025) comprehended the age-specific input data.

China has collected length frequency data of commercial catch through onboard and port samplings since CY2016, and aging of the samples has been started since CY2017. Japan also collects length, weight, maturity and age data from the survey and fishery to support their stock assessment. Russian length frequency and aging data of commercial catch are available since CY2016. The length frequency data obtained through research surveys are available since CY2010.

3.2 Catch-at-age

The catch-at-age is prepared for each Member on quarterly-basis for China and Russia. Japanese catch-at-age is prepared for Eastern Japan and Western Japan due to its difference in catch, size, and season in which the border of two regions is located at Mie-Shizuoka prefectural border.

The Members provided their quarterly catch-at-length data on calendar year basis as follows:

1) China, CY2016 to CY2024/Q2 ;
2) Eastern and Western Japan, CY2014 to CY2024/Q2;
3) Russia, CY2016/Q3 to CY2024/Q2.

The Members provided their quarterly age-length key (ALK) on calendar year basis as follows:

1) China, CY2018 to CY2024/Q2;
2) Eastern and Western Japan, CY2014 to CY2024/Q2.

For the catch-at-age prior to CY2014, Japan provided fishing year-based catch-at-age data for FY1970-FY2013 from the Japanese domestic stock assessment (Yukami et al. 2024). The data contains Russian catch in FY1967-1988 however due to the difficulty of separation into two Members, the catch is incorporated as Japanese catch. For the period of CY2014-2023/Q2, the TWG CMSA has agreed to calculate catch-at-age based on the catch-at-length data and corresponding ALK data of each quarter and region, which the detailed procedures are described in Manabe et al. (2024). The ALK of Russia is substituted by the Eastern Japanese ALK due to the similarity in the area of catch.

For the period with missing catch-at-length, the procedures to supplement the data are as follows:

1) For China CY2015, use mean catch-at-length of China of CY2016-2018 for equivalent quarter;
2) For Russia CY2014-2015, use mean catch-at-length of Russia of CY2016-2018 for equivalent quarter;
3) For Russia CY2022-2023/Q2, use Eastern Japanese catch-at-length of the equivalent quarter/year.

For the period with missing ALK, Eastern Japanese ALK of the equivalent quarter/year is applied to calculate catch-at-length. The calculated catch-at-length from each quarter is converted to fishing year basis by setting the data of age incrementation as July 1st. Ages are subtracted by 1 for the first and second quarters and early caught age 0 fish in those quarters, which are calculated as age -1, are incorporated into the third quarter as age 0. The detailed procedures are described in Manabe et al. (2024, 2025).

Through the procedures described above, catch-at-age data had been prepared for the stock assessment (Figure 4a). Chub mackerel catch was historically composed mainly of fish younger than age 3. In the periods of FY1970s, FY1980s and late-FY2010s to beginning of FY2020s, the catch of fish older than age 3 was prominent. There were differences in age compositions in catch by year and by member from FY2014 to FY2023 (Fig. 6). Catches of ages 1 to 3 were prominent

in FY2014 to FY2016, respectively. In addition, dominant age classes of catch were different among China and Japan.

3.3 Weight-at-age

The Members provided their quarterly weight-at-age data on calendar year basis as follows:

1) China, CY2018 to CY2023/Q2;
2) Eastern and Western Japan, CY2014 to CY2023/Q2;
3) Russia, CY2016 to CY2022.

The TWG CMSA has agreed to calculate a single weight value for each age to convert stock number into biomass (TWG CMSA, 2024). The single weight-at-age were calculated through the following procedure, as described in Manabe et al. (2024, 2025). The proportion of catch number for each quarter is calculated for four regions: China, Eastern Japan, Western Japan, and Russia, using the following equation, where *P* is proportion of catch number, *Na,t,r* represents the catch number of age *a* at year *t*, and region *r*.

$$P_{a,t,r} = \frac{N_{a,t,r}}{\sum N_{a,t,r}} \quad (1)$$

The yearly catch number ratio for each region is then averaged between FY2014-2023 to calculate the constant ratio of catch number across the members.

$$P_{a,r} = \frac{\sum_{t=2014}^{2023} P_{a,t,r}}{10} \quad (2)$$

The weighted mean of weight *W* at age *a* at quarter *q* of year *t* is then calculated as:

$$W_{a,q,t} = P_{china} W_{a,q,t,china} + P_{japan} W_{a,q,t,japan} + P_{russia} W_{a,q,t,russia} \quad (3)$$

The quarterly weight-at-age within a single fishing year is taken an arithmetic mean to calculate the annual weight-at-age, which is used for the stock assessment.

$$W_{a,t} = \frac{\sum W_{a,q,t}}{4} \quad (4)$$

Through this procedure, annual weight-at-age were calculated for FY2014 to FY2023 (Fig. 4b). Since the weight-at-age prior to FY2014 was not reported by other members, the weight-at-age of CM in FY1970 to FY2013 was sourced from the Japanese domestic stock assessment of the Pacific stock of chub mackerel. Historical weight-at-age showed time-varying attributes and decreased obviously in last decade in age groups older than age 0.

3.4 Maturity-at-age

The TWG CMSA has agreed to use the annual maturity-at-age data from Japanese domestic stock assessment (TWG CMSA, 2024) (Fig. 4c). The Japanese maturity-at-age data is derived from the observation of catch from the spawning area, and based on previous studies (Watanabe and Yatsu, 2006; Watanabe, 2010). Chinese maturity-at-age data submitted on a quarterly basis were not included in the base-case maturity-at-age however the alternative maturity-at-age data are prepared

for the sensitivity analysis, which the data preparation and data are described in NPFC-2024-TWG CMSA9-WP02.

Annual maturity-at-age used for base case showed decadal time-varying changes from FY1970 to FY2023 (Fig. 4c). The maturity rate of age 2 and 3 fish is expected to be lower after FY2015 than in the period before FY2014, due to the slow growth of the 2013-year class. In the recent years, maturity rate of age 2 is zero, and that of age 3 is 0.3 in the Japanese national waters.

3.5 Natural mortality

Initially the assessment investigated set two cases of natural mortality (TWG CMSA, 2024). One is M = 0.5 for all age classes while the other is age-specific M (0.80 for age 0, 0.60 for age 1, 0.51 for age 2, 0.46 for age 3,0.43 for age 4, 0.41 for age 5, and 0.40 for age 6+) (Fig. 7). These natural mortality coefficients have been determined according to different natural mortality estimators with biological parameters from various samples (Nishijima et al., 2021). It is assumed that the natural mortalities are time-invariant throughout all years. The TWG CMSA agreed to use the age specific natural mortality estimates for all models at its 9th meeting.

3.6 Abundance indices

The inventory of abundance indices time series shown in Fig. 4d was as follows.

1) Relative number of age 0 fish from the summer survey by Japan from FY2002 to FY2024 (Nishijima et al., 2025a (NPFC-2025-TWG CMSA10-WP08))
2) Relative number of age 0 fish from the autumn survey by Japan from FY2005 to FY 2024 (Higashiguchi et al., 2025 (NPFC-2025-TWG CMSA10-WP05))
3) Relative number of age 1 fish from the autumn survey by Japan from FY2005 to FY 2024 (Higashiguchi et al., 2025 (NPFC-2025-TWG CMSA10-WP05))
4) Relative spawning stock biomass (SSB) from the egg survey by Japan from FY2005 to FY2024 (Nishijima et al., 2025b (NPFC-2024-TWG CMSA10-WP07 (Rev.1)))
5) Relative SSB from the dip-net fishery by Japan from FY2003 to FY2024 (Nishijima et al. 2025c (NPFC-2025-TWG CMSA10-WP06))
6) Relative vulnerable stock biomass from the light purse seine fishery by China from FY2014 to FY2022 (Shi et al., 2025 (NPFC-2025-TWG CMSA10-WP09))
7) Relative vulnerable stock biomass from the trawl fishery by Russia from FY2016 to FY2024 (Chernienko and Chernienko, 2025 (NPFC-2025-TWG CMSA11-WP15))

The seven time series were used during model development and applied for the base case. The abundance indices from Japan and Russia were available until FY2024 and until FY2023 for China.

SPECIFICATION OF STOCK ASSESSMENT

4.1 State-space Stock Assessment Model (SAM)

SAM is a statistical catch-at-age model that accounts for observation errors in catch at age, which was originally developed by Nielsen and Berg (2014). Furthermore, in order to match the nature of data of this stock, improvements have been made to allow more flexible settings (Nishijima and Ichinokawa, 2023), and this assessment used the modified version. The detailed settings are described as follows. SAM consists of two subparts: population dynamics model and observation model.

4.1.1 Population dynamics model

The population dynamics of chub mackerel in SAM basically follows an age-structured model:

$$\log\left(N_{0,y}\right) = \log\left[f\left(SSB_y\right)\right] + \eta_{0,y}, \qquad a = 0 \qquad (5)$$

$$\log\left(N_{a,y}\right) = \log\left(N_{a-1,y-1}\right) - F_{a-1,y-1} - M_{a-1,y-1} + \eta_{a,y}, \qquad 1 \le a \le 5 \qquad (6)$$

$$\log\left(N_{6+,y}\right) = \log\left(N_{5,y-1}e^{-F_{5,y-1}-M_{5,y-1}} + N_{6+,y-1}e^{-F_{6+,y-1}-M_{6+,y-1}}\right) + \eta_{6+,y}\,, \qquad a = 6+ \qquad (7)$$

where $\eta_{a,y}$ is the process error at age a in year y following $\eta_{a,y} \sim N(0, \omega_a^2)$. The recruitment of chub mackerel occurs at age 0, described by a function of SSB and process errors (Eqn. 1). We use a Beverton-Holt stock-recruitment relationship (Beverton and Holt, 1957):

$$f\left(SSB_y\right) = \frac{\alpha \times SSB_y}{1 + \beta \times SSB_y}, \qquad (8)$$

where SSB_y is the sum-product of number (N), weight (w), and maturity (g) at age:

$$SSB_y = \sum_{a=0}^{6+} g_{a,y} w_{a,y} N_{a,y}\,. \qquad (9)$$

For fish older than age 0, the number of each cohort decreases by fishing mortality coefficient ($F_{a,y}$) and natural mortality coefficient ($M_{a,y}$) from the previous year and also be affected by process errors $\eta_{a,y}$ (Eqn. 2). For the plus-age group (6+), the number is described as the sum of surviving numbers of age 5 and age 6+ from the previous year (Eqn. 3).

In SAM, fishing mortality coefficients are assumed to follow a multivariate random walk:

$$\log\left(\boldsymbol{F_y}\right) = \log\left(\boldsymbol{F_{y-1}}\right) + \boldsymbol{\xi}_y\,, \qquad (10)$$

where $\boldsymbol{F_y} = (F_{1,y}, \ldots, F_{A+,y})^T$, $\boldsymbol{\xi_y} \sim \mathrm{MVN}(0, \boldsymbol{\Sigma})$, and $\boldsymbol{\Sigma}$ is the variance-covariance matrix of multivariate normal distribution (MVN). The diagonal elements of matrix $\boldsymbol{\Sigma}$ were σ_a^2, while off-diagonal elements represent covariance of F process errors between age classes. This assumption of F random walk allows us to estimate time-varying selectivity (Nielsen and Berg 2014). For the covariance of MVN, we assume that the correlation coefficient of F between ages a and a' decreases

along with their age differences: $\rho^{|a-a'|}\sigma_a\sigma_{a'}$ ($a \neq a$').

4.1.2 Observation model

SAM is fitted to the data of catch-at-age and abundance indices. SAM uses the Baranov equation for estimates in catch-at-age:

$$\hat{C}_{a,y} = \frac{F_{a,y}}{F_{a,y} + M_{a,y}}\left(1 - \exp\left(-F_{a,y} - M_{a,y}\right)\right)N_{a,y} . \quad (11)$$

In this equation, $F_{a,y}$ and $\underline{N_{a,y}}$ are estimated parameters by random effects, while $\underline{M_{a,y}}$ is the natural mortality coefficient. That is, the predicted catch at age in number ($\hat{C}_{a,y}$) is a derived parameter. SAM then fit to observed catch-at-age in a lognormal assumption:

$$\log\left(C_{a,y}\right) = \log\left(\hat{C}_{a,y}\right) + \varepsilon_{a,y} , \quad (12)$$

where $\varepsilon_{a,y} \sim \mathrm{N}(0, \tau_a^2)$.

We have agreed to use seven abundance indices (Fig. 5d) which represent, respectively,

1. Relative number of age 0 fish from the summer survey by Japan,
2. Relative number of age 0 fish from the autumn survey by Japan,
3. Relative number of age 1 fish from the autumn survey by Japan,
4. Relative spawning stock biomass (SSB) from the egg survey by Japan,
5. Relative SSB from the dip-net fishery by Japan,
6. Relative vulnerable stock biomass to Chinese fleet from the light purse-seine fishery by China, and
7. Relative vulnerable stock biomass from the trawl fishery by Russia.

The predicted values of these abundance indices can be expressed in the following general equation:

$$\hat{I}_{k,y} = q_k \left[\sum_{a=0}^{6+}\left(\chi_{a,y,k}N_{a,y}\right)\right]^{b_k} . \quad (13)$$

The subscripts *k*, *y*, *a* represent index, year, and age, respectively. q_k and b_k are the proportionality constant and the nonlinear coefficient, respectively, for index *k*. Note that this equation does not mean that all the abundance indices are all nonlinear against abundance but includes a linear case (b_k =1). The parameter $\chi_{a,y,k}$ is a multiplier on the number of fish in age *a* and year *y* ($N_{a,y}$) for index *k*. For the abundance indices for age 0 fish number (*k*=1,2),

$$\chi_{a,y,k} = \begin{cases} 1, & a = 0 \\ 0, & \text{otherwise} \end{cases} . \quad (14)$$

For the abundance index for age 1 fish number (*k*=3),

$$\chi_{a,y,k} = \begin{cases} 1, & a = 1 \\ 0, & \text{otherwise} \end{cases} . \quad (15)$$

For the abundance indices for SSB (*k*=4,5),

$$\chi_{a,y,k} = g_{a,y} w_{a,y} . \quad (16)$$

The abundance indices for vulnerable stock biomass to Chinese and Russian fleets (k=6,7) would represent a part of the stock for each fleet or each member's fishery. For the abundance indices for vulnerable stock biomass (k=6,7), therefore,

$$\chi_{a,y,k} = \hat{s}_{a,y,k} w_{a,y,k} , \quad (17)$$

where $\hat{s}_{a,y,k}$ is the estimated fishery selectivity in age a and year y for index (or fleet) k. We cannot estimate fleet-specific F in the current setting of SAM or, therefore, derive fleet-specific predicted catch at age (see Eqn. 14). Since the fleet-specific catch-at-age data is available (Fig. 5a), however, we can approximate the fleet-specific F as follows:

$$F_{a,y,k} \fallingdotseq \frac{C_{a,y,k}}{\sum_f C_{a,y,f}} F_{a,y} , \quad (18)$$

where $C_{a,y,k}$ are the observed catch number in age a and year y for fleet k. This approximation assumes that the fleet-specific F is proportional to fleet-specific "observed" catch at age in number. We then obtain the fleet-specific selectivity:

$$\hat{s}_{a,y,k} = \frac{F_{a,y,k}}{\mathrm{E}[\boldsymbol{F}_{y,k}]} , \quad (19)$$

where $\boldsymbol{F}_{y,k} = (F_{0,y,k}, F_{1,y,k}, \ldots, F_{6+,y,k})^{T}$. It is important to note that $\chi_{k,a,y}$ for k=6 include the estimated parameters ($F_{a,y,k}$), whereas $\chi_{k,a,y}$ for k=1-5 are provided from input data. We used the ratios of catch numbers of China and Russia to the total catch numbers as input data to fit the CPUEs of Chinese light purse seine fishery and Russian trawl fishery. In calculating the vulnerable biomass, fleet- and age- specific weight ($w_{a,y,k}$ in Eqn. 12) is needed. However, since there are no agreed data of fleet- and age- specific weights in fishing year, we took a simpler approach to using the stock weights for biomass calculation: $w_{a,y,k} = w_{a,y}$ (Fig. 4b).

The list of fixed-effect and random-effect parameters is shown in Table 1. The parameters are estimated to maximize the marginal likelihood of summing process-error components and observation error components. The marginal likelihood is computed by the numerical integration using the Laplace approximation via Template Model Builder (TMB: Kristensen et al., 2016). We applied a generic bias-correction estimator for derived quantities calculated as a nonlinear function of random effects (e.g., $N_{a,y}$ is a derived quantity calculated from the random effect of $\log(N_{a,y})$), which is implemented in TMB (Thorson and Kristensen, 2016). Estimation uncertainties including standard errors (SEs) and confidence intervals were computed from the delta method in TMB. In this stock of chub mackerel, the period from July to the following June is treated as a fishing year (NPFC-2025-TWG CMSA09-WP01), and the estimated abundance is that at the beginning of the fishing year (i.e., July).

4.2 Model selection

SAM estimates age-specific process errors for F and N and age-specific observation error for C (σ_a, ω_a and τ_a, respectively: Table 1). Estimating these errors for all ages without any restriction may cause the failure to converge and/or over-parameterization. Estimating the nonlinearity parameters (b_k) for all of the abundance indices also may lead to the same problem. Because some abundance indices might respond linearly to the stock abundance, absence of the nonlinearity parameter of the abundance indices can lead to overestimation or underestimation of resources (Nishijima et al., 2019; Rose and Kulka, 1999). However, at the same time, estimation of nonlinear parameters for indices that actually react linearly to the abundance dynamics might cause overparameterization or even non-convergent estimation.

To address these problems, we conducted a series of model selections. We first focused on the optimization of the settings of the observation and process errors, fixing the relationship of the abundance dynamics and the abundance indices linear (b_k = 1). We introduced restrictions to these errors: For example, the process error for F can be restricted to be identical among ages 0–2 and among ages 3–6+. Because there are huge number of the restriction pattern, we applied a stepwise approach, rather than trying all the possible restriction patterns. We started from the simplest model in which σ_a, ω_a and τ_a were common among all age classes. We assume that the seven abundance indices have different SDs of the measurement errors even in the simplest model because each abundance index is derived from different sources and/or age classes. Then we chose the best between-age breakpoints at which the values of σ_a, ω_a and τ_a changed based on AIC. In this step, one breakpoint was set to each of σ_a, ω_a and τ_a. This process was iterated until no further reduction in AIC was observed. Exceptionally, the N process error (ω_a) breakpoints were not placed between ages 2 and 3 in order to avoid setting independent process errors for each of them. This is because the maturities for ages 2 and 3 have declined to 0 and 0.3, respectively, after 2015 and we suspect that the SSB index does not have sufficient recent information corresponding to these ages.

In the second step, we consider which nonlinear coefficients of abundance indices should be estimated. We classified the seven abundance indices into five categories:

1. Trawl surveys by Japan (summer for age 0 and autumn for ages 0 and 1)
2. Egg survey for SSB by Japan
3. Dipnet fishery CPUE for SSB by Japan
4. Light purse-seine fishery CPUE by China
5. Trawl fishery CPUE by Russia.

We analyzed 32 (= 2^5) cases of all combinations in which the nonlinear coefficients of abundance indices in each category were either estimated or fixed at 1, with the selected restrictions of the errors above. We filtered out models without convergence, models that did not output SE due to non-positive definite of Hessian matrix, or models having very large SE of any of the fixed-effect

parameters (>10). Among models meeting these criteria, the simplest model with ΔAIC < 2.0 was selected.

4.3 Agreed base case scenario

In this assessment, we consider two scenarios as candidates for the base case analysis. The difference between these two base case scenarios is exclusion or inclusion of the latest abundance indices. The first scenario, namely S01-InitBase, excludes the six abundance indices in 2024 (Note that Chinese light purse-seine fishery CPUE has no 2024 data). The other scenario, S02-Index24_1, includes the 2024 indices. Because SAM requires biological parameters (weight at age and maturity at age) in 2024 and the proportion of Russian catch number in 2024 to estimate the 2024 population status, we assume they are the averages of themselves over 2016–2023 and 2021–2023, respectively. The sensitivity analysis for these settings confirmed that the assumption has a minor effect on the stock assessment results (NPFC-2025-TWG CMSA11-WP07).

The TWG CMSA based this year's stock assessment on the previous assessment and included the following scenarios as candidate base cases:

- **S01-InitBase.** This scenario is based on the TWG CMSA 09 base case (S28-Proc Est), which excluded the latest abundance indices. Therefore, the abundance indices up to FY2023 were used as input in this scenario (FY2024 indices were excluded).

- **S02-Index24_1.** This scenario included the FY2024 abundance indices from Japanese and Russian fisheries and Japanese surveys. The weight and maturity at age for FY2024 were assumed to be their averages throughout FY2016–FY2023. The proportion of Russian catch out of the total catch was assumed to be its average over FY2021–FY2023. Although the catch in FY2024 is not available, stock status at the beginning of FY2024 can be calculated because stock status is determined before exploitation.

Seventeen other sensitivities were used to investigate the effect of alternative assumptions regarding the biological parameters in FY2024, Russian catch proportion in FY2024, nonlinearity for abundance indices, stock-recruit relationship, maturity processes and assumptions regarding process error in numbers at age.

The TWG CMSA agreed to select S02-Index24_1 as the base case scenario because it showed a smaller Mohn's rho in both the retrospective analysis and retrospective forecasting, as well as better performance in hindcasting cross-validation compared with S01-InitBase (Nakayama et a. 2025, Nishijima et al. 2025e). The selection also reflected the robustness of the stock assessment results

to the assumptions about the FY2024 biological and catch composition data (, Nishijima et al. 2025e).

4.4 Model diagnostics

For the selected base case models, we applied several model diagnostics to check the reliability from a statistical point of view. Firstly, we performed a jitter analysis in which the initial values of the parameters were varied and re-estimated to confirm that the estimated parameters reach the global optimum. We checked whether the final gradients of the fixed effect parameters are close to zero, which is a necessary condition for model convergence.

We then plotted residuals in the catch number by age and in abundance indices to examine whether the residuals have temporal patterns. We also examined residuals in process errors for numbers by age ($\eta_{a,y}$ in Eqns. 1-3) and F by age (diagonal components of ξ_y in Eqn. 6). to show the stock abundance historically changed by these process errors. To visualize the effect of the process errors for numbers by age on the biomass-at-age, we plotted the deviances between the biomass-at-age estimated with the process error and the biomass-at-age expected with *no* process error. The deviances were calculated by $\widehat{N}_{a,y} \times \omega_{a,y} \times \left[\exp\left(\hat{\eta}_{a,y}\right) - 1\right]$. Furthermore, we performed one-step-ahead (OSA) projections using the parameters estimated with full data and visualized the residuals between observation and projection to check whether there are temporal patterns in the OSA residuals in catch-at-age and the abundance indices.

A five-year retrospective analysis was performed to examine if the estimates had systematic bias for the removal (updating) of data. Mohn's rho was calculated for total biomass, SSB, recruitment, and mean F. We also performed a retrospective forecasting, which excludes the stock index values and catch number by age from the latest year and compares the results of a one-year-ahead forecasting from the terminal year of those data (in which age-specific weight and maturity rates were used) with estimates from the model using all data. We fixed the nonlinear coefficients (b_k) at the estimates with the full data in the retrospective analysis.

The leave-one-out (LOO) index analysis was next conducted by excluding the seven abundance indices one by one and comparing the estimates with the results obtained when all indices were used. This analysis allows us to examine the impact of each index on abundance estimates and check their robustness.

To evaluate whether the parameters converged to the maximum likelihood estimate (MLE) and the uncertainty of the estimate, we lastly examined the log-likelihood when the parameters were varied around the estimate. The parameters profiled are those related to the stock-recruitment relationship and proportionality constants for the abundance indices. For the indices for which nonlinear coefficients were estimated, the likelihood profile was obtained by fixing the nonlinear coefficients to the estimated values, because it was shown that the likelihood did not change much if the value of the proportionality constant was changed, and it was unclear whether the index had sufficient information on stock abundance. We also change the value of natural mortality coefficient (M), given as input data, and its effects on the likelihood and abundance estimates.

4.5 Setting and equations for biological reference points and future projections

The population dynamics model for stochastic future projections is the same as is used in SAM. Future projections were conducted assuming a constant catch a fixed amount (ranging from 0 to 200 thousand mt in increments of 10 thousand mt) each year from FY2026 to FY2036. Constant F projections were also conducted under Fcur and Constant-F scenarios where the catch was calculated by a fixed fishing mortality (ranging from F30%SPR to F70%SPR in increments of 5%SPR) each year since FY2026. For all scenarios the catch in FY2024 and FY2025 is based on the assumption that the fishing mortality in FY2024 and FY2025 would be the same as the FY2023 fishing mortality estimated by SAM.

Two assumptions regarding biological parameters were used for the calculation of reference points, one where the future biological parameters are assumed to equal the average of the recent eight (FY 2016–FY2023) years, and another where the mean biological parameters for the entire model time period (FY1970–FY2023) are used to calculate the reference points. The TWG CMSA recommends the use of the recent average based on the assumption that the prevailing conditions will likely persist for the near future.

4.5.1 Reference points

F-based reference points

The TWG CMSA calculated these reference points along with commonly used biological reference points such as F%SPR (30%, 40%, 50%, 60% and 70%), F0.1, with mean biological parameters and selectivity of the current fishing mortality (F_{cur}, average in FY2021 to FY2023). In particular, the biological parameters such as weight-at-age and maturity-at-age used for calculation of biological reference points are assumed as the average values during the most recent 8 years (FY2016 to FY2023), which represents the recent shift in biological parameters. As a comparable, the average of the biological parameters over the stock assessment period is used for the calculation

of these reference points.

B-based reference points

While the F-based reference points are relatively robust to the time-varying biological parameters, commonly used B-based reference points such as SSB_{MSY} and SSB0 are found to be significantly affected by the changes of biological parameters in this stock as well as by the assumptions of stock recruitment relationships and model configurations. Owing to the uncertainty, the TWG CMSA explored some empirical reference points based on percentiles of historical SSB in FY1970–FY2023. The 25th percentile of SSB could be regarded as the limit, being above the SSB levels when the stock has been severely depleted during the 1990's and early 2000's. The remaining two reference points ($SSB_{REFERENCE\_A}$ and $SSB_{REFERENCE\_B}$) are the 50th and 70th percentiles of historical estimated SSB.

Although these levels of SSB are significantly lower than the theoretically calculated SSB_{MSY} under the assumption of Beverton-Holt type SR relationship without considering the time-varying nature of biological parameters, the two SSB reference points are about 20% of $SSB_{F=0\_RECENT}$ and about 40% of $SSB_{F=0\_RECENT}$, respectively, which is calculated as the multiplier between average lifetime contribution to the spawning stock biomass per fish assuming no fishing (SPR0) and average number of recruitment during the most recent 8 years. The quantity roughly approximates the level of SSB that could have been attained on average over the last decade if there had been no fishing.

4.5.2 Equations for calculating and population dynamics in future projection

The population dynamics model for future projections is the same as that used in SAM. The calculation was conducted by an R package named *frasyr* (https://github.com/ichimomo/frasyr), which has been developed for the stock assessment of Japanese domestic fisheries resources. In particular, we used the functions for future projection and the calculation of biological reference points in *frasyr*. The general equations of the forward calculation of the population dynamics are

$$N_{a,y}^{i} = \begin{cases} \dfrac{\hat{\alpha} SSB_y^i}{1+\hat{\beta} SSB_y^i} \exp\left(\eta_{0,y}^i\right) \ \ (a=0) \\ N_{a-1,y-1}^i \exp\left(-M_{a-1} - F_{a-1,y-1}^i\right) \exp\left(\eta_{a,y}^i\right) \ (0<a<6) \\ N_{a-1,y-1}^i \exp\left(-M_{a-1} - F_{a-1,y-1}^i\right) \exp\left(\eta_{a,y}^i\right) + N_{a,y}^i \exp\left(-M_a - F_{a,y}^i\right) \exp\left(\eta_{a,y}^i\right) \ \ (a=6+) \end{cases} \tag{24}$$

where $\hat{\alpha}$ and $\hat{\beta}$ are stock recruitment parameters estimated by SAM, $N_{a,y}^i$ is the number of fish in year y and age a at ith iteration, $F_{a,y}^i$ is fishing mortality coefficient in year y and age a at ith iteration, $\eta_{a,y}^i \sim N(0, \hat{\omega}^2)$ where $\hat{\omega}^2$ is the variance of process error at recruitment estimated by SAM, and SSB_y^i is SSB defined as $\sum_{a=0}^{6} N_{a,y}^i w_{a,y} g_{a,y}$. The equations are generally

applied from the end year of the stock assessment period with the initial conditions of $N^i_{a,2024} = \widehat{N}_{a,2024}$ in the base case scenario S02-Index24_1, where $\widehat{N}_{a,y}$ is the point estimates by SAM. Before management measures are implemented in 2026, we assumed that the fishing mortality in FY2024 and FY2025 would be the same as the 2023 fishing mortality estimated by SAM. If we were to assume the average fishing mortality for FY2021–2023 (F_{CUR}) during this period, the projected catch in the FY2024 would exceed 200,000 tons, which is unrealistically high considering current fishing situation. The fishing mortality in FY2023 was lower than in FY2021–2022, and using F2023 results in projected catches for FY2024–2025 that are similar to FY2023 (170,000 –180,000 tons), so we adopted this assumption. The future biological parameters of w_a and m_a are the averages of the most recent 8 years.

Two types of future harvesting methods were considered: constant-catch scenarios and constant-F scenarios. In the constant-catch scenarios, a total catch (*CC*) was predetermined ranging from 0 to 200,000 tons. Catch number at age $C^i_{y,a}$ in year *y* and age *a* is calculated with the Baranov catch equation

$$C^i_{y,a} = \frac{F^i_{y,a}}{F^i_{y,a} + M_a}\left(1 - \exp\left(-F^i_{y,a} - M_a\right)\right)N^i_{y,a}\,, \tag{25}$$

where $F^i_{y,a}$ is equal to x^i_yFcur with the same selectivity as Fcur and adjustment factor of x^i_y that is determined to satisfy the equation of $\sum_{a=0}^{6+} w_a C^i_{y,a} = CC$. If we cannot find x^i_y to satisfy the equation because of too small number of fishes, we took the smaller of the two numbers, $x_i = \exp(10)$ or fishing mortality corresponding to 99% of total catches when $x_i = \exp(100)$.

In the constant-F scenarios, we examined F ranging from F30%SPR to F70%SPR in 5% increments. In the Baranov equation above, $F^i_{y,a}$ was set as xF_{CUR}, where *x* used the values obtained when calculating the biological reference points. The constant-catch and constant-F scenarios were initiated in FY2026, and population dynamics were projected through to 2036, ten years later. We also conducted a future scenario in which the stock is exploited with current F since FY2026 to inform the current fishing impact on the stock in the future. The stochastic simulations were conducted 3,000 times for each model and scenario.

STOCK ASSESSMENT RESULTS

5.1 Base case model results

The TWG CMSA based this year's stock assessment on the previous assessment and included the following scenarios as base cases:

- **S01-InitBase.** This scenario is based on the TWG CMSA 09 base case (S28-Proc Est),

which excluded the latest abundance indices. Therefore, the abundance indices up to FY2023 were used as input in this scenario (FY2024 indices were excluded).

- **S02-Index24_1.** This scenario included the FY2024 abundance indices from Japanese and Russian fisheries and Japanese surveys. The weight and maturity at age for FY2024 were assumed to be their averages throughout FY2016–FY2023. The proportion of Russian catch out of the total catch was assumed to be its average over FY2021–FY2023.

For both scenarios the model estimates the nonlinear coefficients only for the three trawl surveys by Japan which was identified by the lowest AIC in S01-InitBase and obtained the second lowest AIC in S02-Index24_1, the difference of AIC under this setting and the lowest AIC was only 0.48 and this was the simplest setting among those with ΔAIC < 2.0.

The chub mackerel stock in the NWPO has experienced large changes in biological parameters over the time period of the model. The main temporal changes are a recent decrease in maturity at age, along with a recent decrease in the weight at age, both of which were observed to change over the model time period to cause temporal changes of biological reference points. Fixed Effects parameter estimates are shown in Table 2, and the management related quantities are listed in Table 3.

5.1.1 Parameter estimates

The estimated fixed effects parameters for the base-case scenario (S02-Index24_1) are shown in Table 2. For all parameters, the final gradient values were very close to 0 and the SE values were less than 2.5. We found no problems in jitter analysis (results not shown). Correlation coefficients from the covariance matrices of the fixed effects parameters showed that q_k and b_k for age-0 and age-1 fish in the Japanese trawl surveys were highly negatively correlated (Fig. 8). In addition, the parameters α and β of the Beverton-Holt stock-recruitment relationship were highly positively correlated. However, since β is a function of α, this is to be expected (Beverton & Holt 1957). These strong correlations between α and β are explained by the scales of abundance and SSB (for details, see Discussion in TWG CMSA 2025), and there were no problems with model convergence, as indicated by the absolute values of the final gradients approaching zero and sufficiently small SEs for these parameters (Table 2). The nonlinear coefficients in the Japanese trawl survey indices were estimated in the range of 1.7−2.4 (Table 2), suggesting that they have a tendency of hyperdepletion (Fig. 9).

5.1.2 Time-series estimates for abundances and fishing impacts

The two scenarios obtained almost identical population dynamics. Since 1970, total biomass, SSB, and recruitment of chub mackerel have drastically fluctuated (Table 4, Fig.10). Specifically, stock levels were historically high in the 1970s, but declined in the 1980s, were maintained at fairly low levels from the 1990s to the early 2000s; stock levels gradually recovered in the late 2000s and

increased rapidly after the occurrence of the strong year class in 2013. However, after peaking in 2018, the stock levels rapidly dropped again. In 2023, the spawning stock biomass was only 16% of the respective peak levels. Neither of the peaks in 2017 in 2018 reached the stock levels observed in the 1970s. In addition, the spawning stock biomass in 2024 further declined from 2023, to 14% of the peak in 2018. Exploitation rate (estimated catch biomass / total biomass) and mean F remained constant, with some fluctuations, until the 2000s, but decreased thereafter (Fig. 10).

5.1.3 Stock-recruitment relationship

The estimated Beverton-Holt stock-recruitment relationship is shown in Fig. 11 for the final base case (S02-Index24_1). The estimated stock-recruitment relationships were slightly convex, suggesting that the density-dependent effect in the stock-recruitment relationship is not strong in the chub mackerel population dynamics. The SD of recruitment variability was 0.78 in S02-Index24_1 (Table 2).

5.2 Model diagnostics

5.2.1 Residual plots

In this assessment, the predicted catch and the observed catch do not match because of the assumption of observation error in the age-specific catch numbers, but the difference between these values was small, except in some years (Fig. 12). Observation errors for catch-at-age were larger in the young and old age (ages 0, 1, and 6+) groups than those in the intermediate age (ages 2–5) groups which resulted in larger estimates of expected catch than the observed catches (Figs. 12 and 13). The time-series trend of the residuals was weak.

For the abundance indices, observation error was notably high in the Russian trawl fishery CPUE (Figs. 14 &15). The summer age-0, and autumn age-1 indices tended to have positive residuals in recent years, except for the 2023 autumn (Figs. 14 & 15).

The process errors in log(*N*) for age-0 fish fluctuated strongly, and those for age 1 and 2 fish fluctuated moderately, compared to those for older ages (Fig. 16, top, and Fig. 17). The recruitment residual has been positive after 2020. In addition, the first seven years from 1971 had positive recruitment residuals (except 1974), but for the next 13 years through 1990, the residuals were negative in all years except 1985. A large positive process error was observed in age 2 in 2015, resulting in a large positive deviance in the same year and age (Fig. 17).

Process errors for log(*F*) (deviation from random walk) were larger in ages 0 and 1 than in the other

ages (Fig. 17, bottom). The pattern of random walks for each age was very similar, as evidenced by the very high correlation coefficient of 0.98 between the closely adjacent ages (Tables 5 and 6).

5.2.2 Retrospective analysis

In the retrospective analysis, the biomass and recruitment tended to be revised downward as the data were updated and as a result, F shows negative retrospective pattens in the base-case scenario S02-Index24_1 (Fig. 18). SSB had much smaller retrospective pattern compared to biomass and recruitment.

The same tendencies, the positive retrospective patterns in the biomass, recruitment and SSB were obtained in the retrospective forecasting (Fig. 19), but the Mohn's rho values were expanded relative to those in the retrospective analyses.

5.2.3 Leave-one-out index analysis

In the LOO index analysis, although the abundance, SSB, recruitment, and exploitation rate somewhat varied in recent years depending on the index removed, the patterns observed were largely consistent, indicating that the stock estimates are robust (Fig. 20). Among the abundance indices, the absence of summer Japanese trawl survey for age 0 had relatively large effect on the recruitment. This is natural because this index was slightly inconsistent with the autumn Japanese trawl survey index for age 0 (e.g., 2021 year class). The absence of Japanese trawl surveys for age 0 in summer and for age 1 in autumn also led to the increase of the recent exploitation rate, presumably because of the smaller estimated recruitment.

5.2.4 Evaluation of the One Step Ahead residuals

OSA residuals were calculated for the age composition data the indices of abundance (Figs. 21 & 22). Absolute values of residuals for catch-at-age were larger between the late 1980s and the mid 2000s. In general, the catch-at-age OSA residuals tended to be small and lacked any consistent patterning. The OSA residuals from the fits to the indices of abundance showed a similar lack of patterning and did not suggest systematic model deficiencies such as underfitting or overfitting. Overall, the OSA residuals indicate no issues with the model's performance. In the one-step-ahead projection, we observed no clear temporal tendencies in the residuals for catch-at-age and the indices except that the Japanese dipnet fishery's standardized CPUE (Fig. 22). The residuals almost followed a normal distribution (Fig. 23).

5.2.5 Likelihood profiling

To evaluate whether the recruitment parameters converged to the maximum likelihood estimate

(MLE) and the uncertainty of the estimate, we examined the log-likelihood when the parameters were varied around the estimate. The negative log-likelihood had a convex shape against the parameters, with the MLE as the smallest, indicating convergence to the optimal value (Fig. 24). The dip of the negative log-likelihood of β was not as sharp as those of other parameters, suggesting a greater uncertainty in the density-dependent parameter. We also investigated likelihood profiles for proportionality constants for the seven abundance indices, indicating converged estimation of these parameters (Fig. 25).

Finally, the effect of the natural mortality coefficient (M), given as input data, was examined: the change in log likelihood was examined by adding values of -0.3 to 0.5 simultaneously from the values of M in the two scenarios. The results revealed that the negative log-likelihood monotonically decreases (i.e., the likelihood increases) as M is decreased (Fig. 26). This suggests that it is difficult to estimate M from these data inside SAM.

5.2.6 Comparison with previous assessments

Comparing the current two scenarios (S01-InitBase, S02-Index24_1) with the previous base case (S28-ProcEst, TWG CMSA 2024a), the estimated historical population dynamics were also almost consistent (Fig. 27). However, focusing on the recent population dynamics, inclusion of 2023 indices revised the biomass, SSB, and recruitment downward considerably (Fig. 28). This is presumably because all abundance indices consistently decreased in 2023 and this information was not included in the previous base case. The decrease in the 2023 indices contributed to the increase in the retrospective patten this year from last year (NPFC-2025-TWG CMSA11-WP08. Some degree of revision to stock estimates due to data updates is an essential part of the annual assessment process.

5.3 Reference points

5.3.1 Historical change in spawning potential of SPR0

SPR0 has changed annually according to the biological parameters that changed each year (Fig. 29). In particular, SPR0 decreased significantly from FY2015 onwards, reaching a minimum in 2019 and remaining low during the FY2020-2023 period. The average SPR0 for the 2020s (FY2020-2023) was 166 g in Scenario S02-Index24_1 which is about half of the SPR0 averaged for other decades.

5.3.2 Reference Points

F-based reference points

The TWG CMSA calculated these reference points along with commonly used biological reference points such as F%SPR (30%, 40%, 50%, 60% and 70%), F0.1, with mean biological parameters and selectivity of the current fishing mortality (F_{cur}, average in FY2021 to FY2023) (Table 3). In

particular, the biological parameters such as weight-at-age and maturity-at-age used for calculation of biological reference points are assumed as the average values during the most recent 8 years (FY2016 to FY2023), which represents the recent shift in biological parameters. As a comparable, the average of the biological parameters over the stock assessment period is used for the calculation of these reference points.

B-based reference points

While the F-based reference points are relatively robust to the time-varying biological parameters, commonly used B-based reference points such as SSB_{MSY} and SSB0 are found to be significantly affected by the changes of biological parameters in this stock as well as by the assumptions of stock recruitment relationships and model configurations. Owing to the uncertainty, the TWG CMSA explored some empirical reference points based on percentiles of historical SSB in FY1970–FY2023 (Fig. 24). The 25^{th} percentile of SSB could be regarded as the limit, being above the SSB levels when the stock has been severely depleted during the 1990's and early 2000's. The remaining two reference points ($SSB_{REFERENCE\_A}$ and $SSB_{REFERENCE\_B}$) are the 50^{th} and 70^{th} percentiles of historical estimated SSB (Fig. 29).

Although these levels of SSB are significantly lower than the theoretically calculated SSB_{MSY} under the assumption of Beverton-Holt type SR relationship without considering the time-varying nature of biological parameters, the two SSB reference points are about 20% of $SSB_{F=0\_RECENT}$ and about 40% of $SSB_{F=0\_RECENT}$, respectively, which is calculated as the multiplier between average lifetime contribution to the spawning stock biomass per fish assuming no fishing (SPR0) and average number of recruitment during the most recent 8 years. The quantity roughly approximates the level of SSB that could have been attained on average over the last decade if there had been no fishing (Fig. 30).

5.4 Future projections

Constant F projections were conducted under F_{cur} and Constant-F scenarios where the catch was calculated by a fixed fishing mortality (ranging from F30%SPR to F70%SPR in increments of 5%SPR) each year since FY2026 (Fig. 31). Future projections were also conducted under constant catch scenarios (i.e. a fixed amount ranging from 0 to 200 thousand mt in increments of 10 thousand mt) each year from FY2026 to FY2036 (Fig. 32). The probability that future SSB on July 1, at the beginning of the fishing year, is above $SSB_{REFERENCE\_B}$, $SSB_{REFERENCE\_A}$, and SSB_{LIMIT} (70^{th} percentile, 50^{th} percentile and 25^{th} percentile, respectively) under constant catch and fishing mortality projections for the base case scenario S02_24_Index1 are shown in Tables 5 & 6.

Two assumptions regarding biological parameters were used for the calculation of reference points, one where the future biological parameters are assumed to equal the average of the recent eight (FY

2016–FY2023) years, and another where the mean biological parameters for the entire model time period (FY1970–FY2023) are used to calculate the reference points. The TWG CMSA recommends the use of the recent average based on the assumption that the prevailing conditions will likely persist for the near future.

DISCUSSION

In this working paper, a stock assessment of Northwestern Pacific chub mackerel was conducted using SAM with existing agreed data. SSB gradually decreased from the high period in the 1970s to the 1980s, and SSB remained at a low level from the 1990s to the early 2000s; the beginning of the decreasing trend in SSB in the 1980s can be explained by a reversal from the positive recruitment residuals that often appeared until FY1977 to negative residuals that often appeared thereafter, shown in the plot for process errors (Fig. 17). High fishing mortalities were found since FY1986 thorough the 1990s, causing the extremely low levels of SSB for this time period. In the late 2000s, SSB gradually recovered as fishing pressure slowly decreased, and after the occurrence of the strong year class in FY2013. Although SSB recovered in the 2010s, it was still lower than in the late 1970s. Recent declines in the estimated biomass and recruitment trends (Fig. 10) correspond with both the CPUE (Fig. 14) series as well as a shift to lower SPR0 (Fig. 30). This may be due to the overall effect of the change in weight and maturity at age (Fig. 4).

Retrospective analysis revealed a negative pattern in fishing mortality, which was related to a small positive bias in recruitment and total biomass. These retrospective patterns are consistent with the catch history and the available data on maturity and catch at age. The LOO index analysis showed that the effect of excluding one index was small, suggesting that the age-0 and age-1 fish indices have similar information to each other and the SSB indices have similar information to each other.

For this stock, the choice of the stock-recruitment relationship is a difficult issue. In this case, we used the Beverton-Holt model, which is the simplest model and fits well with chub mackerel, but recruitment shows almost proportional relationship with SSB and the density-dependent effect is very small. Therefore, the uncertainty of the parameters related to the density dependence was large.

Estimating stock recruitment relationships in an assessment model is inherently challenging due to the complex interplay of biological and environmental factors that influence fish population dynamics. Variability in recruitment can result from factors such as fluctuating environmental conditions, changes in predator-prey interactions, and genetic diversity within the stock (Myers, 1998). Additionally, data limitations, such as insufficient time series data, measurement errors, and biases in sampling methods, further complicate the estimation process (Maunder & Deriso, 2013). These difficulties are exacerbated by the non-linear and often unpredictable nature of recruitment,

making it hard to develop reliable models that accurately capture the true dynamics of fish populations (Hilborn & Walters, 1992). From the viewpoint of stock assessment and management for chub mackerel, it will be necessary to consider how the stock-recruitment relationship should be characterized in the future.

The chub mackerel stock in the NWPO has experienced large changes in biological parameters over the time period of the model. The main temporal changes are a recent decrease in maturity at age, along with a recent decrease in the weight at age, both of which were observed to change over the model time period to cause temporal changes of biological reference points. Maximum sustainable yield (MSY)-based reference points are highly variable over the time series of the assessment because the weight- and maturity- at age of chub mackerel has varied widely which impacts the productivity of the stock. Unfished spawning biomass per recruit (SPR0) represents the theoretical equilibrium productivity per fish assuming no fishing. SPR0 has varied remarkably over time (Fig. 27).

In addition, as there is little recruitment compensation in the stock-recruitment relationship within the range of historically observed SSB and recruitment (Fig. 11), estimates of biomass-based MSY reference points are extreme explorations that are highly sensitive to model configuration.

Because of the above reasons, commonly used reference points such as MSY-related or SPR-related reference points vary over time and are uncertain, and do not take into account non-stationarity of key population dynamics parameters. are potentially misleading with respect to stock status. The TWG CMSA explored empirical biomass-based reference points based on percentiles of historical SSB in FY1970–FY2023. These empirical reference points attempt to account for the non-stationarity in key population parameters, future research on this topic is recommended.

SUMMARY

Stock status overview

Total biomass, Spawning Stock Biomass

The time series of estimated chub mackerel total biomass and SSB generally declined from the 1970s through the 1990s (Fig. 10). The stock began to recover in the early 2000s, peaking in FY2018, then SSB has declined to 16% of that peak in 2023. The spawning stock biomass in 2023 is slightly higher than SSB_{LIM} ($SSB_{2023}/SSB_{LIM}=1.23$) but lower than $SSB_{REFERENCE\_A}$ and $SSB_{REFERENCE\_B}$ (Table 3).

Recruitment

The level of recruitment in the 1970s was estimated to be high (~15 billion individuals on average)

and reached a low period between the 1990s and the 2010s (Fig. 10). Recruitment in the most recent decade (FY2014–FY2023) was also high on average (~7.4 billion), but not as high as in the 1970s and had a decreasing trend since the last peak in 2018. The estimated Beverton-Holt stock recruitment relationship was slightly concave (Fig. 11), suggesting that the density-dependent effect in recruitment is not strong.

Exploitation status

Estimated exploitation rate generally fluctuated between 10% and 35%, with over 40% and below 10% in several years, following the estimated F dynamics. No clear temporal trend was observed (Fig. 10). The current fishing mortality (F_{cur}) corresponds to 16% SPR, and higher than the commonly used F-based reference points such as F0.1 and F30–70%SPR (Table 3). Fishing mortality related reference points indicate that the stock is at approximately 16% SPR, indicating that current fishing mortality are also reported for percent FSPR values, in relation to the current F (Fcur, average FY2021–FY2023) for FSPR from the recent period (FY2016–FY2023) as well as over the entire time period (FY1970–FY2023; Table 3).

Conclusions and recommendations

The chub mackerel stock in the NWPO has experienced large changes in biological parameters over the time period of the model. The main temporal changes are a recent decrease in maturity at age, along with a recent change in the weight at age, both of which were observed to impact the model time period to cause temporal impacts on biological reference points. MSY-based reference points are highly variable over the time series of the assessment because the weight- and maturity- at age of chub mackerel have varied widely (Fig 4.), which impacts the productivity of the stock. Unfished spawning biomass per recruit (SPR0) has varied remarkably over time (Fig. 30).

Besides such uncertainty, the current fishing mortality (average FY2021–FY2023) is higher than the commonly used reference points such as F%30–60%, and SSB in FY2024 is lower than the reference levels of median and 70th percentiles ($SSB_{REFERENCE\_A}$ & $SSB_{REFERENCE\_B}$, respectively), but slightly above the SSB_{LIM}.

Harvest Recommendations

Given the uncertainty in biological parameters in future, which has a large impact on the projection results, the TWG CMSA considers it is not appropriate to provide long-term harvesting recommendations at this time. However, in response to the request from COM09, 10 year projection was undertaken to assess the effects of varying catch and F levels based on the most recent eight years' biological data (Figs. 31 & 32, Tables 7 & 9). Projections indicate that current fishing mortality is unsustainable, and probabilities of achieving various reference levels under catch-constant as well as F-constant scenarios are provided in Tables 5 & 6. It is recommended to reduce

fishing mortality to recover SSB to the reference levels.

Data and Research needs

The assessment results, including projections, are dependent on biological parameters and processes which are uncertain. Therefore, future studies should be focused on collecting and analyzing biological information, e.g., maturity-at-age and weight-at-age, which would improve the assessment. Fisheries-dependent data, such as fleet-specific catch-at-age, are also critical to develop Member-specific fishing fleet and age-specific abundance indices. It is also important to explore the factors that contributed to the lower-than-expected presence of the 2018 year class in catch-at-age data, despite strong signals in survey indices.

A critically important recommendation that should be carried out in 2-3 years is to develop a harvest control rule (HCR) specific to this stock via a Management Strategy Evaluation (MSE) process. This HCR should be dynamic and able to adjust annual total catches depending on the stock abundance as well as the target and limit reference points. During the process of the development of MSE, uncertainties in parameter estimates, time-varying or density-dependent biological parameters, stock-recruitment assumptions, process errors, and selectivity should be considered.

Timely collection of biological information and further research on biological parameters and processes, including the effect of environment and climate change, are critically important to facilitate the accurate estimation of reference points.

REREFENCES

Baryshko M.E. 2009. Fisheries of mackerel and sardine-Ivasi in the Far East. Vladivostok DGTRU. 472 c.

Beverton, R. J. H., & Holt, S. J. (1957). On the dynamics of exploited fish populations. Chapman and Hall, London, Fish and Fisheries Series No. 11, fascimile reprint 1993.

Chernienko, I. and Chernienko E. (2025). Standardized CPUE of Russian commercial trawl fishery of chub mackerel in the Northwest Pacific up to 2024. NPFC-2025-TWG CMSA11-WP05.

Higashiguchi, K., Nishijima, S., Ichinokawa, M. and Yukami, R. (2025). Standardized Abundance Indices for Ages 0 and 1 Fish of Chub Mackerel from Northwest Pacific Autumn Surveys up to 2024. NPFC-2025-TWG CMSA10-WP05.

Hilborn, R., & Walters, C. J. (1992). Quantitative Fisheries Stock Assessment: Choice, Dynamics, and Uncertainty. Springer.

Iizuka, K. (2002). Stock and fishing grounds of chub mackerel in 1960s and 1970s. *Gekkan Kaiyo*, 34, 273–279 (in Japanese).

Kasamatsu, F. & Tanaka, S., 1992. Annual changes in prey species of minke whales taken off Japan, 1948–1987. Nippon Suisan Gakkaishi (Japanese Society of Fisheries Science), 54, pp.637–651.

Kamimura, Y., Taga, M., Yukami, R., Watanabe C. and Furuichi S. (2021). Intra- and inter specific density dependence of body condition, growth, and habitat temperature in chub mackerel (*Scomber japonicus*). ICES J. Mar. Sci., 78, 3254-3264.

Kanamori, Y., Takasuka, A., Nishijima, S., and Okamura, H. (2019). Climate change shifts the spawning ground northward and extends the spawning period of chub mackerel in the western North Pacific. Marine Ecology Progress Series. 624, 155-166. https://doi.org/10.3354/meps13037

Kawabata, A., Nakagami, M., Suyama, T., Yatsu, A., Takagi, K. & Takeda, Y., 2006. [Seasonal distribution and migration of mackerel and sardine species estimated from recent large-scale research vessel surveys.] Abstracts of the 2006 Annual Meeting of the Japanese Society of Fisheries Oceanography, p.94.

Kawasaki, T., 1965. [Ecology and resources of skipjack tuna (I).] Fisheries Research Series, 8, p.148.

Kawasaki, T., 1968. [Ecology of immature chub mackerel of the Pacific stock.] Bulletin of the Tokai Regional Fisheries Research Laboratory, 55, pp.59–113.

Koizumi, M., 1992. [Observations on eggs, larvae, and juvenile chub mackerel collected around the Izu Islands.] Fisheries Oceanography, 56, pp.57–64.

Kato, M. and Watanabe, C., (2002). Maturation, spawning and feeding habitat of chub and blue mackerels. *Gekkan Kaiyo*, 34, 366–272 (in Japanese).

Kristensen, K., Nielsen, A., Berg, C. W., Skaug, H., and Bell, B. M. (2016). TMB: Automatic

differentiation and laplace approximation. Journal of Statistical Software, 70(5), 1–21. https://doi.org/10.18637/jss.v070.i05

Kuroda, K., 1992. [Trends in spawning season, spawning grounds, and spawning intensity of Scomber species along the Pacific coast of Japan.] Fisheries Oceanography, 56, pp.65–72.

Konishi, K., Isoda, T. & Tamura, T., 2016. Decadal change of feeding ecology in sei, Bryde's, and common minke whales in the offshore western North Pacific. Paper SC/F16/JR23 submitted to the JARPNII Review Workshop, Tokyo, February 2016, 19 pp

Ma, Q., Liu, B. and Dai, L. (2023) Overview surveys from 2021 to 2023 by Chinese research vessel "Song Hang" in the NPFC convention area. NPFC-2023-SC08-WP12.

Manabe, A., Higashiguchi, K., Yukami, R. and Oshima, K. (2024). The data description for the base case stock assessment of chub mackerel Scomber japonicus in the northwestern Pacific Ocean. NPFC-2024-TWG CMSA09-WP01.

Manabe, A., Mora Gazi, K. and Oshima, K. (2025). The data description for the base case stock assessment of chub mackerel *Scomber japonicus* in the northwestern Pacific Ocean for 2025 assessment. NPFC-2025-TWG CMSA11-WP03 Rev. 1.

Maunder, M. N., & Deriso, R. B. (2013). A stock–recruitment model for highly fecund species based on temporal and spatial extent of spawning. Fisheries Research, 146, 96-101.

Meguro, K., Nashida, K., Mitani, T., Nishida, H. & Kawabata, A., 2002. [Distribution and migration of chub mackerel and spotted mackerel—Adults.] Kaiyō Monthly (Ocean), 34, pp.256–260.

Murayama, T., Mitani, I., Aoki, I. (1995) Estimation of the spawning period of the Pacific mackerel Scomber japonicus based on the changes in gonad index and the ovarian histology. Bull .Jpn. Soc. Fish. Oceanogr. 59, 11-17 (in Japanese, with English abstract).

Myers, R. A. (1998). When do environment-recruitment correlations work? Reviews in Fish Biology and Fisheries, 8(3), 285-305.

Nagasawa, K., 1999. [Distribution and ecology of piscivorous fishes in the Kuroshio–Oyashio transition region.] Kaiyō Monthly (Ocean), 34, pp.245–250.

Nakayama, S., Nishijima, S., Ichinokawa, M., Manabe A., Oshima K. and Rice, J. (2025) Candidate Base Case Scenarios for the 2025 Chub Mackerel Stock Assessment in the Northwest Pacific Ocean. NPFC-2025-TWG CMSA11-WP06.

Nielsen, A., and Berg, C. W. (2014). Estimation of time-varying selectivity in stock assessments using state-space models. Fisheries Research, 158, 96–101. https://doi.org/10.1016/j.fishres.2014.01.014

Nishida, H., Kawabata, A., Meguro, K., Nashida, K. & Mitani, T., (2001). [Distribution and migration of chub mackerel and spotted mackerel—Juveniles.] Fisheries Oceanography, 65, p.201.

Nishijima, S., Kamimura, Y., Yukami, R., Manabe, A., Oshima, K., and Ichinokawa, M. (2021). Update on natural mortality estimators for chub mackerel in the Northwest Pacific Ocean.

NPFC-2021-TWG CMSA04-WP05.

Nishijima, S., Suzuki, S., Ichinokawa, M., and Okamura, H. (2019). Integrated multi-timescale modeling untangles anthropogenic, environmental, and biological effects on catchability. Canadian Journal of Fisheries and Aquatic Sciences, 76(11), 2045–2056. https://doi.org/https://doi.org/10.1139/cjfas-2018-0114.

Nishijima, S., and Ichinokawa, M. (2023). On the description and flexibility of state-space assessment model. NPFC-2023-TWG CMSA07-WP07.

Nishijima, S., Kamimura, Y., Ichinokawa, M. and Yukami, R. (2025a). Standardized abundance index for recruitment of chub mackerel from Northwest Pacific summer surveys up to 2024. NPFC-2025-TWG CMSA10-WP08.

Nishijima, S., Ichinokawa, M. and Yukami, R. (2025b). Standardizing monthly egg survey data as an abundance index for spawning stock biomass of chub mackerel in the Northwest Pacific. NPFC-2024-TWG CMSA10-WP07 (Rev.1).

Nishijima, S., Yukami, R. and Ichinokawa, M. (2025c). Standardized CPUE of Japanese commercial dip-net fishery targeting spawners of chub mackerel in the Northwest Pacific up to 2024. NPFC-2025-TWG CMSA10-WP06.

Nishijima, S., Ichinokawa M., Oshima K., and Rice, J. (2025d) Biological reference points and future projections in the 2025 stock assessment for the Northwestern Pacific chub. NPFC-2025-TWG CMSA11-WP09.

Nishijima, S., Ichinokawa M., Manabe, A., Nakayama, S., Oshima, K., and Rice, J. (2025e) Sensitivity analyses of the 2025 chub mackerel stock assessment in the Northwest Pacific Ocean. NPFC-2025-TWG CMSA11-WP07.

Oozeki, Y., A. Takasuka, H. Kubota and M. Barange (2007) Characterizing spawning habitats of Japanese sardine (*Sardinops melanostictus*), Japanese anchovy (*Engraulis japonicus*), and Pacific round herring (*Etrumeus teres*) in the northwestern Pacific. CalCOFI Reports, 48, 191-203

Pozdnyakov S. E., Vasilenko A.V. (1994). Distribution, migration routes and helminth fauna of the Japanese mackerel *Scomber japonicus* in the north-western part of the Pacific Ocean // Vopr. ichthyol. T. 34. №1, C. 22-34.

Pyrkov V.N., Solodilov A.V., Degaj A.Yu. (2015) Sozdanie i vnedrenie novyh sputnikovyh tekhnologij v sisteme monitoringa rybolovstva // Sovremennye problemy distancionnogo zondirovaniya Zemli iz kosmosa. —. — T. 12, No 5. — S. 251–262.

Rose, G., and Kulka, D. (1999). Hyperaggregation of fish and fisheries: how catch-per-unit-effort increased as the northern cod (*Gadus morhua*) declined. Canadian Journal of Fisheries and Aquatic Sciences, 56(S1), 118–127. https://doi.org/10.1139/cjfas-56-S1-118

Shi, Y., Zhang, H. and Han, H. (2025). Standardized CPUE of Chub mackerel (*Scomber japonicus*) caught by the China's lighting purse seine fishery up to 2023. NPFC-2025-TWG CMSA10-WP09.

Tamura, T., Fujise, Y. & Shimazaki, K., (1998). Diet of minke whales Balaenoptera acutorostrata in the northwestern North Pacific in summer, 1994 and 1995. Fisheries Science, 64, pp.71–76.

Tamura, T., Konishi, K. & Isoda, T., (2016). Updated estimation of prey consumption by common minke, Bryde's, and sei whales in the western North Pacific. Paper SC/F16/JR15 submitted to the JARPNII Review Workshop, Tokyo, February 2016, 58 pp.

Thorson, J. T., and Kristensen, K. (2016). Implementing a generic method for bias correction in statistical models using random effects, with spatial and population dynamics examples. Fisheries Research, 175, 66–74. https://doi.org/10.1016/j.fishres.2015.11.016

Technical Working Group on Chub Mackerel Stock Assessment (2023) 7th Meeting Report. NPFC-2023-TWG CMSA07-Final Report. 53 pp. (Available at www.npfc.int)

Technical Working Group on Chub Mackerel Stock Assessment. (2024) 8th Meeting Report. NPFC-2023-TWG CMSA08-Final Report. 32 pp. (Available at www.npfc.int)

Technical Working Group on Chub Mackerel Stock Assessment. (2025) 10th Meeting Report. NPFC-2025-TWG CMSA10-Final Report. 30 pp. (Available at www.npfc.int)

Usami, S. (1973) Ecological studies of life patter of the Japanese mackerel *Scomber japonicus* HOUTTUYN on the adult of the Pacific subpopulation. Bull. Tokai. Reg. Fish. Res. Lab., 76, 71-178 (in Japanese, with English abstract).

Vasilenko A.V. Intraspecific structure and commercial value of Japanese mackerel populations. 1990. Avtoref. diss.... candidate of biological sciences. Vladivostok, 24 p.

Watanabe, T. (1970) Morphology and ecology of early stages of life in Japanese common mackerel, *Scomber japonicus* HOUTTUYN, with special reference to fluctuation of population. Bull. Tokai. Reg. Fish. Res. Lab., 62, 1-283 (in Japanese, with English abstract).

Watanabe, C., Hanai, T., Meguro, K., Ogino, R., Kimura, R. (1999) Spawning biomass estimates of chub mackerel *Scomber japonicus* of Pacific subpopulation off central Japan by a daily egg production method. Bull. Jpn. Soc. Sci. Fish., 65(4),695-702 (in Japanese, with English abstract).

Watanabe, C. and A. Yatsu (2004) Effects of density-dependence and sea surface temperature on inter-annual variation in length-at-age of chub mackerel (*Scomber japonicus*) in the Kuroshio-Oyashio area during 1970–1997. Fish. Bull., 102, 196-206.

Watanabe, C. and A. Yatsu (2006) Long-term changes in maturity at age of chub mackerel (Scomber japonicus) in relation to population declines in the waters off northeastern Japan. Fish. Res., 78, 323-332.

Watanabe, C. (2010). Changes in the reproductive taraits of the Pacific stock of chub mackerel Scomber japonicus and their effects on the population dynamics. Bull. Jpn. Soc. Fish. Oceanogr., 76, 46-50.

Yamada, T., Aoki, I., Mitani, I. (1999) Spawning time, spawning frequency and fecundity of Japanese chub mackerel, *Scomber japonicus* in the waters around the Izu Islands, Japan. Fisheries Research., 38, 83-89.

Yukami, R., Nishijima, S., Kamimura, Y., Isu, S., Furuichi, S., Watanabe, R., Higashiguchi, K., Saito, R. and Ishikawa, K. (2024). Stock assessment and evaluation for Chub Mackerel Pacific stock (fiscal year 2023). FRA-SA2024-AC005. In Marine fisheries stock assessment and evaluation for Japanese waters (fiscal year 2023/2024). Japan Fisheries Agency and Fisheries Research and Education Agency of Japan. Tokyo, 71pp. https://abchan.fra.go.jp/wpt/wp-content/uploads/2024/03/details_2023_05.pdf

Zhang, H., Han, H., Sun, Y., Xiang, X., Li, Y. and Shi, Y. (2023) Data description on fisheries bycatch in the chub mackerel fisheries in China. NPFC-2023-TWG CMSA07-WP12 (Rev. 1). 3pp. https://www.npfc.int/system/files/2023-09/NPFC-2023-TWG%20CMSA07-WP12%28Rev%201%29%20Data%20description%20on%20fisheries%20bycatch%20in%20CM%20fisheries%20in%20China.pdf

TABLES

Table 1

The list of mathematical notations for SAM, including the symbol used, its type (Index, Data, random effects: RE, fixed effects: FE, and derived quantities: DQ, and its description).

Symbol	Type	Description
a	Index	Age class (from 0 to 6+)
y	Index	Fishing year (from 1970 to 2022)
k	Index	Fleet ID for abundance index (from 1 to 6)
$C_{a,y}$	Data	Observed catch number at age *a* in a year *y*
$w_{a,y}$	Data	Stock weight at age *a* in a year *y* (also used as catch weight for simplicity)
$g_{a,y}$	Data	Maturity at age *a* in a year *y*
$M_{a,y}$	Data	Natural mortality coefficient at age *a* in a year *y*
$N_{a,y}$	RE	Number at age *a* in a year *y*
$F_{a,y}$	RE	Fishing mortality coefficient at age *a* in a year *y*
ω_a	FE	SD for the process error in number at age *a*
σ_a	FE	SD for the process error in F at age *a*
ρ	FE	Correlation coefficient in MVN of F random walk between adjacent age classes
τ_a	FE	SD for the measurement error in catch at age *a*
q_k	FE	Catchability coefficient for abundance index *k*
v_k	FE	SD for the measurement error in abundance index *k*
b_k	FE	Nonlinear coefficient for abundance index *k*
α	FE	Slope of stock-recruitment relationship at the origin
β	FE	Strength of density dependence in stock-recruitment relationship
$\hat{C}_{a,y}$	DQ	Predicted catch number at age *a* in a year *y*
$\hat{s}_{a,y}$	DQ	Selectivity at age *a* in a year *y*

Table 2

Fixed-effect parameters (FE), their maximum likelihood estimates (MLE), their standard errors (SE), their final gradients, symbols including the information on age class and index fleet, and unlinked value (inverse link function of MLE) under Scenario S02-Index24_1.

FE	MLE	SE	Gradient	Unlinked value
logQ (JPN summer survey)	-15.6792	2.30289004	-7.62E-06	1.55E-07
logQ (JPN autumn survey age 0)	-14.504035	2.31148929	1.79E-05	5.02E-07
logQ (JPN autumn survey age 1)	-10.55497	1.60459597	1.43E-05	2.61E-05
logQ (JPN egg survey)	-0.2258006	0.12389846	8.10E-06	0.79787717
logQ (JPN dipnet)	-2.4622594	0.15433565	-1.21E-05	0.08524213
logQ (CHN purse sein)	-5.4552764	0.13437866	-3.17E-05	0.0042737
logQ (RUS trawl)	-4.1736122	0.24869381	1.02E-05	0.01539654
logB (JPN summer survey)	0.86975	0.11907331	-9.39E-05	2.3863142
logB (JPN autumn survey age 0)	0.8151345	0.12543536	0.00033094	2.25947956
logB (JPN autumn survey age 1)	0.5671192	0.12302012	0.00020807	1.76318035
logσ (age 0–1)	-0.7204778	0.18383944	-9.29E-07	0.48651976
logσ (age 2)	-1.0075574	0.19443062	-3.99E-05	0.36510972
logσ (age 3–)	-1.2833983	0.17074541	2.87E-05	0.27709406
logω (age 0)	-0.2462263	0.12565032	3.35E-05	0.78174529
logω (age 1–)	-1.1454601	0.13351863	-3.37E-05	0.31807753
logτ (age 0)	-0.254829	0.13671048	-1.85E-05	0.77504905
logτ (age 1)	-0.6482389	0.16962969	-1.94E-05	0.52296595
logτ (age 2–3)	-1.6101614	0.33527145	-2.33E-05	0.19985535
logτ (age 4–5)	-0.9270467	0.13953189	1.34E-05	0.39572066
logτ (age 6+)	-0.1216399	0.13187202	3.20E-05	0.88546719
logν (JPN summer survey)	-0.3178417	0.2609826	-1.23E-05	0.72771799
logν (JPN autumn survey age 0)	-0.4051246	0.27451485	-2.19E-05	0.66689369
logν (JPN autumn survey age 1)	-0.4699654	0.24942735	1.47E-06	0.6250239
logν (JPN egg survey)	-1.0565971	0.18352748	1.24E-05	0.34763676
logν (JPN dipnet)	-0.5338454	0.16441418	-1.07E-05	0.58634587
logν (CHN purse sein)	-1.278561	0.25989131	1.77E-06	0.27843769
logν (RUS trawl)	-0.473255	0.24889304	5.76E-06	0.62297121
logα	-4.3024831	0.19719966	-8.53E-06	0.01353491
logβ	-8.0077947	1.33589477	9.39E-08	0.00033286
logitρ	4.06929803	0.83600232	-8.99E-06	0.98319776

Table 3

Reference points for the base case scenario (S02-Index24_1). F-based reference point values that are dependent on time varying parameters are calculated by holding F_{cur} the same for all calculations, but by varying the time period (either FY2016–FY2023 or FY1970–FY2023) over which the biological parameters are estimated. Refer to Glossary in the stock assessment report for the definitions. *For the description of the biological parameters, see Table ANNEX 3.*

Reference Points	Biological parameters	
	FY2016–FY2023	FY1970–FY2023
F-based reference points		
Current%SPR	**16.2**	27.8
$F0.1/F_{cur}$	**0.838**	0.838
$FpSPR.30.SPR/F_{cur}$	**0.580**	0.911
$FpSPR.40.SPR/F_{cur}$	**0.412**	0.609
$FpSPR.50.SPR/F_{cur}$	**0.295**	0.416
$FpSPR.60.SPR/F_{cur}$	**0.207**	0.282
$FpSPR.70.SPR/F_{cur}$	**0.139**	0.184
Biomass-based reference points		
$SSB_{F=0\_RECENT}$	**1399**	–
25th Percentile Historical SSB (SSB_{LIM}) (thousand mt)	**107**	
50th Percentile Historical SSB ($SSB_{REFERENCE\_A}$) (thousand mt)	**289**	
70th Percentile Historical SSB ($SSB_{REFERENCE\_B}$) (thousand mt)	**585**	
SSB_{2023}/ SSB_{LIM}	**1.23**	
$SSB_{2023}/ SSB_{REFERENCE\_A}$	**0.46**	
$SSB_{2023}/ SSB_{REFERENCE\_B}$	**0.23**	
$SSB_{LIM} / SSB_{F=0\_RECENT}$	**0.08**	–
$SSB_{REFERENCE\_A} / SSB_{F=0\_RECENT}$	**0.21**	–
$SSB_{REFERENCE\_B} / SSB_{F=0\_RECENT}$	**0.42**	–

Table 4

Time series of estimates of total biomass, spawning stock biomass, recruitment, catch, and exploitation rate (catch/biomass) and their standard error (SE) under Scenario ScenarioS02-Index24_1. *The SEs were derived using the delta method.*

Fishing	Biomass (1000 MT)		SSB (1000 MT)		Recruitment (billion)		Catch (1000 MT)		Exploitation rate	
year	**MLE**	**SE**	**MLE**	**SE**	**MLE**	**SE**	**MLE**	**SE**	**MLE**	**SE**
1970	4326.1	744.5	733.6	94.5	19.4	7.0	883.6	129.6	0.209	0.042
1971	4924.1	795.3	911.2	121.6	22.4	7.6	896.5	111.9	0.186	0.034
1972	5227.4	931.3	757.8	107.1	9.7	3.4	699.6	101.1	0.137	0.027
1973	4524.1	675.8	986.7	132.0	8.0	2.7	808.9	95.4	0.182	0.031
1974	4214.5	573.6	1398.7	198.4	12.5	4.2	882.7	102.4	0.212	0.033
1975	3685.5	512.2	1160.8	154.7	19.4	6.5	864.8	100.1	0.238	0.038
1976	4693.4	785.8	1122.3	149.4	23.7	7.9	735.3	87.2	0.160	0.030
1977	5768.0	899.8	1257.0	158.9	18.5	6.1	990.4	128.6	0.175	0.030
1978	5928.0	855.1	1382.0	164.1	13.2	4.4	1416.4	188.6	0.242	0.038
1979	3812.0	500.0	1352.3	170.0	6.5	2.2	1096.3	134.3	0.290	0.043
1980	2301.9	308.9	1079.1	154.0	7.2	2.4	596.8	71.6	0.262	0.039
1981	2531.6	423.6	756.8	114.8	8.8	2.9	396.6	52.3	0.160	0.031
1982	2389.7	377.8	581.2	79.2	5.9	1.9	380.8	47.5	0.162	0.029
1983	1928.2	270.6	548.1	69.1	6.3	2.1	394.4	46.0	0.208	0.033
1984	2443.7	373.9	619.7	76.2	7.6	2.4	517.4	62.4	0.215	0.035
1985	2098.1	301.7	498.3	59.5	7.7	2.5	463.6	62.2	0.224	0.035
1986	1626.0	221.0	379.9	44.7	3.5	1.1	569.5	87.9	0.352	0.045
1987	974.4	117.9	330.5	36.8	1.3	0.4	362.9	48.6	0.374	0.044
1988	604.2	71.8	282.7	38.2	0.6	0.2	253.0	33.0	0.420	0.046
1989	345.4	52.2	150.5	21.1	0.5	0.2	109.6	14.2	0.321	0.051
1990	255.7	49.1	78.0	13.1	0.6	0.2	30.6	4.0	0.123	0.028
1991	359.7	81.3	62.4	10.3	1.3	0.4	26.7	3.7	0.077	0.018
1992	665.3	153.7	69.9	10.4	3.0	1.0	57.2	11.7	0.089	0.024
1993	698.9	121.1	106.5	15.4	1.0	0.3	243.5	63.4	0.349	0.064
1994	421.6	59.2	109.6	14.0	0.9	0.3	119.1	17.1	0.285	0.043
1995	402.5	64.4	90.5	11.2	1.5	0.5	116.0	19.9	0.291	0.045
1996	712.8	177.5	52.0	6.1	4.3	1.5	165.2	43.4	0.235	0.046
1997	672.7	139.6	44.5	5.0	0.7	0.2	286.1	78.8	0.422	0.061
1998	337.3	46.4	94.6	14.7	0.4	0.1	104.7	17.0	0.312	0.046
1999	313.3	58.1	89.0	12.5	1.0	0.3	74.6	11.5	0.243	0.041
2000	263.3	47.8	54.5	6.9	0.6	0.2	61.1	12.6	0.234	0.045

2001	178.7	27.6	63.0	8.9	0.4	0.1	42.7	6.9	0.242	0.046
2002	273.4	46.3	40.4	5.9	1.5	0.4	31.3	6.0	0.116	0.025
2003	357.8	58.5	55.3	6.9	1.2	0.3	61.8	12.8	0.174	0.034
2004	845.3	142.9	138.0	18.8	4.3	1.0	131.4	22.9	0.157	0.029
2005	839.5	136.2	87.8	10.3	1.5	0.3	195.8	41.0	0.234	0.040
2006	747.4	99.2	281.1	43.1	0.5	0.1	223.9	36.4	0.301	0.043
2007	684.6	87.2	266.8	37.5	2.3	0.5	153.1	19.0	0.225	0.032
2008	657.5	85.2	156.7	21.2	1.3	0.3	153.3	23.8	0.234	0.036
2009	683.9	86.0	162.9	22.0	2.2	0.4	138.7	18.6	0.204	0.032
2010	765.7	105.4	144.4	21.1	1.9	0.4	122.2	18.2	0.161	0.028
2011	879.3	123.0	199.1	30.9	1.2	0.3	100.2	13.5	0.115	0.020
2012	1160.7	159.1	295.7	43.7	3.0	0.6	130.1	15.6	0.113	0.019
2013	2474.5	398.9	334.3	49.1	11.6	2.7	209.1	30.6	0.085	0.016
2014	2267.4	362.7	364.6	53.6	3.3	0.8	237.5	37.6	0.106	0.020
2015	2684.6	409.2	257.4	43.5	4.6	0.9	318.5	46.4	0.120	0.020
2016	3107.9	411.8	457.9	77.3	8.3	1.9	358.1	45.1	0.116	0.018
2017	3127.7	394.5	799.2	145.6	9.1	2.0	403.3	49.5	0.130	0.020
2018	3900.7	558.9	800.8	133.6	16.8	4.1	495.1	58.1	0.128	0.021
2019	2869.2	374.0	694.7	121.5	5.1	1.0	410.8	49.7	0.144	0.023
2020	2439.2	300.7	549.8	93.5	7.9	1.7	476.4	53.2	0.196	0.029
2021	2087.1	293.9	391.1	66.7	8.7	2.0	415.9	49.6	0.201	0.032
2022	1772.1	265.2	250.9	45.5	7.0	1.6	278.3	37.6	0.159	0.029
2023	1375.3	231.3	131.6	28.0	3.4	0.9	172.9	23.4	0.127	0.026
2024	1220.9	233	111.5	27.2	3.6	0.9	NA	NA	NA	NA

Table 5

Probability that future SSB on July 1, at the beginning of the fishing year, is above $SSB_{REFERENCE\_B}$, $SSB_{REFERENCE\_A}$, and SSB_{LIMIT} (70^{th} percentile, 50^{th} percentile and 25^{th} percentile, respectively) under constant catch projections for the base case scenario. The projection towards FY2036 is shown below.

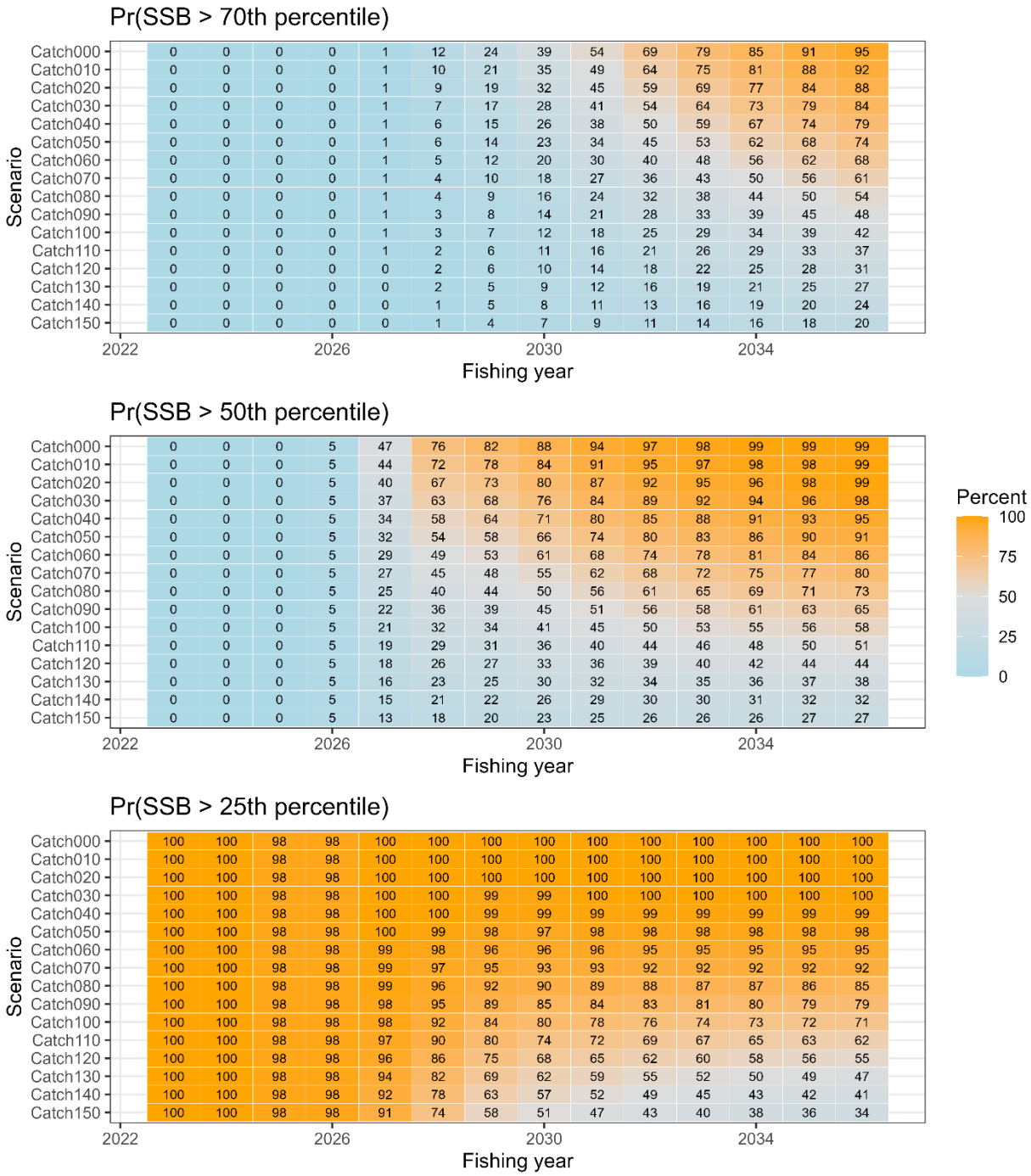

Table 6

Probability that future SSB on July 1, at the beginning of the fishing year, is above $SSB_{REFERENCE\_B}$, $SSB_{REFERENCE\_A}$, and SSB_{LIMIT} (70^{th} percentile, 50^{th} percentile and 25^{th} percentile, respectively) under constant fishing mortality projections for the base case scenario. The projection towards FY2036 is shown below.

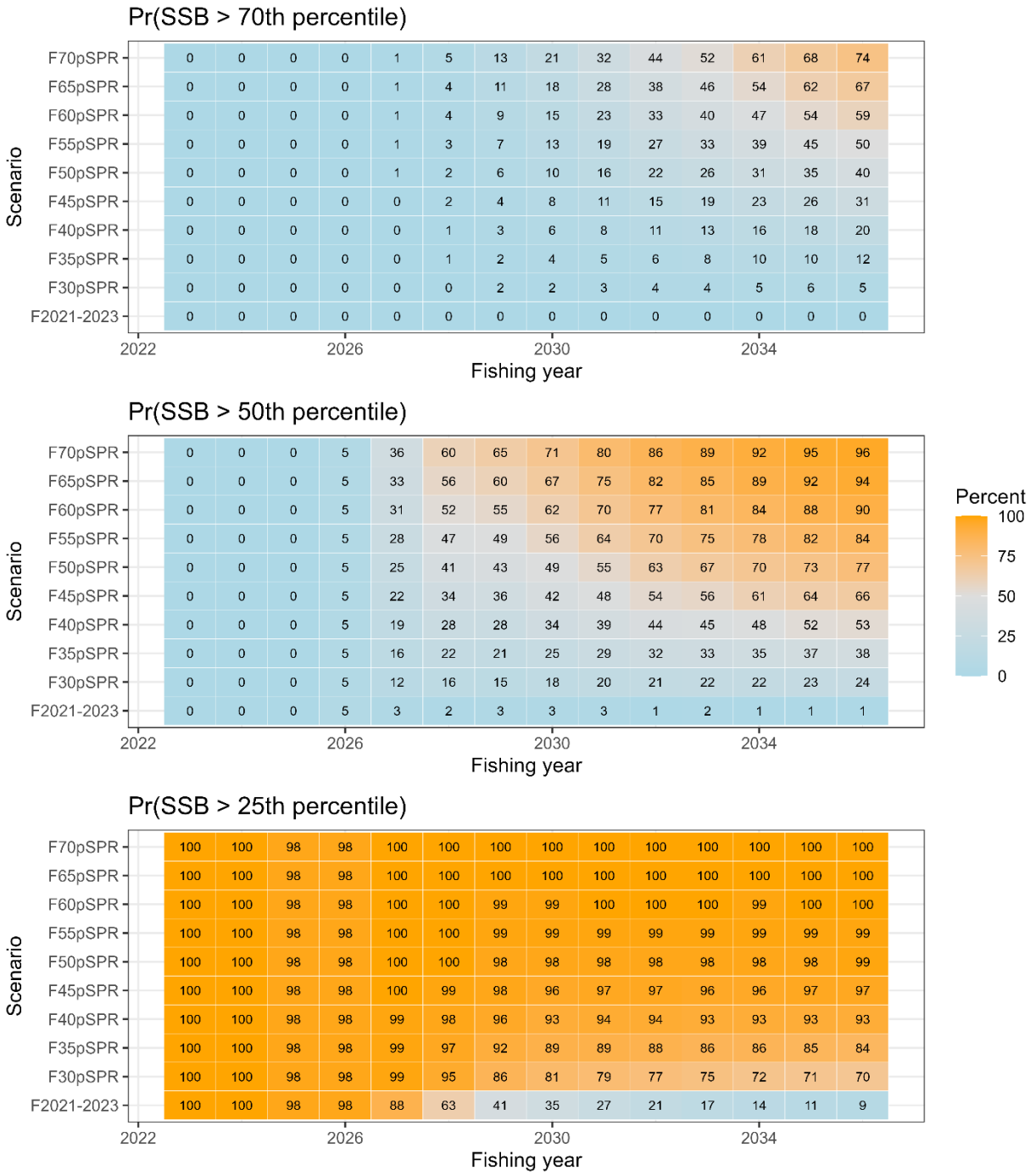

Table 7

Median catch and median SSB based on constant-catch scenarios (ranging from 0 mt to 150 thousand mt).

Table 8

Median catch and median SSB based on projections using constant F scenarios.

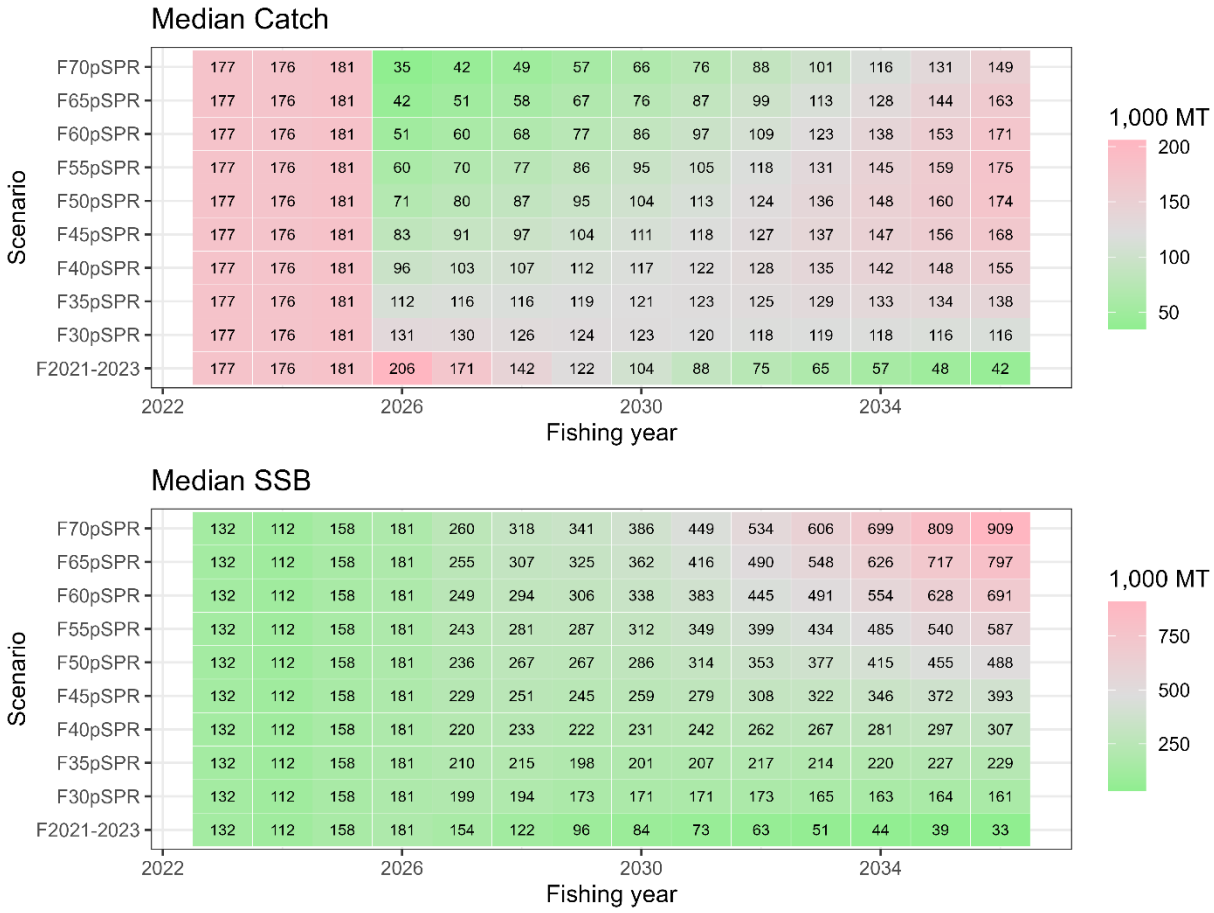

FIGURES

Figure 1

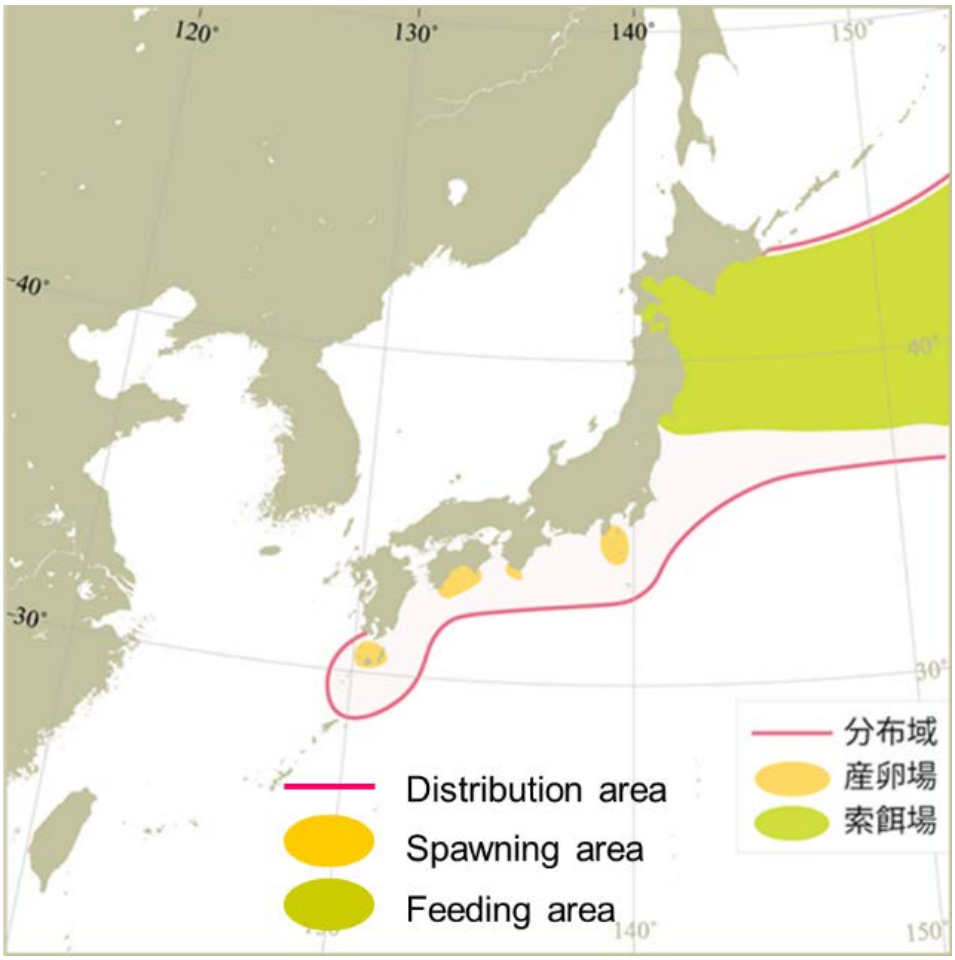

Map of distribution of chub mackerel in the North Pacific (Yukami et al. 2024).

Figure 2

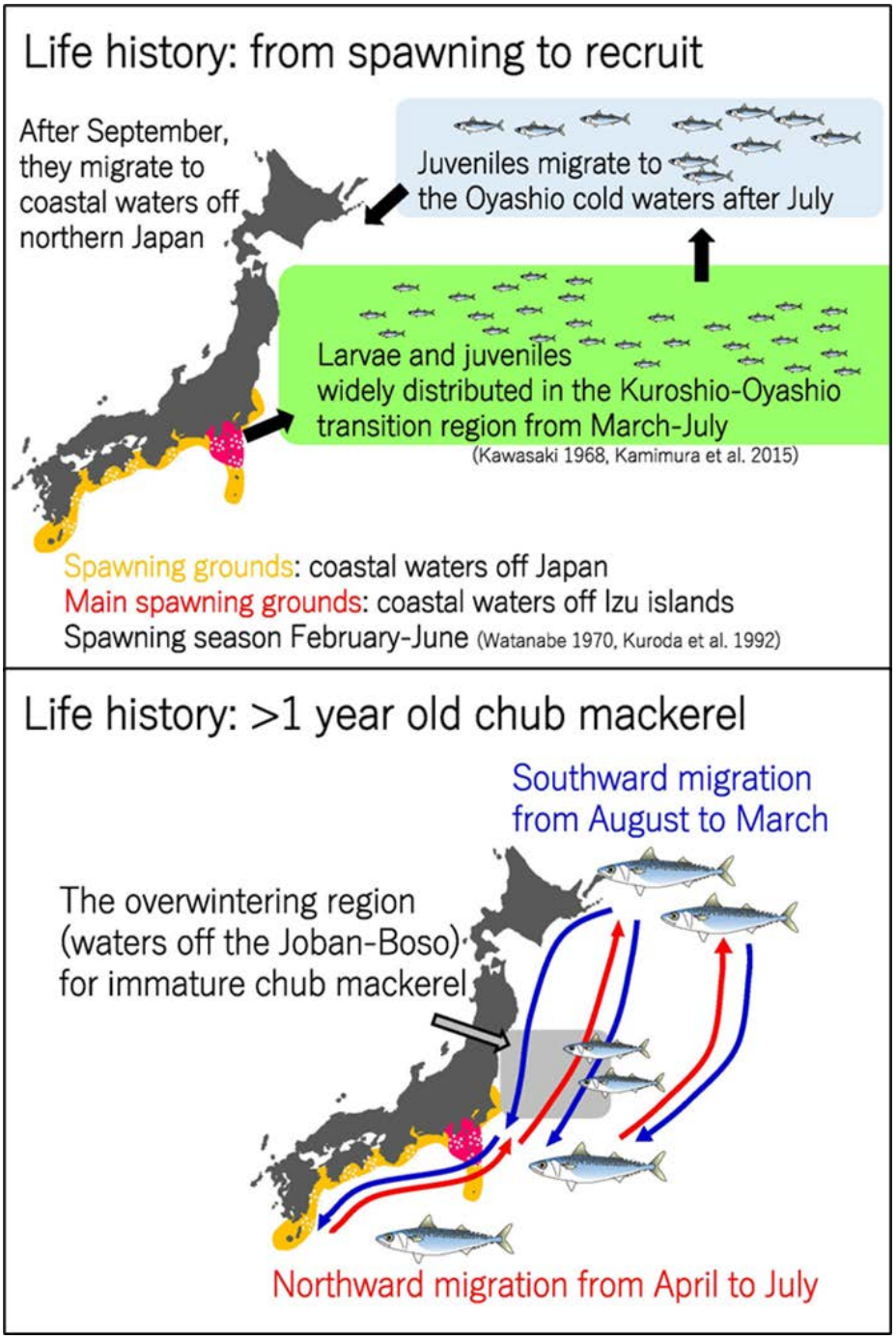

Migration pattern of chub mackerel by growth stage. The upper and bottom panels show seasonal movement of age 0 fish from spawning to recruitment and fish at age 1 and older, respectively (Kamimura, 2017).

Figure 3

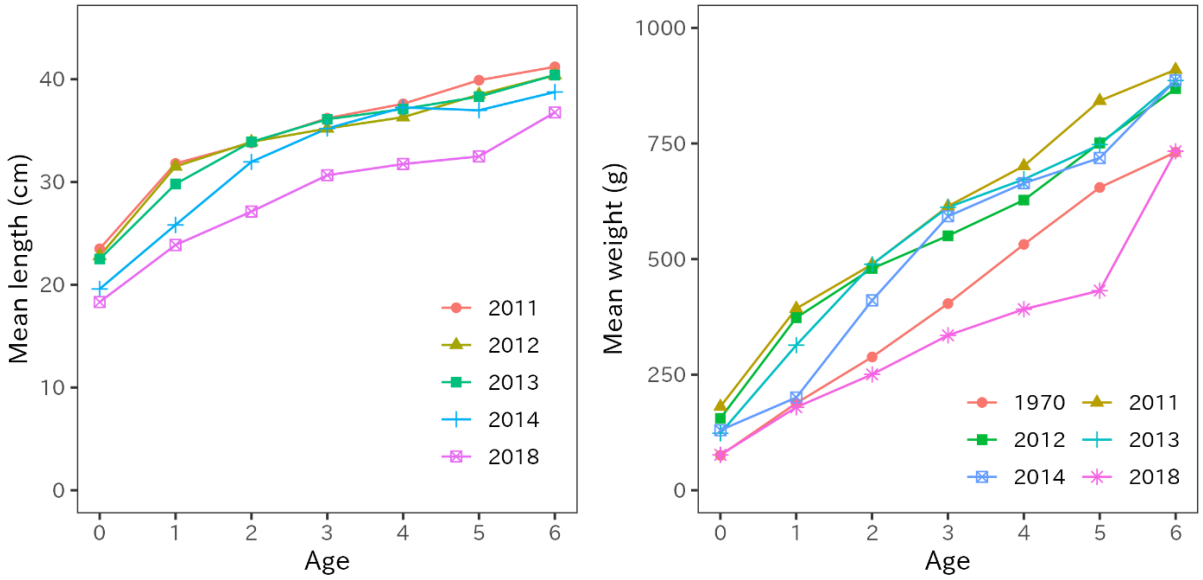

Mean fork lengths of chub mackerel at ages 0 to 6 in FY2011-2014 and FY2018 (left panel). Mean weight at age in FY1970s, FY2011-2014 and FY2018 (right panel).

Figure 4

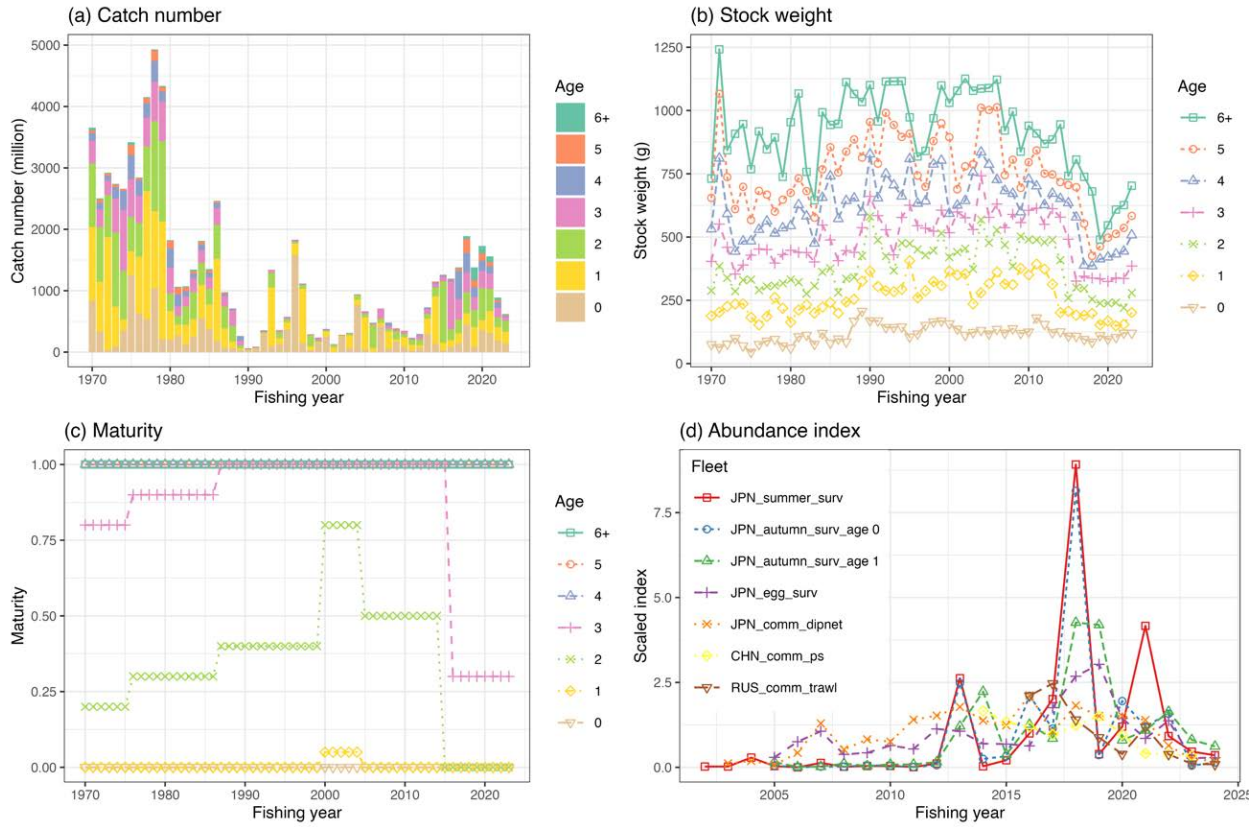

The time series data used for the base case scenario of chub mackerel stock assessment. (a) catch number by age, (b) weight by age, (c) maturity by age, (d) abundance index. Each abundance index is scaled by its mean value for visualization. Note that the Japanese and Russian abundance indices are included through FY2024.

Figure 5

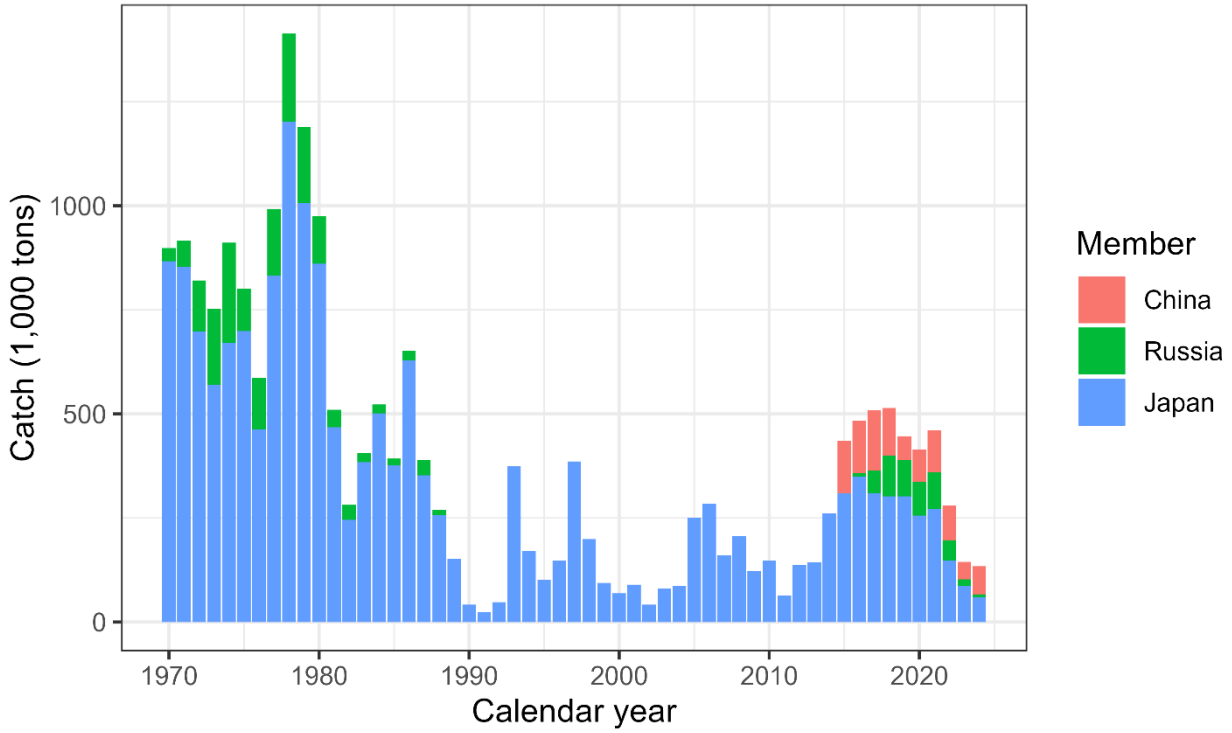

Historical chub mackerel catch in weight by Member. The provisional Chinese catch for CY2024 is estimated using the historical ratio for chub mackerel and blue mackerel. Blue mackerel has been excluded from the catch using the chub-to-blue-mackerel ratio. Catch data for China was obtained from the Annual Summary Footprint, which is available at https://www.npfc.int/summary-footprint-chub-mackerel-fisheries and adjusted using this ratio. Russia's catch data is sourced from the Annual Summary Footprint which reflects no blue mackerel catches. Japan's catch data was collected from coastal prefectures along the Pacific Ocean, where chub mackerel are typically captured. The catch data of this figure is different from the catch data described in the data section above.

Figure 6

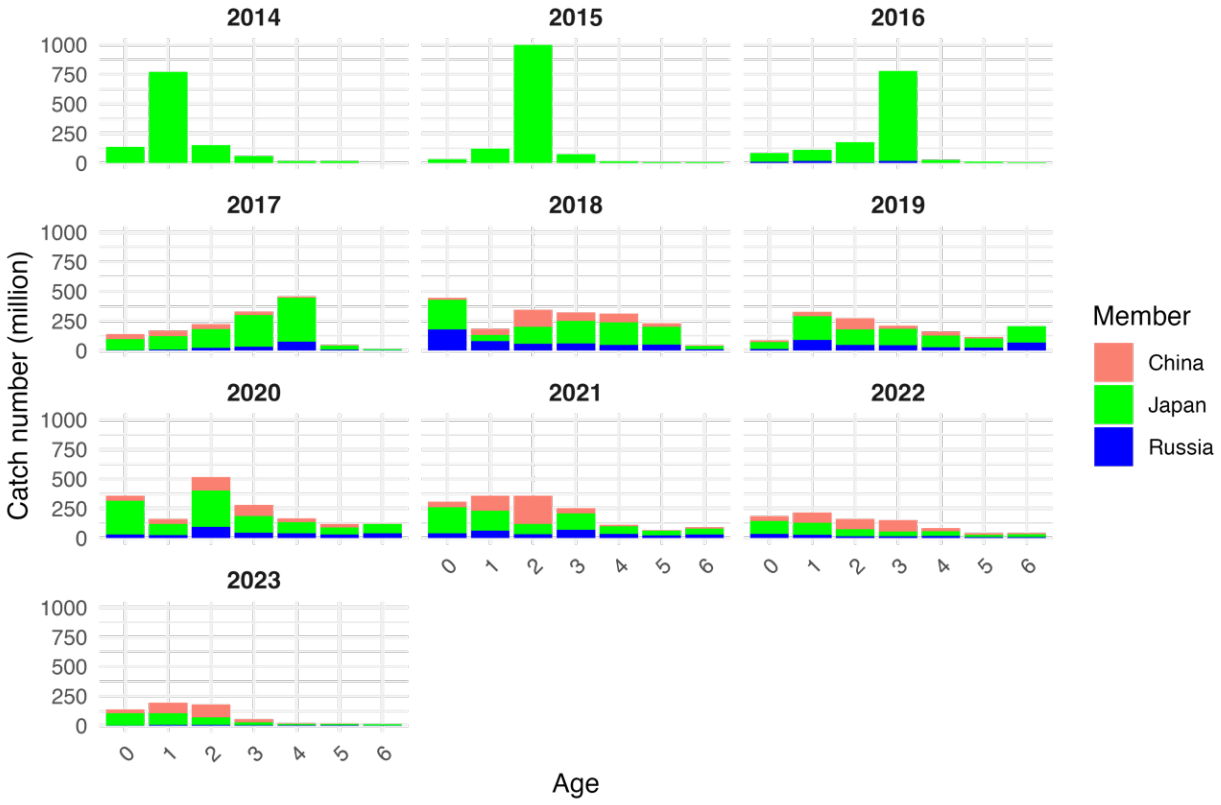

Catch number of chub mackerel by member by age by year from FY2014 to FY2023.

Figure 7

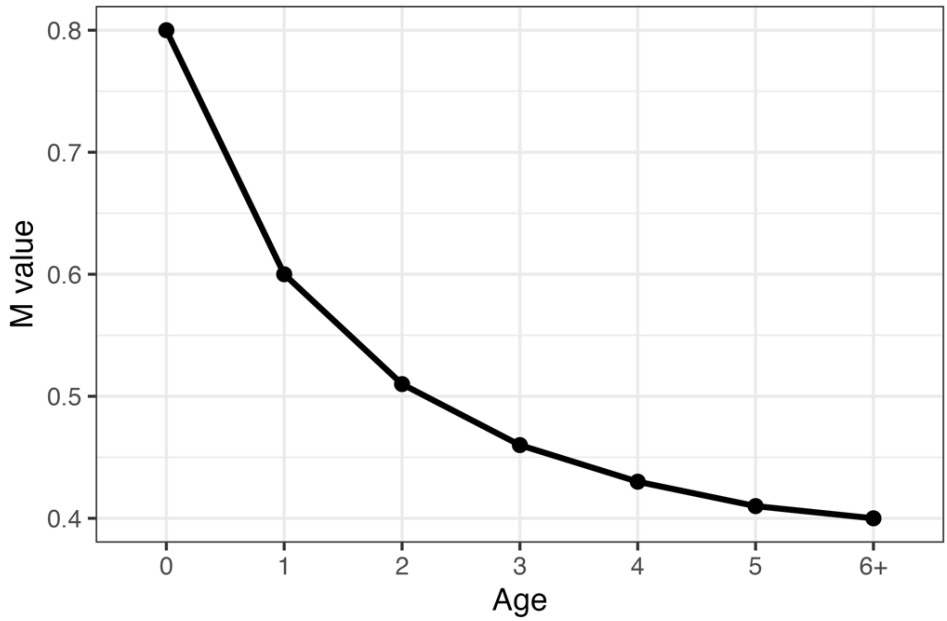

Natural mortality (M) values under the two candidate base case scenarios.

Figure 8

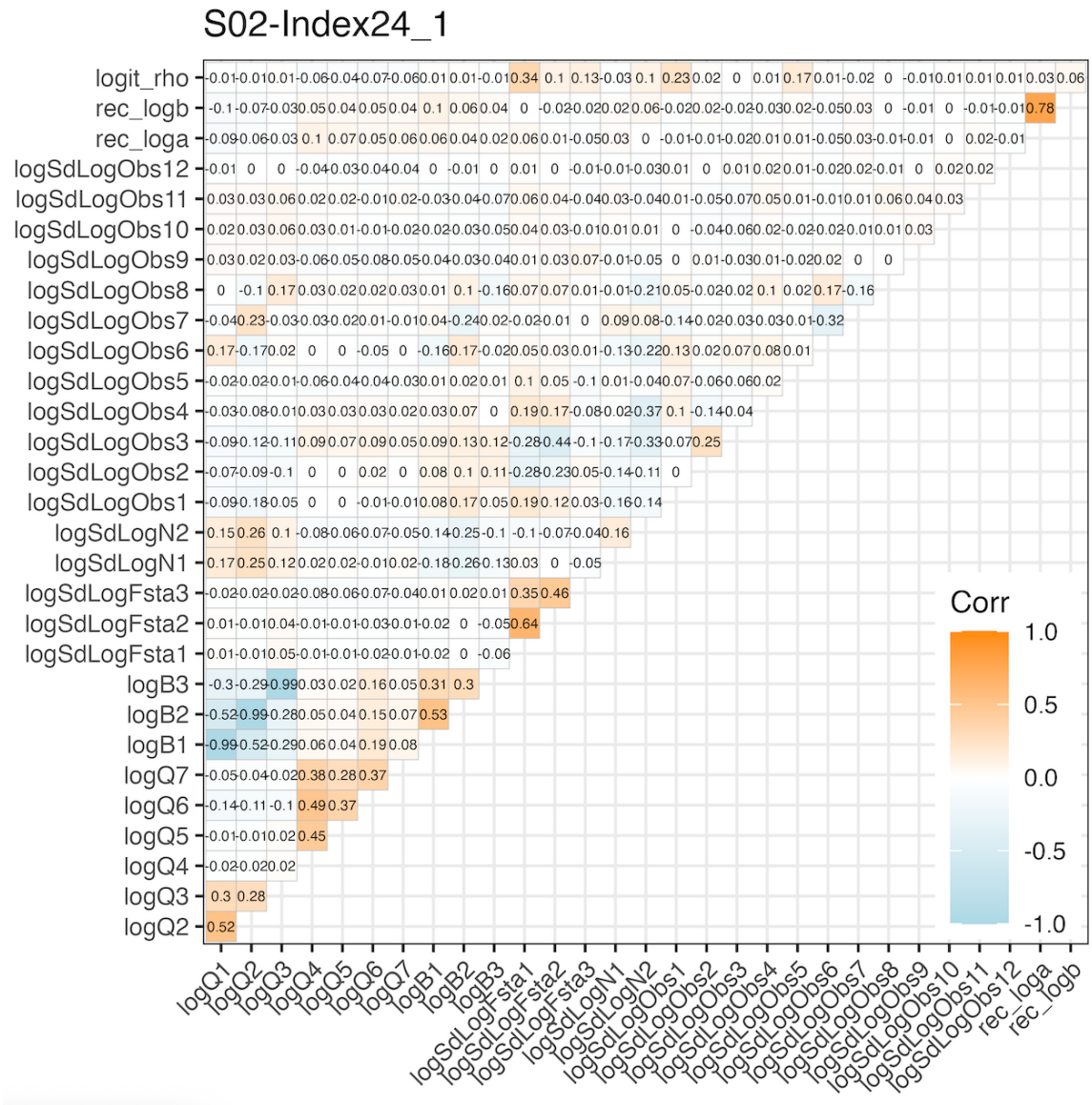

Plot of the correlation matrix obtained from the covariance matrix of the fixed effects parameter estimates, for the base case scenario (Scenario S02-Index24_1). Orange colors indicate positive correlation, while light blue indicates negative correlation.

Figure 9

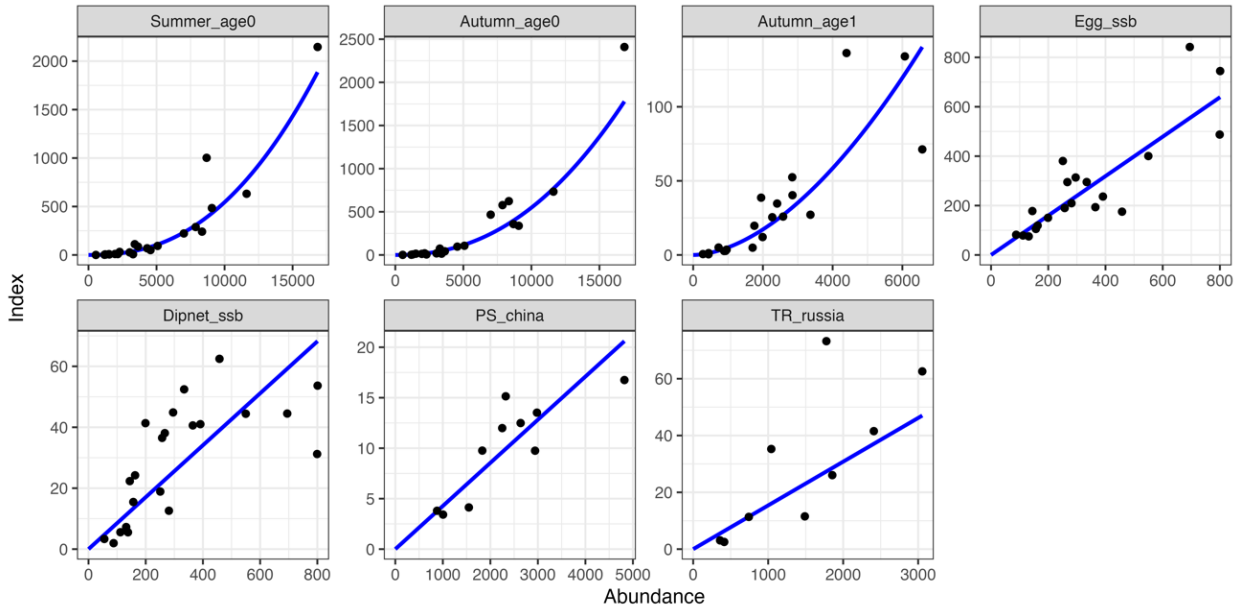

Relationship between seven abundance indices and their corresponding abundance estimates under the base case scenario (Scenario S02-Index24_1). The blue lines indicate the precited relationships.

Figure 10

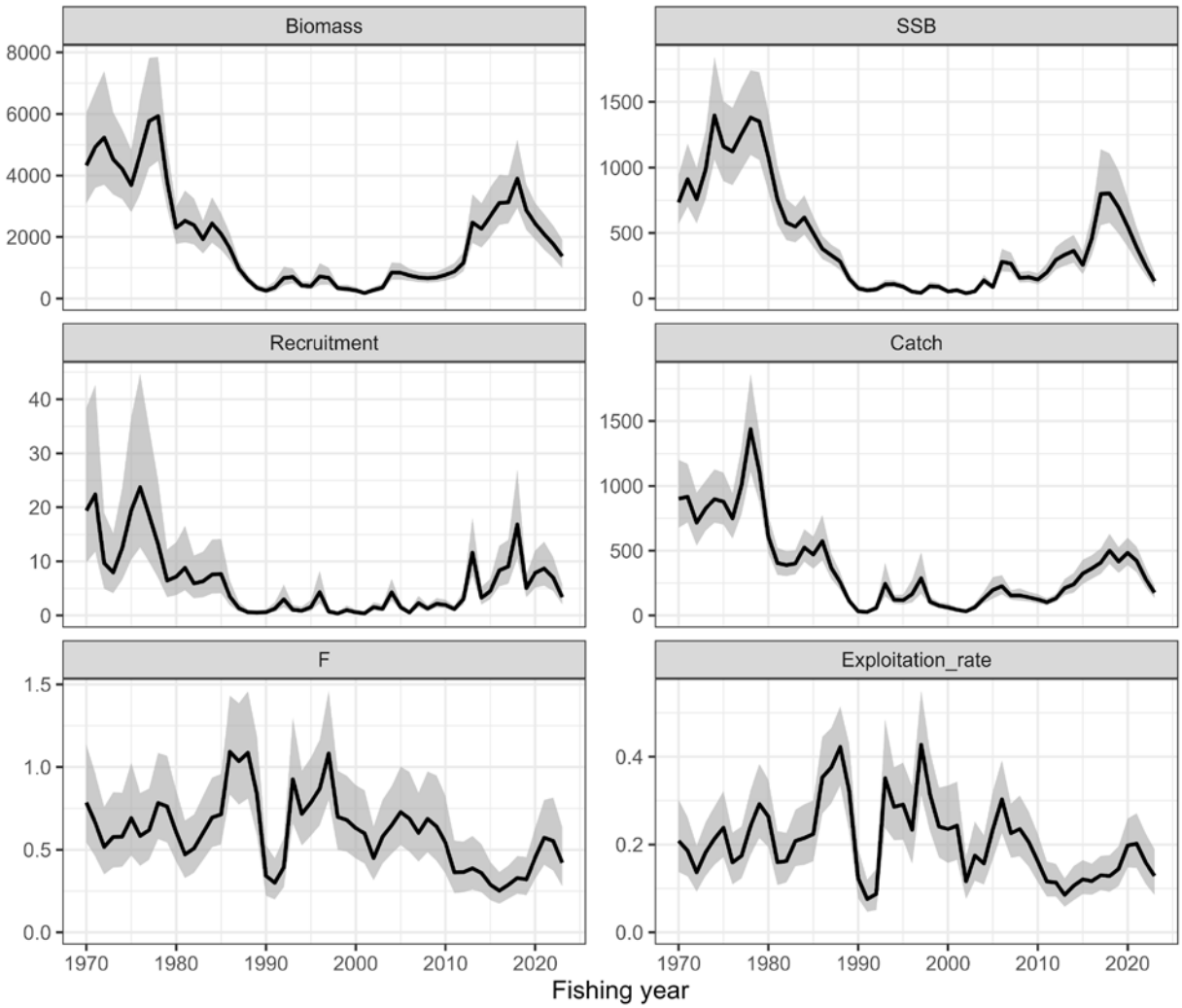

Time series of estimates of total biomass (1,000 MT), SSB (1,000 MT), recruitment (billion), catch (1,000 MT), mean F, and exploitation rate (catch divided by total biomass) of chub mackerel under the base case scenario (Scenario S02-Index24_1).

Figure 11

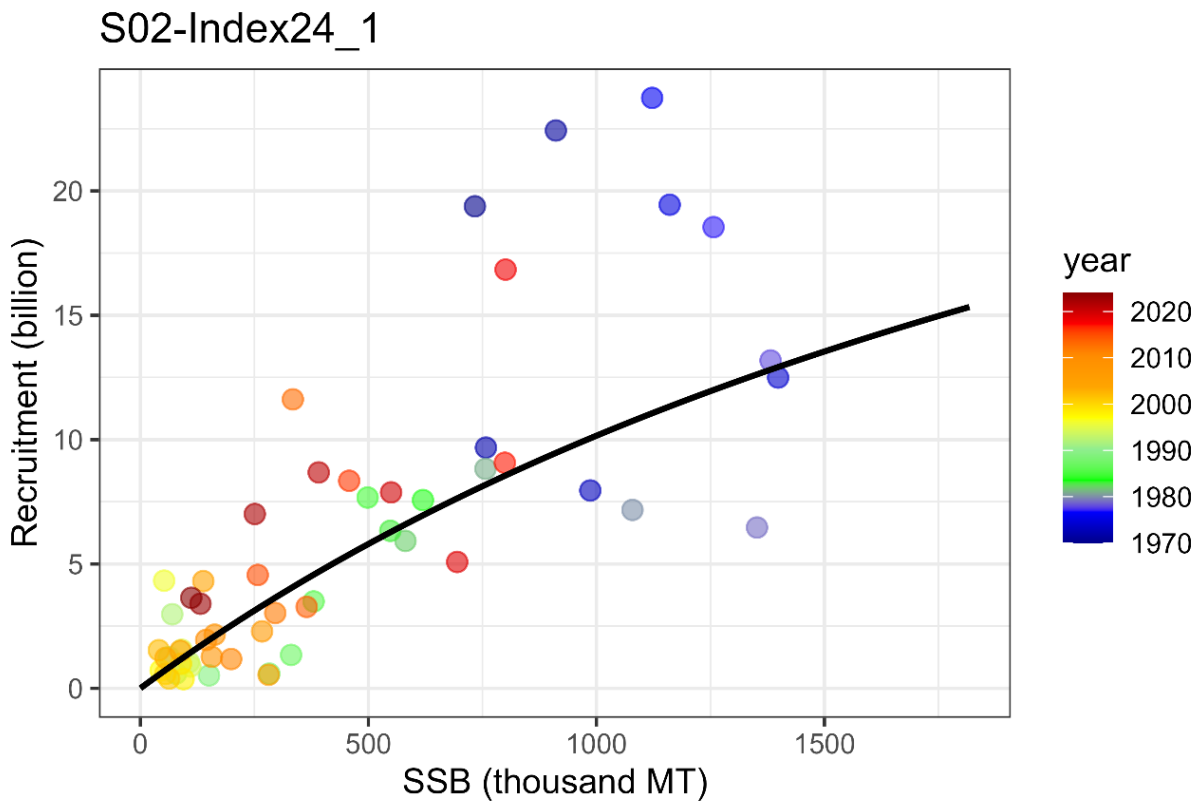

Estimated Beverton-Holt stock recruitment relationship of chub mackerel under the base case scenario (Scenario S02-Index24_1) (black line) and estimated past SSB and number of recruits (circles colored by decade).

Figure 12

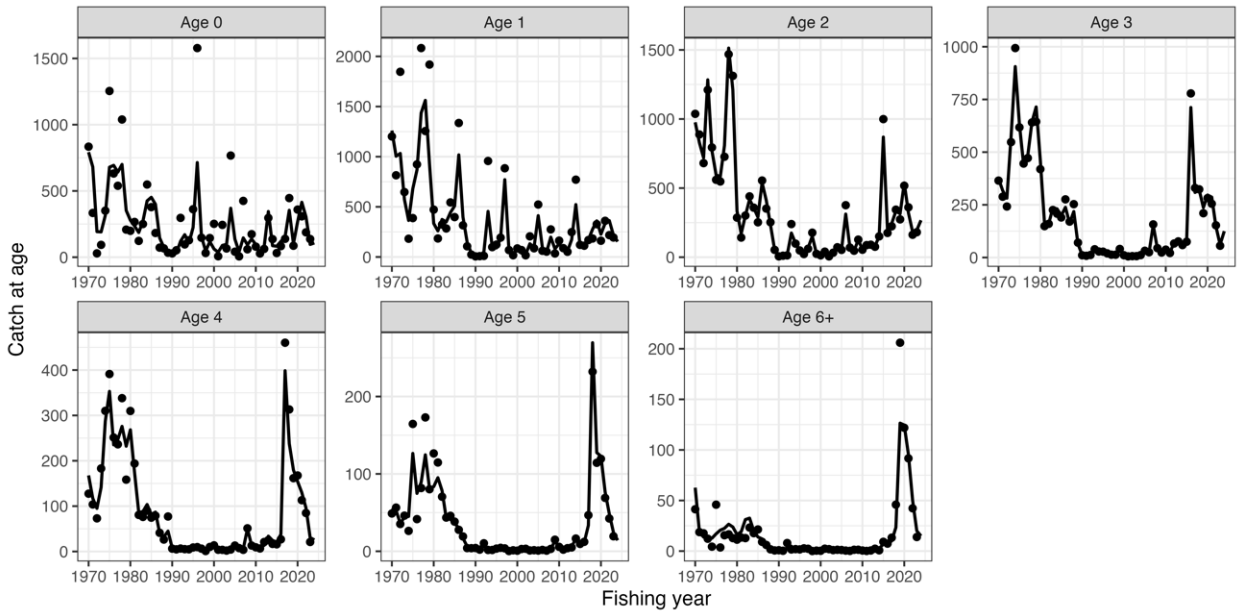

Observed catch numbers by age (dots) and their predicted values (lines)of chub mackerel under the base case scenario of Scenario S02-Index24_1.

Figure 13

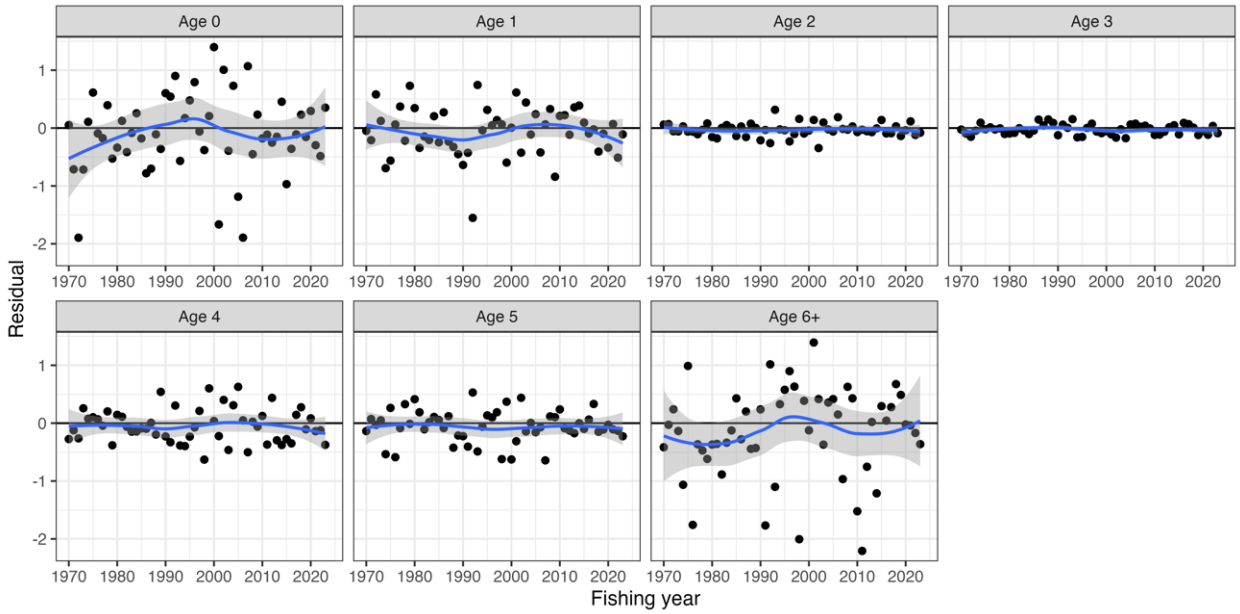

Residual plot for catch numbers of chub mackerel by age under the base case scenario of Scenario S02-Index24_1. Blue curves and shaded areas indicate smoothed curves estimated by LOESS and their 95% confidence intervals.

Figure 14

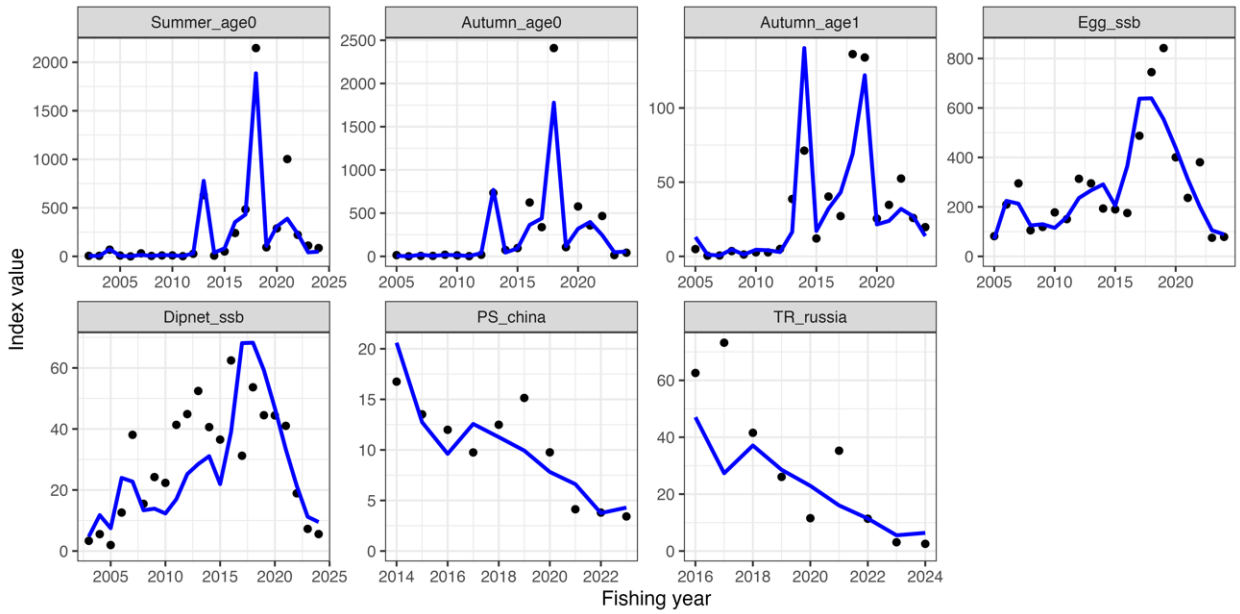

Trends of abundance indices used (dots) and their predicted values (lines) of chub mackerel under the base case scenario of Scenario S02-Index24_1.

Figure 15

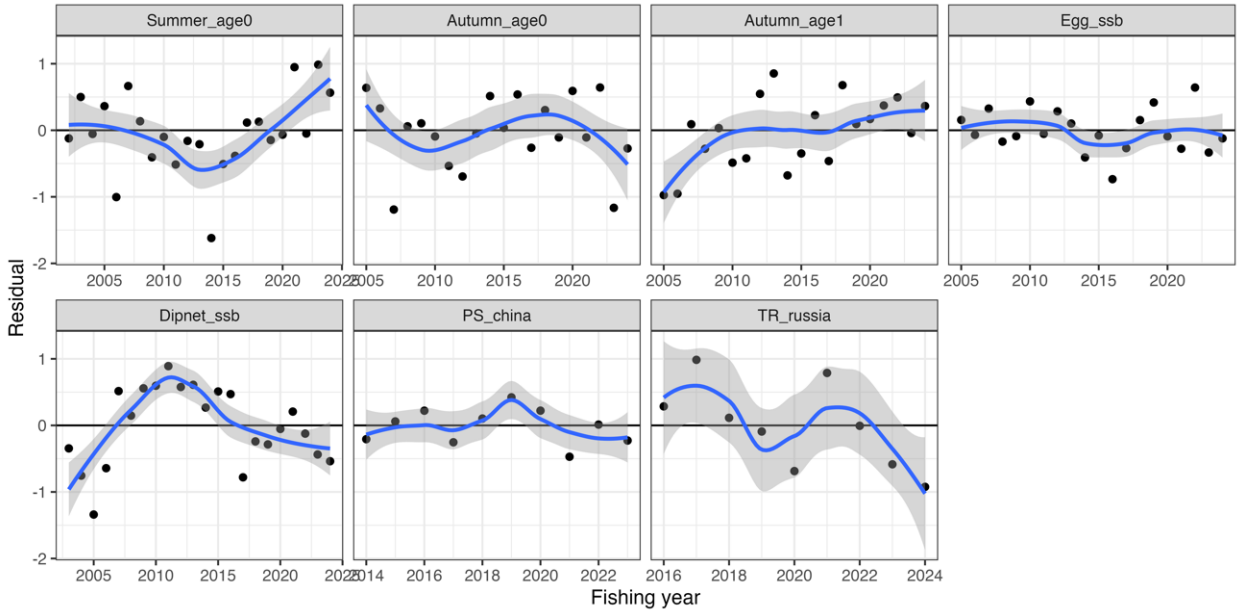

Residual plot for abundance indices of chub mackerel under the base case scenario of Scenario S02-Index24_1. Blue curves and shaded areas indicate smoothed curves estimated by LOESS and their 95% confidence intervals.

Figure 16

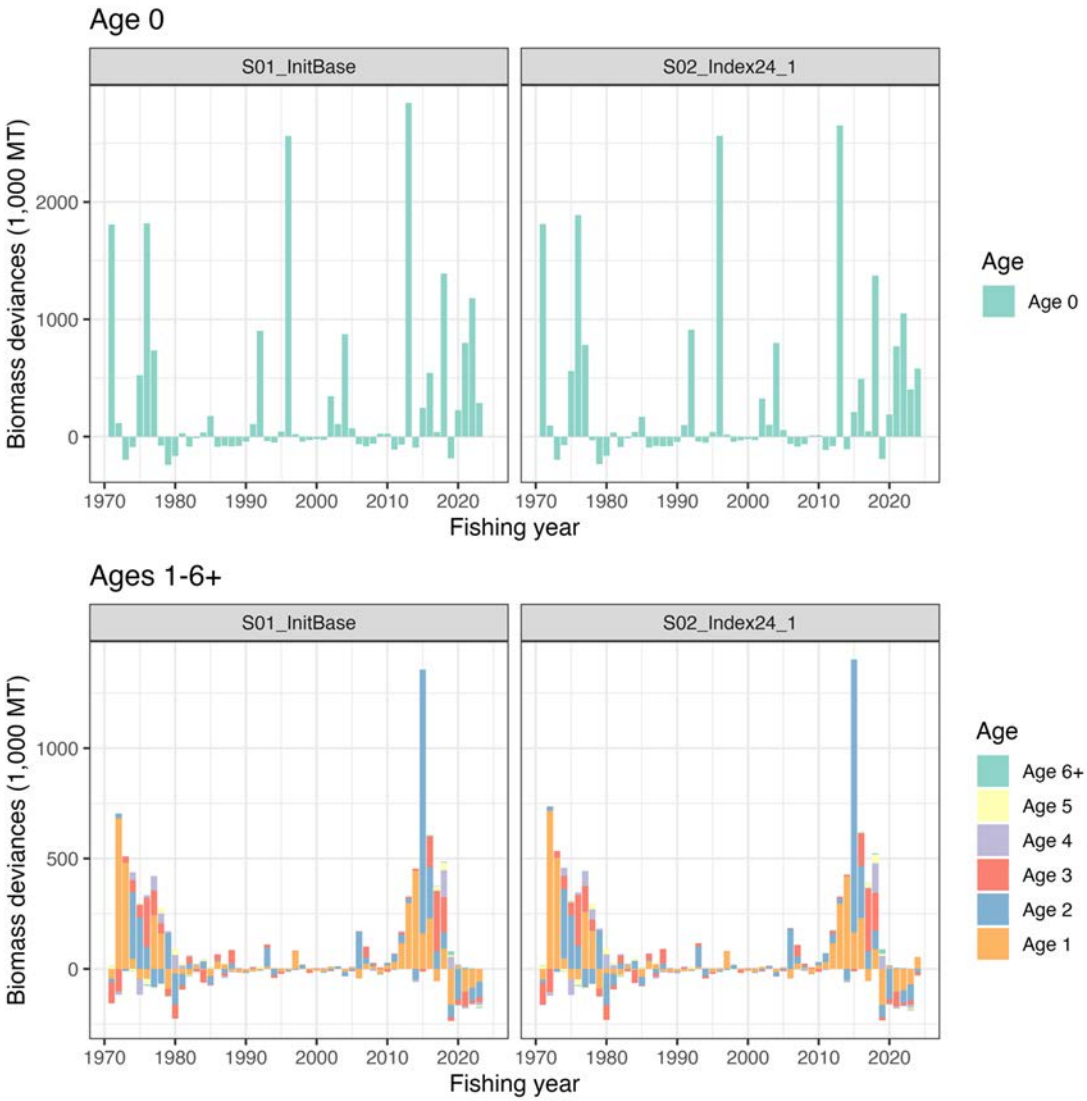

Deviances of abundances under S01-InitBase (left) and S02-Index24_1 (right) scenarios. Only Age 0 deviances are plotted separately (Top) because of the different scale of the observed deviances.

Figure 17

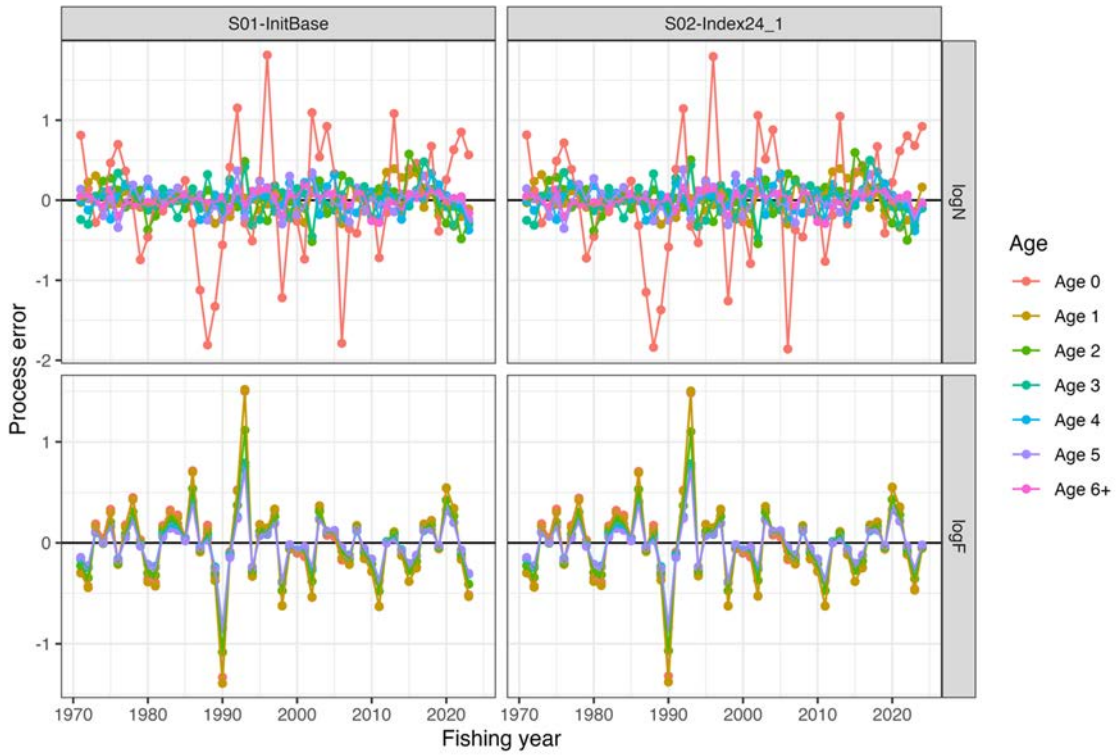

Process errors log(N) (top) and log(F) (bottom) under S01-InitBase (left) and S02-Index24_1 (right) scenarios.

Figure 18

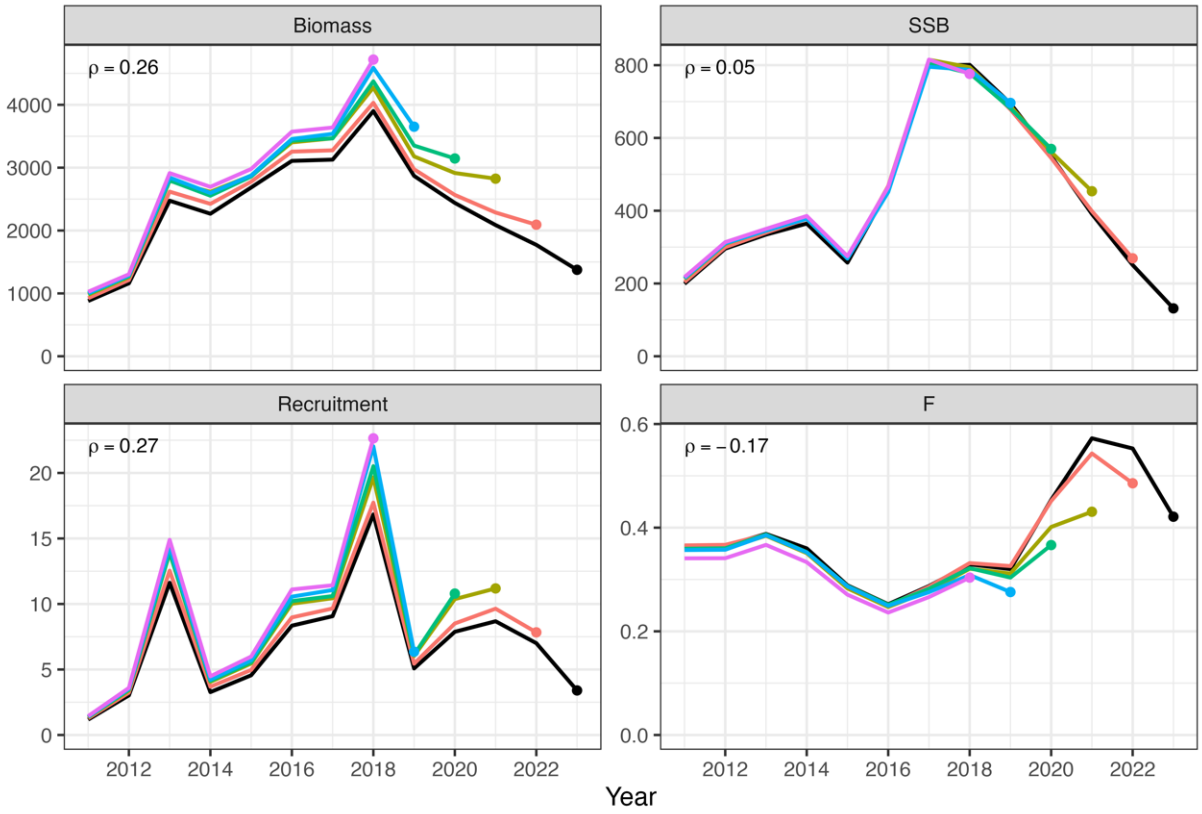

Retrospective patterns for total biomass (top left), SSB (top right), recruitment (bottom left), and mean F (bottom right) of chub mackerel under the base case scenario of Scenario S02-Index24_1. Black Lines represent models with all data, and colored lines represent models with the most recent data trimmed. Mohn's rho is shown in the upper left corner. The dots indicate the terminal year for the calculation of Mohn's rho.

Figure 19

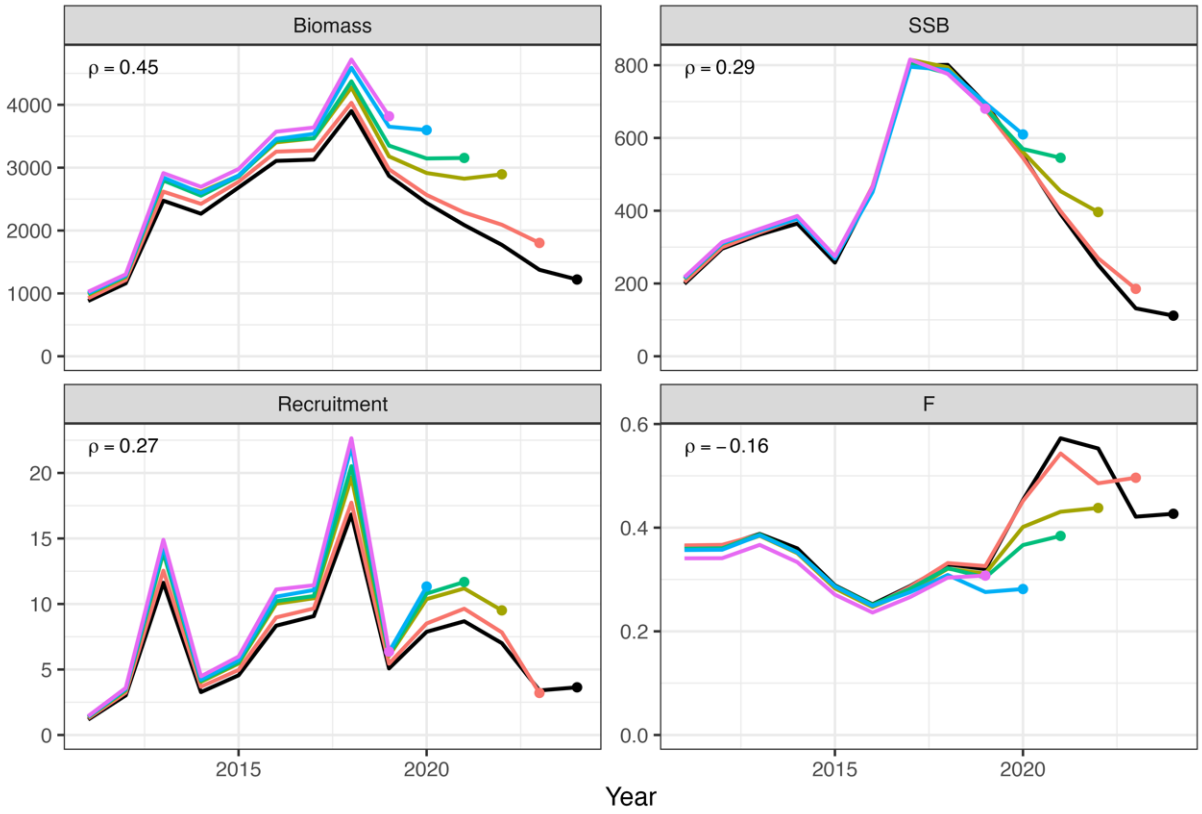

Patterns of retrospective forecasting for total biomass (top left), SSB (top right), recruitment (bottom left), and mean F (bottom right) of chub mackerel under the base case scenario of Scenario S02-Index24_1. Black Lines represent models with all data, and colored lines represent models with the most recent data trimmed. Mohn's rho is shown in the upper left corner. The dots indicate the year of one-year-ahead forecasting, used for the calculation of Mohn's rho.

Figure 20

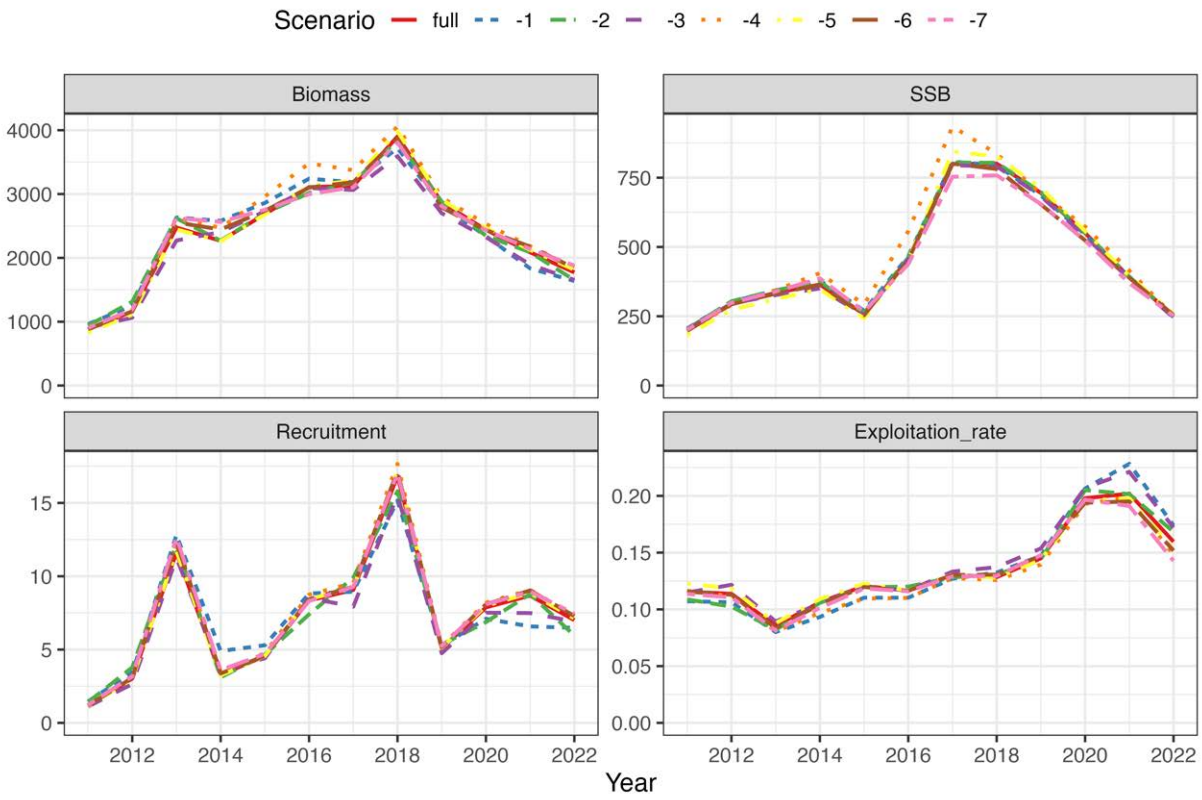

Comparison of the results of the estimates of chub mackerel when all index values are used and when each indicator is excluded for the base case scenario of Scenario S02-Index24_1. The IDs of the index are as follows: (1) relative stock number of age 0 from the summer survey by Japan, (2) relative stock number of age 0 from the autumn survey by Japan, (3) relative stock number of age 1 from the autumn survey by Japan, (4) relative SSB from the egg survey by Japan, (5) relative SSB from the dip-net fishery by Japan, and (6) relative vulnerable stock biomass from the light purse-seine fishery by China.

Figure 21

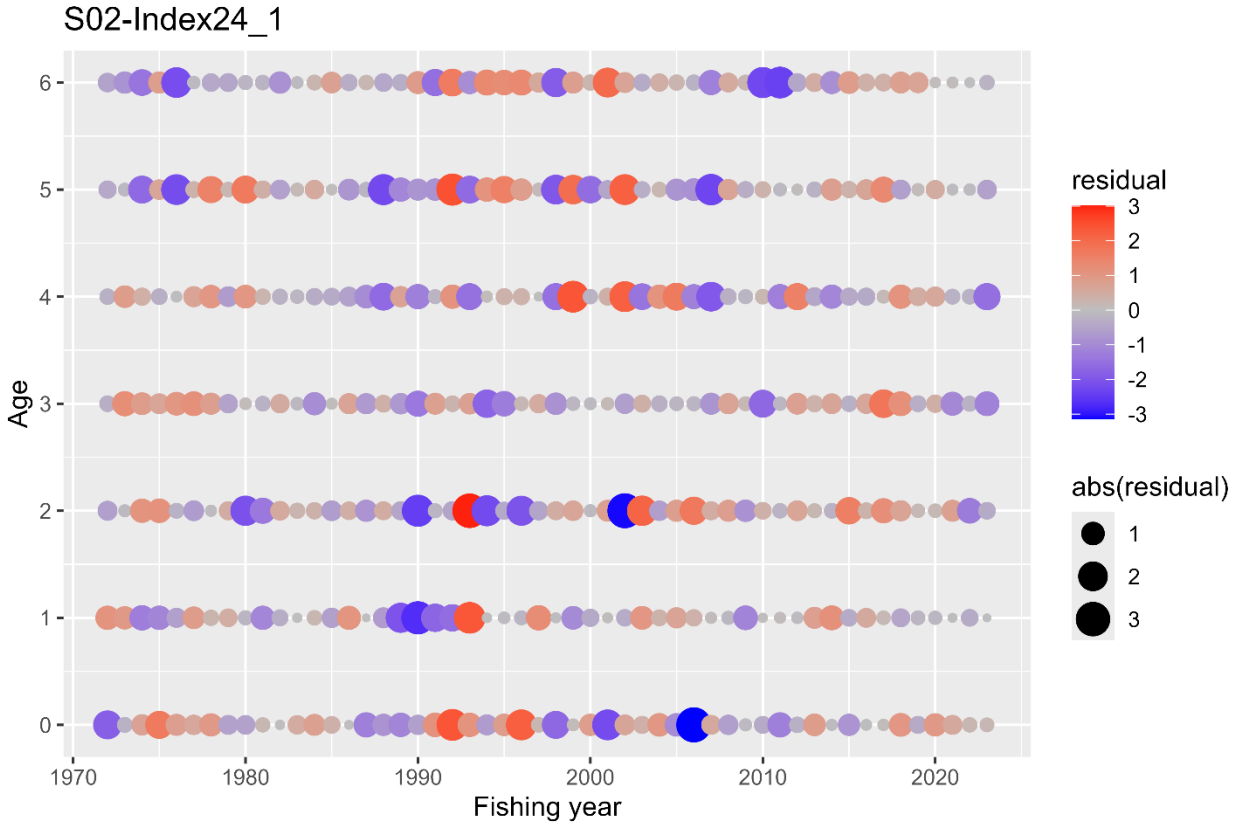

One-Step-Ahead residuals for the catch at age for the base case scenario S02-Index24_1.

Figure 22

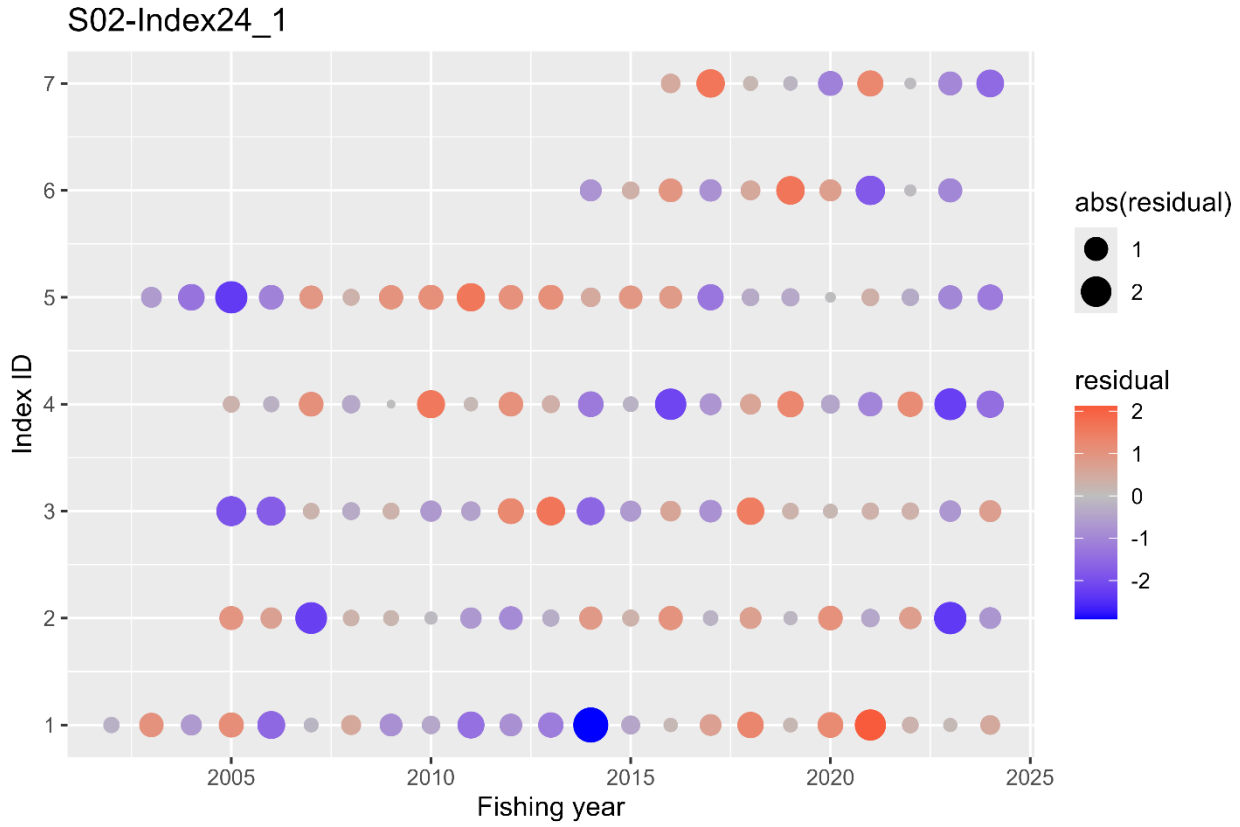

One-Step-Ahead residuals for the indices of abundance for the base case scenario S02-Index24_1. The IDs of the index are as follows: (1) relative stock number of age 0 from the summer survey by Japan, (2) relative stock number of age 0 from the autumn survey by Japan, (3) relative stock number of age 1 from the autumn survey by Japan, (4) relative SSB from the egg survey by Japan, (5) relative SSB from the dip-net fishery by Japan, and (6) relative vulnerable stock biomass from the light purse-seine fishery by China.

Figure 23

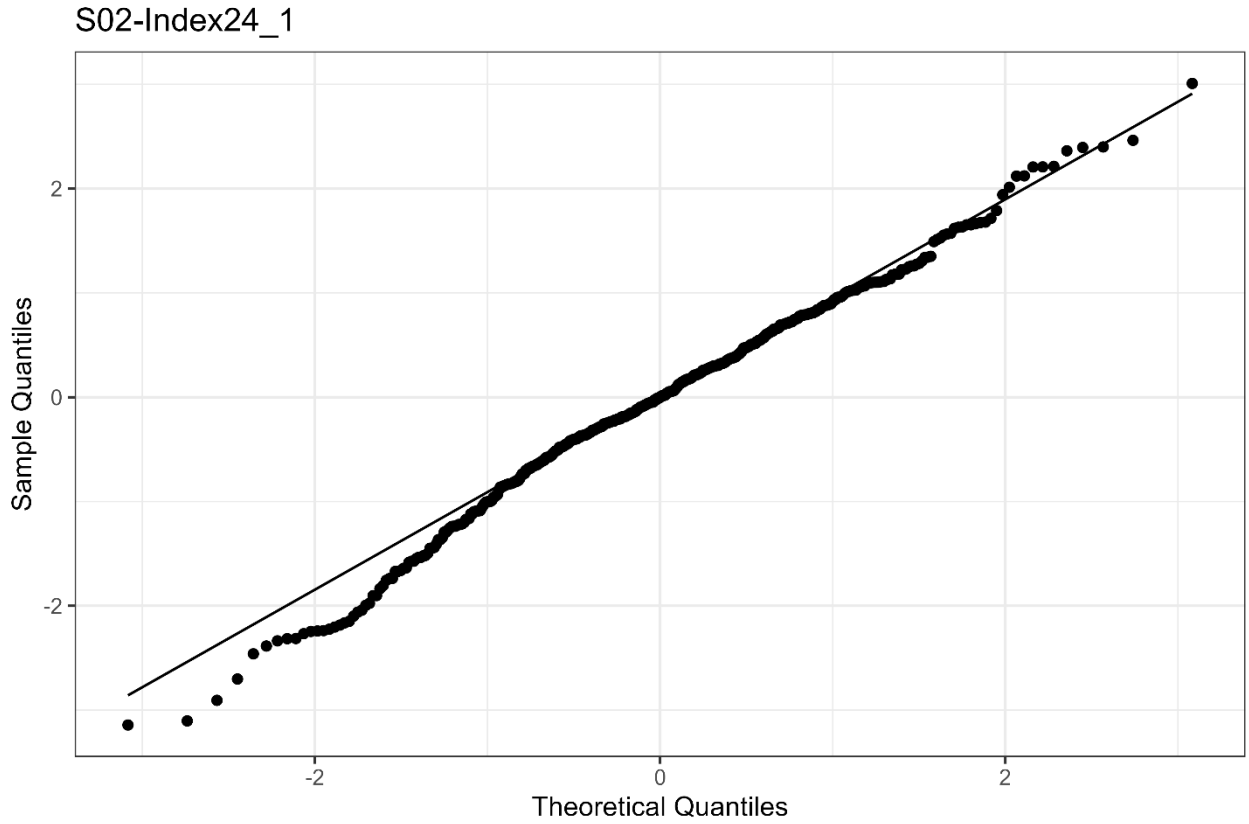

QQplot of the One-Step-Ahead residuals from the indices and catch-at-age for the base case scenario S02-Index24_1.

Figure 24

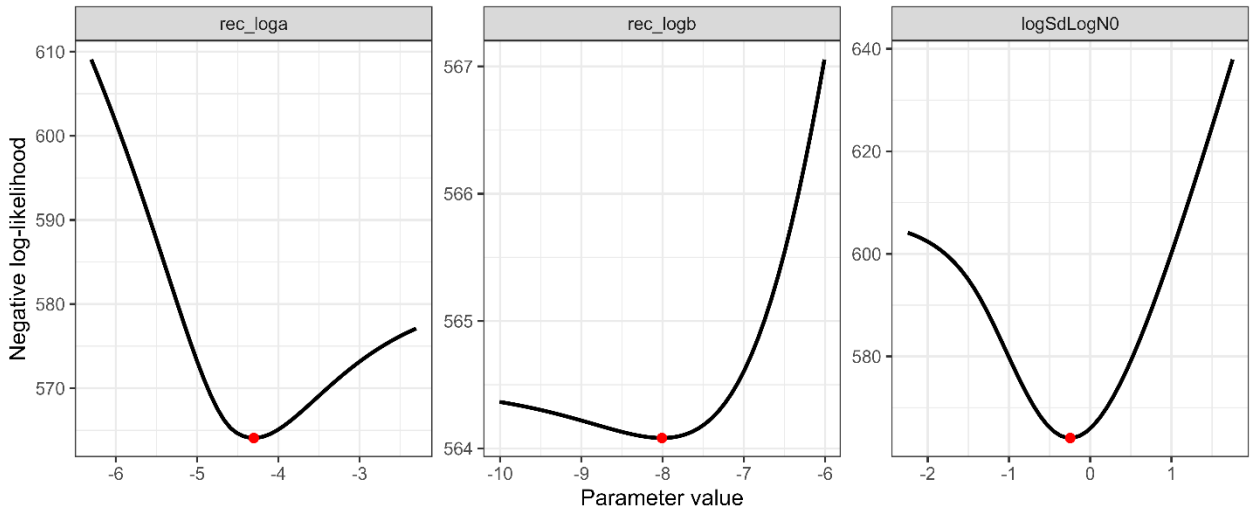

Changes in negative log-likelihoods by varying parameters related to the stock-recruitment relationship (α, β, ω_0 in log space).

Figure 25

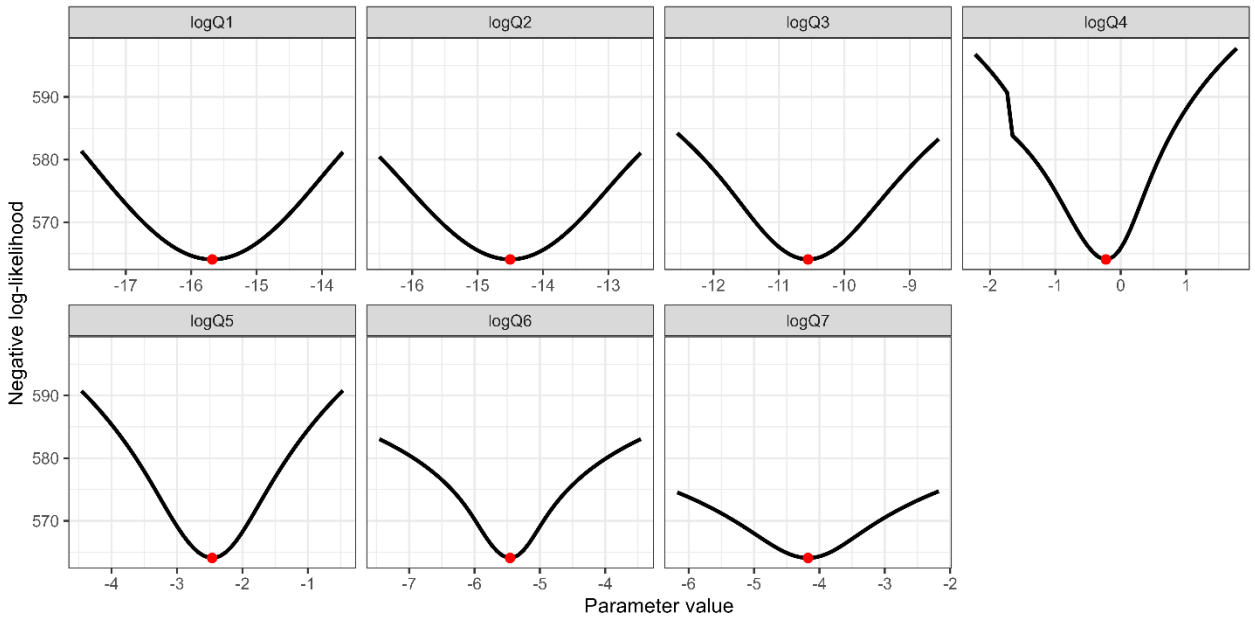

Changes in negative log-likelihoods by varying parameters of proportionality constants for abundance indices (q_k in log space). The red dotes indicate the input values for the base case scenarios.

Figure 26

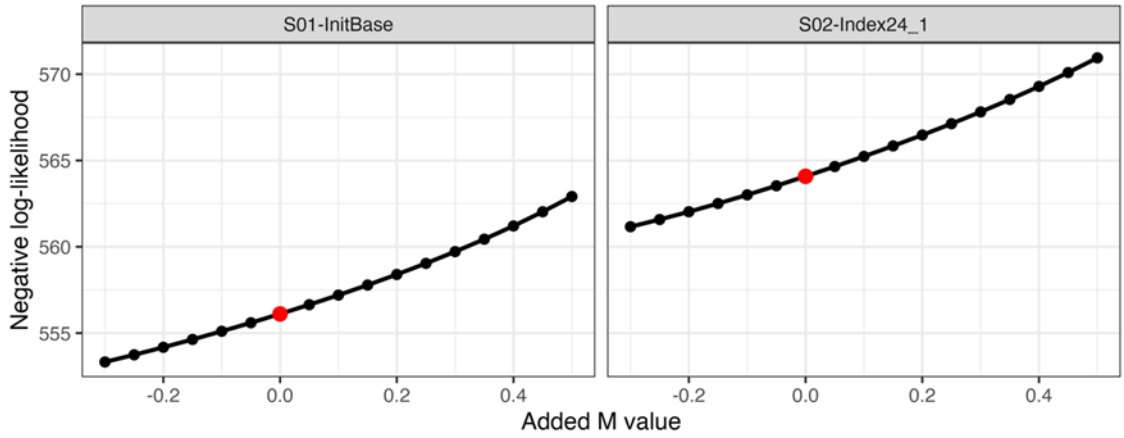

Changes in negative log-likelihood by adding different M values. The red dotes indicate the input values for the base case scenarios.

Figure 27

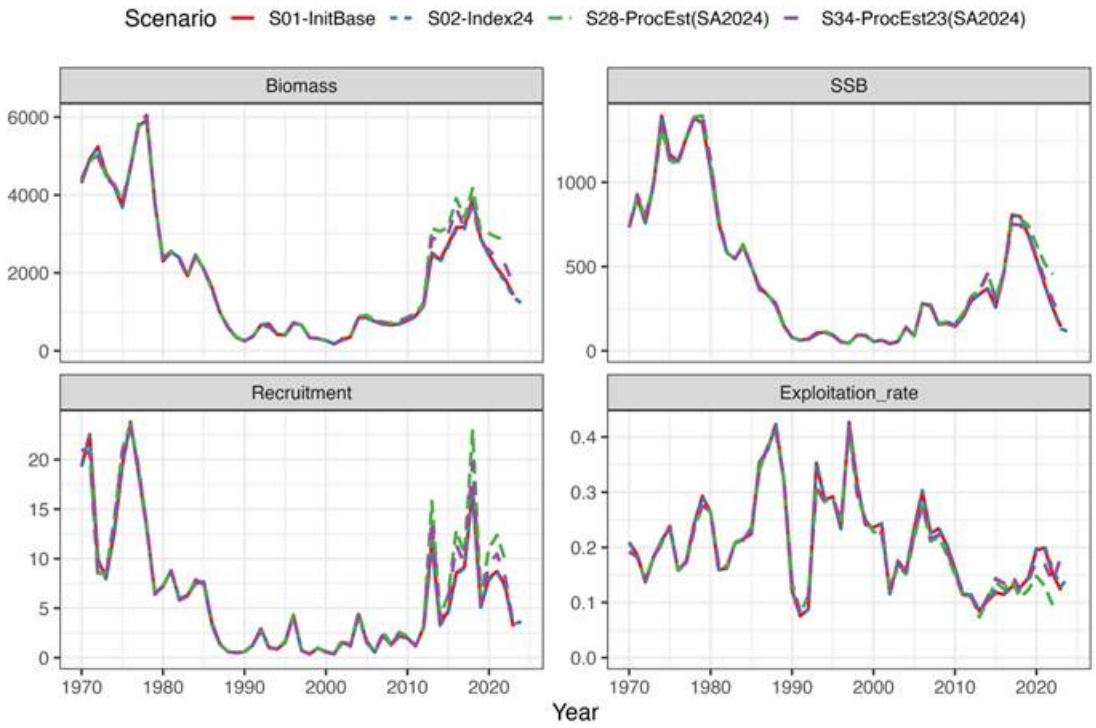

Comparison of the estimated population dynamics between current (red and blue for S01-InitBase and S02-Index24_1, respectively) and previous (S28ProcEst, denoted by green) stock assessments. Note that the purple line indicates S34-ProcEst23, a representative scenario in the previous stock assessment, in which the 2023 indices were used.

Figure 28

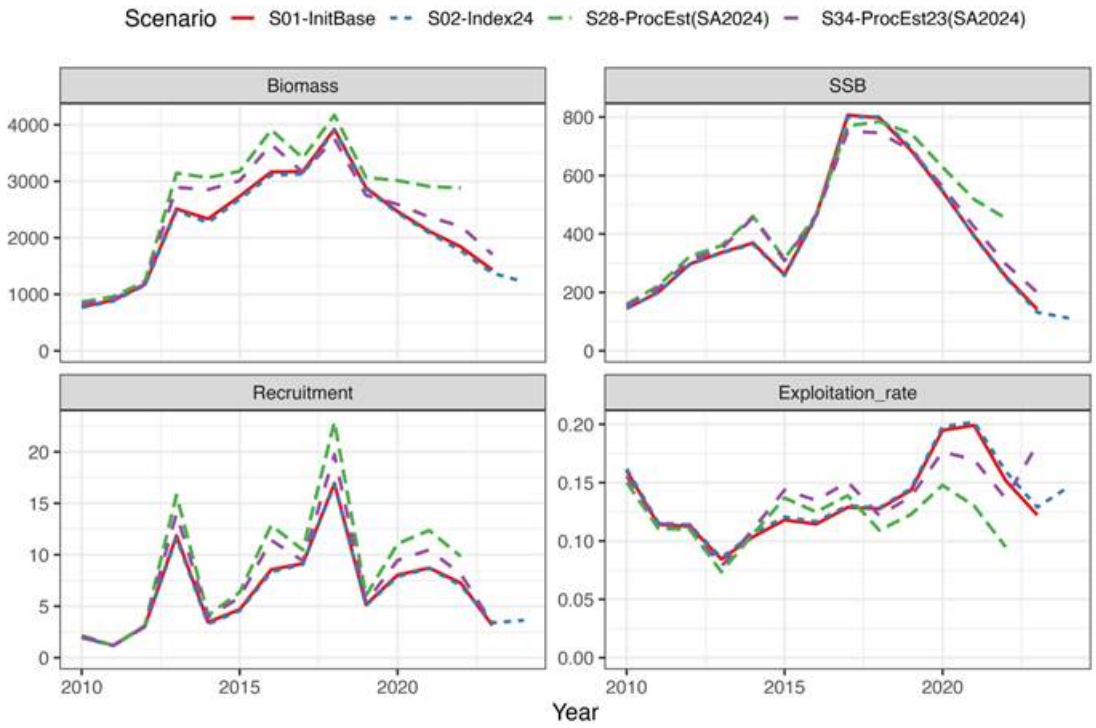

Same as Figure 27, but focusing on the recent years.

Figure 29

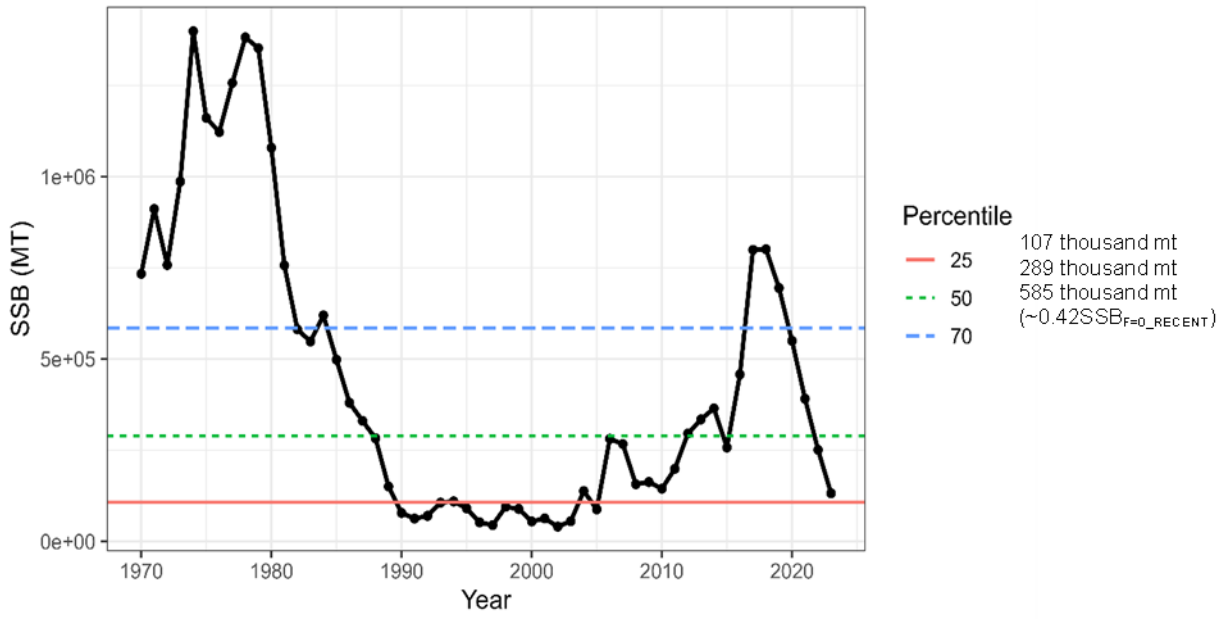

Estimated spawning stock biomass and its 25th, 50th and 70th percentiles.

Figure 30

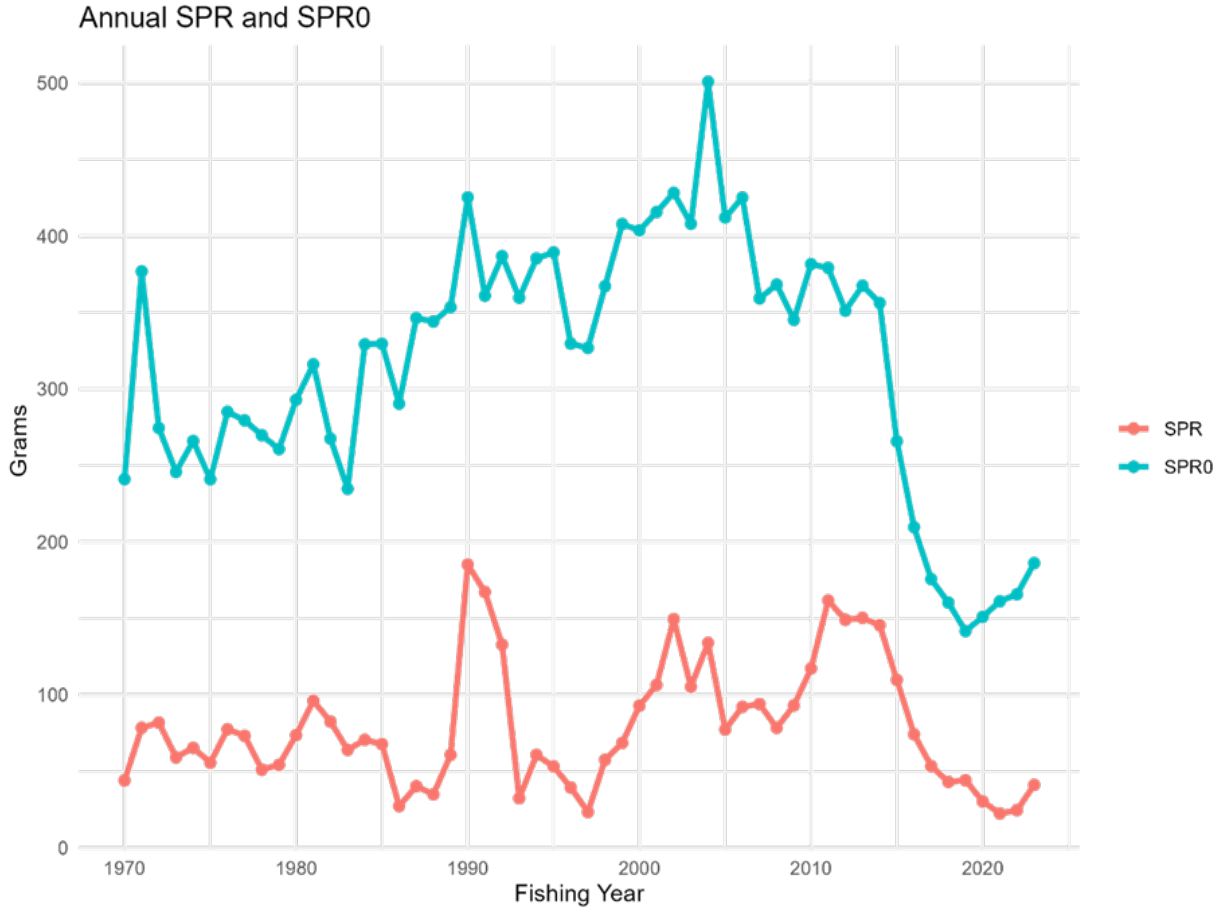

Trajectories of spawners per recruit with (SPR) and without fishing (SPR0).

Figure 31

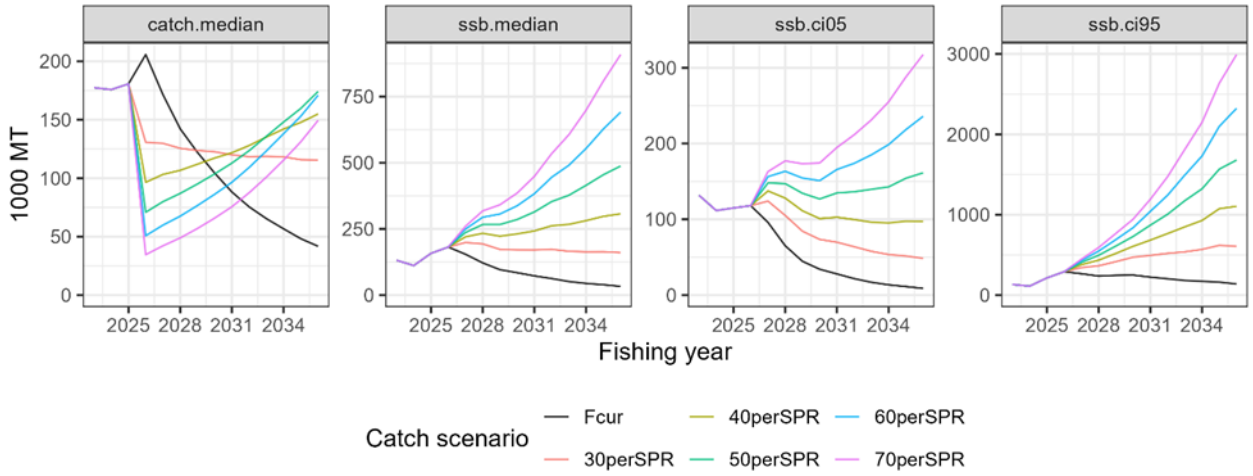

Future trajectories median catch (left), median SSB (second from left), 5% lower limit of predictive interval for SSB (third from left) and 95% SSB (right) with mean biological parameters for the entire time series. 30–70%SPR and "F_{cur}" in "Catch scenarios" indicate total amount of catches (mt) in constant fishing mortality scenarios of F30–70%SPR in increments of 10% and current fishing morality, respectively.

Figure 32

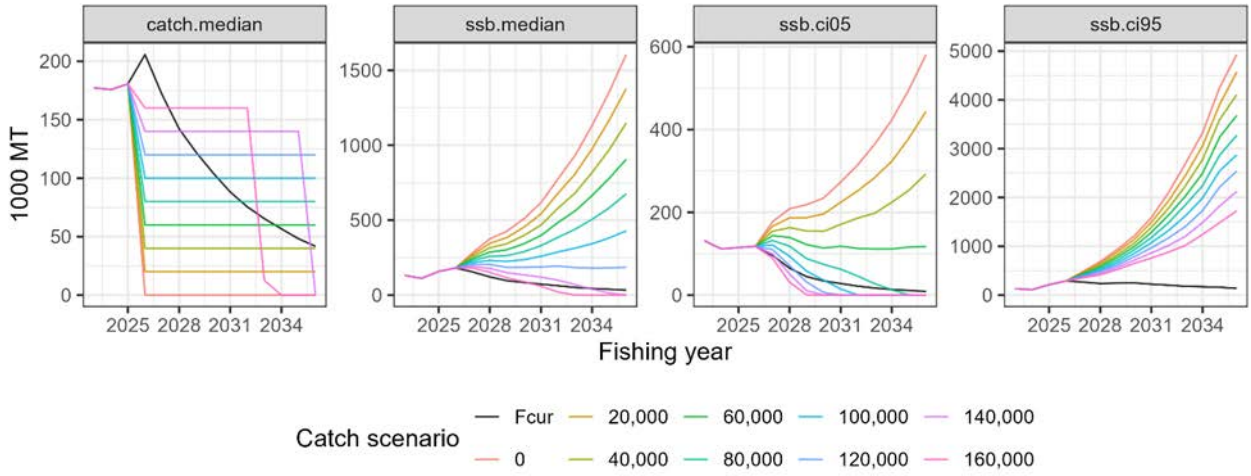

Future trajectories of median catch (left), median SSB (second from left), 5% lower limit of predictive interval for SSB (third from left) and 95% SSB (right) with mean biological parameters in recent 8 years. Numbers and "F_{cur}" in "Catch scenarios" indicate total amount of catches (mt) in constant catch scenarios of 0 to 160 thousand mt in increments of 20 thousand mt and current fishing mortality, respectively.

ANNEX 1 Additional Tables

Table A1. Descriptions of common terms in the assessment. For terms that are time specific (either a year or a range of years), examples are given for 2023, although the text may refer to alternative years.

Term	**Description**
TBy2023	Total stock biomass in FY2023 (1,000 MT)
SSBy2023	Spawning stock biomass in FY2023 (1,000 MT)
Ry2023	The number of recruits in FY2023 (million)
AFy2023	Weighted average of F-at-age by estimated catch-at-age in FY2023
Ey2023	Exploitation rate (estimated catch divided by stock biomass) in FY2023
CurrentSPR/SPR0	Ratio of spawners per recruit (SPR) in the average of FY2021-2023 to that without fishing
SSBmedian	Median spawning biomass from FY1970 to 2023
F0.1/ F_{cur}	Ratio of F0.1 to current F (average F in FY2020-2023)
FpSPR.30.SPR/ F_{cur}	Ratio of F30%SPR to current F (average F in FY2020-2023)
FpSPR.40.SPR/ F_{cur}	Ratio of F40%SPR to current F (average F in FY2020-2023)
FpSPR.50.SPR/F_{cur}	Ratio of F50%SPR to current F (average F in FY2020-2023)
FpSPR.60.SPR/F_{cur}	Ratio of F60%SPR to current F (average F in FY2020-2023)
FpSPR.70.SPR/F_{cur}	Ratio of F70%SPR to current F (average F in FY2020-2023)
F_{MSY}/F_{cur}	Ratio of FMSY to current F (average F in FY2020-2023)
B_{MSY}	Deterministic MSY reference point for total biomass (1,000 MT)
SSB_{MSY}	Deterministic MSY reference point for spawning stock biomass (1,000 MT)
h	Steepness
SSB0	Virgin spawning stock biomass (1,000 MT)
SSB_{MSY}/SB_0	Ratio of SB_{MSY}Y to SB_0
F_{MSY}SPR	%SPR for F_{MSY}
B/B_{MSY}	Ratio of total biomass in FY2023 to B_{MSY}
SSB/SSB_{MSY}	Ratio of spawning biomass in FY2023 to SSB_{MSY}
$SSB_{MSY}y/SSB_{MAX}$	Ratio of SSB_{MSY} to the historical maximum of spawning biomass

Table A2. Settings and specifications of SAM for S02-Index24_1.

Model configuration	**Parameter**	**Option(s) addressed after input data fixed by TWG CMSA11(?)**
Recruitment	$N_{0,y}$	Parameterized Beverton-Holt stock-recruitment relationship with α and β estimated in the model (base case)
Catchability or proportionality constant for abundance indices	q_k	Assumed constant across years
Nonlinear coefficient for abundance indices	b_k	Searching the best option(s) about how constraints are imposed on which indices based on AIC etc. b is estimated for the three Japanese trawl surveys, whereas fixed at 1 for other indices.
Years of F random walk	-	Include the Markov process for all years as the base case
Correlation of age classes in F random walk	ρ	Using a simple function of age difference ($\rho^{\lvert a-a' \rvert}$)
Process errors in numbers older than age 0	ω_a $(a>0)$	Searching the best option(s) about how constraints are imposed on which age classes based on AIC etc., prohibiting setting breakpoints between ages 2 and 3 (base case).
SD in F random walk	σ_a	Searching the best option(s) about how constraints are imposed on which age classes based on AIC etc. Estimate SDs of F random walk for ages 0‑1, 2, and above 3.
SD in measurement errors of catch at age	τ_a	Searching the best option(s) about how constraints are imposed on which age classes based on AIC etc. Estimate SDs in measurement errors of catch at age for age 0, 1, 2‑3, 4‑5, and 6+.
SD in measurement errors of abundance indices	v_a	Assuming different measurement errors among abundance indices
Number of fleets	-	Single fleet

Natural mortality	M	Age-specific M (0.80 for age 0, 0.60 for age 1, 0.51 for age 2, 0.46 for age 3, 0.43 for age 4, 0.41 for age 5, and 0.40 for age 6+) (base case)
Maturity-at-age		JPN Maturity-at-age (base case)
Catch-at-age	$C_{a.y}$	See Annex F, NPFC-2025-TWG CMSA11-WP03 Rev.1
Weight-at-age		To compute total biomass and SSB using an average, weighted by age-specific catch number with the same ratio across all years (FY2014–FY2023) by Member, of CHN, E/W JPN and RUS WAA
Summer survey index (age 0)		Used for SA (NPFC-2025-TWG CMSA10-WP08)
Autumn survey indices (ages 0, 1)		Used for SA (NPFC-2025-TWG CMSA10-WP05)
Egg abundance (SSB)		Used for SA (NPFC-2025-TWG CMSA10-WP07 (Rev. 1))
Dipnet fishery (SSB)		Used for SA (NPFC-2025-TWG CMSA10-WP06)
Chinese fishery CPUE		Used for SA (NPFC-2025-TWG CMSA10-WP09)
Russian fishery CPUE		Used for SA (NPFC-2025-TWG CMSA11-WP05)

Table A3. Future projection settings for the base case scenario, S02-Index2.

Projection Aspect	**Future Projection Settings**
Type of simulation	Stochastic (3,000 times)
Duration	10 years after introduction of management
Start year for incorporating management	2026
Catch or F levels	・Constant catch of 0 to 160 thousand mt in increments of 20 thousand mt ・Constant F, with values of F30–70%SPR in increments of 10% and current fishing mortality (F_{CUR}).
Estimation of catch from terminal year (FY 2024) to current year (FY 2025)	The most recent F (F2023)
Process error other than Age 0	Consider as random stochasticity with the estimated variances in SAM when it is estimated
Recruitment level	Model-based approach using S-R relationship–
Error structure in recruitment	Parametric with process error.
Biological parameters	Recent 8-years average